JOURNAL OF HAZARDOUS MATERIALS

JOURNAL OF
HAZARDOUS
MATERIALS

VOL. 34 (1993)

Abstracted/indexed in:
Applied Science and Technology Abstracts
ASM International/The Institute of Metals — Materials Information
Cambridge Scientific Abstracts
Centre de Documentation Scientifique et Technique — PASCAL database
Chemical Abstracts
CIS Documentation
Coal Abstracts
Current Awareness in Biological Sciences (CABS)
Current Contents (Engineering, Technology & Applied Sciences)
Engineering Index Abstracts
Environmental Periodicals Bibliography
Laboratory Hazards Bulletin/Chemical Hazards in Industry
NIOSHTIC
Système de Documentation et Information Métallurgique

Announcement from the Publisher

Elsevier Science Publishers encourages submission of articles on floppy disk.

All manuscripts may now be submitted on computer disk, with the eventual aim of reducing production times still further.

The preferred storage medium is a 5¼ or 3½ inch disk in MS-DOS format, although other systems are welcome, e.g. Macintosh.

After final acceptance, your disk plus one final, printed and exactly matching version (as a printout) should be submitted together to the editor. It is **important that the file on disk and the printout are identical.** Both will then be forwarded by the editor to Elsevier.

Illustrations should be provided in the usual manner.

Please follow the general instructions on style/arrangement and, in particular, the reference style of this journal as given in 'Instructions to Authors'.

Please label the disk with your name, the software & hardware used and the name of the file to be processed.

Contact the Publisher for further information:

ELSEVIER SCIENCE PUBLISHERS

Field-scale rotary kiln incineration of batch loaded toluene/sorbent. I. Data analysis and bed motion considerations

Christopher B. Leger[a], Vic A. Cundy[a,*], Arthur M. Sterling[b], Alfred N. Montestruc[a], Allen L. Jakway[a] and Warren D. Owens[c]

[a]*Mechanical Engineering Department and* [b]*Chemical Engineering Department, Louisiana State University, Baton Rouge, LA 70803 (USA)*
[c]*Mechanical Engineering Department, The University of Utah, Salt Lake City, UT 84112 (USA)*

Abstract

In this study, a field-scale rotary kiln incinerator was used for experiments on the processing of toluene contaminated sorbent contained in plastic packs. The incinerator was probed with instruments in several different locations. The results obtained in this study agree in many ways with previous studies on xylene and dichloromethane in the same incinerator. The species and temperature stratification observed near the kiln exit is consistent with previous observations. The moderate mixing induced by turbulence air addition is similar to that observed during the xylene and dichloromethane studies. The bed motion was different from that of previous experiments, and this difference affected the measured responses. Additional instrumentation has provided a clearer view of the processes occurring within the incinerator and through the entire system. The second paper in this series will expand upon the analysis of this data. Mass balances will be performed on the system, the evolution rates of toluene will be calculated, and the characteristic times for the toluene evolution will be determined.

Introduction

The study of hazardous waste incineration in rotary kilns is receiving increased attention in the U.S. and abroad, especially as landfill restrictions are expanding to an ever broader range of solid waste materials. Also, as the regulations on hazardous waste incinerators in the U.S. become increasingly stringent, predictive ability for the performance of these systems, even in a rudimentary sense, is needed. Because of the considerable complexity of the process, however, much remains to be learned. As part of our comprehensive

---

*To whom correspondence should be addressed.

study of this process at Louisiana State University, we have recently empha-sized the need to broaden the full-scale experimental data base. Such data are needed to provide insight into this complicated process, for use in both model development and validation, and in scaling analyses [1]. Initially, our field-scale efforts focused on obtaining species and temperatures at the exit of an industrial rotary kiln during quasi-steady processing of liquid carbon tetrachlo-ride [2–4]. Subsequent work focused on obtaining continuous gas and temper-ature measurements during transient processing of polyethylene packs con-taining clay sorbent charged with toluene [5], xylene [6], and dichloromethane [7]. These studies were performed on the rotary kiln incinerator operated by the Louisiana Division of The Dow Chemical Company at their facility in Plaquemine, Lousiana.

The studies of transient behavior have focused on characterizing the incin-erability of an aromatic and a chlorinated hydrocarbon in a rotary kiln environment. Toluene was selected as the aromatic test liquid because it is commonly used as a surrogate waste during trial burns in the permitting process, and because we have used it extensively in bench- and pilot-scale work [8–10]. Unfortunately, Federal regulations precluded our use of toluene at the Dow facility after the first experiment; thereafter xylene was sub-stituted. Recent facility additions, however, have allowed us to complete our study using toluene. With the experience gained from previous full-scale transient experiments, we have, in this most recent study, been able to perform a much more detailed study of the Dow incinerator system. The experimental variables and conditions have remained largely the same for comparison purposes. The experimental procedures have been improved, and the number of continuous measurements has been greatly increased. The details of this most recent study, including descriptions of the instrumenta-tion and the operating conditions studied as well as some preliminary results, were presented by Leger et al. [11]. Therefore, only a brief summary of the experimental methods will be presented here.

Materials and methods

Facility

The rotary kiln at the Louisiana Division of Dow Chemical USA is 3.2 m in diameter and 10.7 m long, with a design firing capacity of 17 MW and 800 °C outlet temperature. Gases flow through the kiln exit plane into a transition section and then into the afterburner. The afterburner has a design firing capacity of 7 MW, a design outlet temperature of 1000 °C, and a minimum residence time of 2 seconds. Gases exiting the afterburner pass through a quench chamber, a series of wet scrubbers and wet electrostatic precipita-tors, through an induced draft fan, and up a stack. A simplified schematic of the system is shown in Fig. 1.
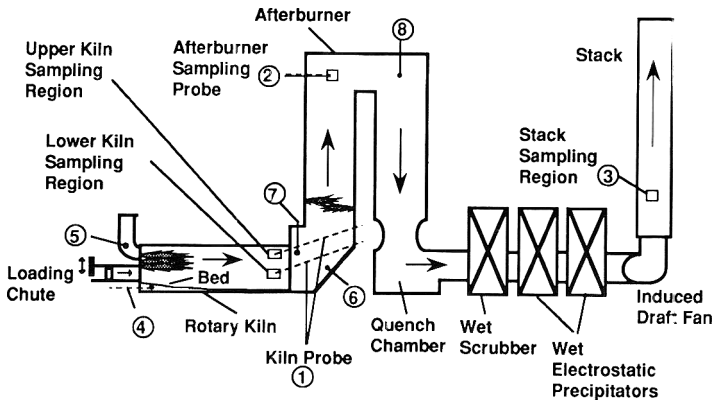
Fig. 1. Schematic of the Dow rotary kiln incinerator facility showing the measurements taken at each location. (1) Kiln sampling probe O_2, CO_2, CO, THC concentrations, gas temperature, (2) afterburner probe O_2, CO_2, CO, THC concentrations, gas temperature, (3) stack sampling O_2*, CO concentrations (2)*, (4) bed thermocouple temperature, (5) kiln feed end pressure*, (6) kiln exit pressure*, (7) kiln exit temperature*, and (8) afterburner temperature*. (*Indicates measurements from instruments that are a permanent part of the facility.)

Experimental conditions

Polyethylene packs. each containing 18.9 l of toluene on 22.7 kg of sorbent (montmorillonite granules of approximately 6 mm diameter), were prepared by Dow personnel before the experiments. Blank packs (sorbent only) were also prepared. One pack was fed into the kiln every 10 minutes throughout the experiment; blank packs were fed while changing operating conditions to maintain bed thickness in the kiln. Two nozzles, located on the stationary kiln face, allow the injection of compressed air (at ambient temperature) into the kiln to promote turbulence, bulk mixing, and combustion; we further shall refer to this as turbulence air (TA). Continuous gas measurements and gas temperatures were obtained during four different test modes: operation with and without the addition of turbulence air and operation at two kiln rotation rates, 0.1 and 0.25 rpm. Table 1 gives the experimental test matrix that was used on the two consecutive days of testing.

To the greatest extent possible, all operational parameters were held constant during each test mode. These parameters included: kiln rotation rate, natural gas and air feed rates to the kiln burners, and the turbulence air injection rate. Stack measurements, taken by Dow personnel using EPA approved methods, verified that incinerator emissions remained well within regulatory limits during the entire test period.

Sampling and instrumentation

As in previous studies [2, 6, 7], two water-cooled probes were used to obtain gas samples and gas temperature measurements within the kiln and

TABLE 1

Experimental test matrix for each day

No. of packs	Contents	Sampling	Rotation rate[a]	Turbulence air
4	Blank	None	Fast	Off
6	Toluene	Continuous	Fast	Off
3	Blank	None	Fast	Changing
6	Toluene	Continuous	Fast	On
3	Blank	None	Changing	On
6	Toluene	Continuous	Slow	On
3	Blank	None	Slow	Changing
6	Toluene	Continuous	Slow	Off
2	Toluene	Sample bomb	Slow	Off

[a] Fast = 0.25 rpm, slow = 0.1 rpm.
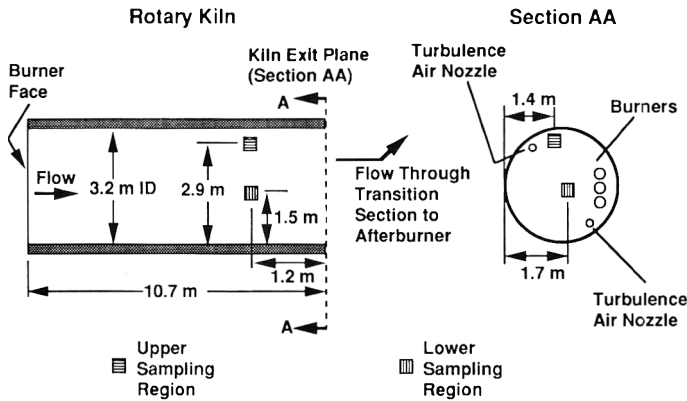
Fig. 2. Location of the two sampling regions near the kiln exit plane. The locations are estimated to within ±0.15 m (see Ref. [12]). This diagram is not to scale.

afterburner. Figure 1 shows the probe sampling locations and the measurements taken at each location. Each probe is equipped with a radiation-shielded type K thermocouple at its tip. The kiln probe, 7.8 m in length, was inserted through the transition section and drew samples from near the kiln exit. Only two access ports were available; one allowed the probe to reach a point in the upper half of the kiln, while the other allowed the probe to reach a point in the lower half of the kiln. The locations of these two sampling points are shown in Fig. 2. The kiln probe was inserted into the upper access port on the first day of experiments (3 October 1990) and it remained there for the entire day. On the second day (4 October 1990), the probe was inserted into the lower access port and the experiments were replicated. The afterburner probe, 3.8 m in length, was inserted in a different location from previous studies in an effort to sample from a better-mixed region of the afterburner. Sample gases were drawn

through each probe using an air-driven jet pump. These gases were cooled by passage through the probe and any condensate was removed using a cyclone separator. The sample gases were next drawn through a teflon sample tube to a rotary sample pump, then passed through a particulate filter, a chiller, and another condensate trap. The dried sample gas was metered through a flow controller into a series of gas analyzers. All continuous data were recorded using Omega® data acquisition packages on Macintosh SE® computers, at a frequency of 1 Hz. A more detailed discussion of the instruments and sample treatment is given by Leger et al. [11].

Along with these measurements, the readings of several facility instruments were continuously recorded during these experiments. Oxygen and CO concentrations in the stack, temperatures in the kiln and afterburner, and pressures in the kiln feed end and transition section were recorded. These locations are also indicated in Fig. 1.

Measurement of the temperature of the solids bed in the kiln was attempted using a 19 mm diameter heavy wall stainless steel pipe supporting a 3.175 mm diameter stainless steel sheathed type K thermocouple. This probe was not cooled and was inserted 1 m into the kiln, where the thermocouple tip was immersed in the bed of solids. Figure 1 shows the location of this probe.

The sample gas from the kiln and afterburner probes could also be diverted into one-liter glass sample bottles for later analysis using GC and GC/MS techniques. To simplify the sampling procedure, these grab samples were not taken simultaneously with the continuous measurements. Instead, during the incineration of a single pack at the end of each day, the continuous analyzers were disconnected and a series of grab samples was taken from both the kiln and afterburner probes at predetermined intervals.

Leger et al. [11] and Leger [12] presents the details of this experimental study and the continuous record of the oxygen concentration measured in the kiln, afterburner, and stack. These data show the variation of the transient oxygen concentration as a function of operating condition at different locations within the system. Because the data were for individual packs, differences from pack to pack under the same operating conditions could be observed. These differences were seen to persist through the entire system. Comparison between operating conditions was somewhat obscured by the variation of individual pack responses. Vertical stratification of the oxygen concentration at the kiln exit, however, was readily observed and agreed well with previous transient studies [6,7]. Although the baseline levels of oxygen were affected by the addition of turbulence air to the system, it was unclear if the oxygen response of individual packs was influenced by the turbulence air. Whether kiln rotation rate had any effect on the oxygen response was also unclear.

In this paper, the data from all monitored channels are considered. The data are averaged over several packs during each experimental condition to reduce the effects of individual pack variations. These averaged data characterize the conditions at each sampling location and demonstrate the influence of the kiln rotation rate and turbulence air addition. In a companion paper [13], mass

balances will be performed on the data, the evolution rates of toluene will be characterized, and the influence of bed motion on the evolution rates will be discussed.

Data reduction

For these experiments, the independent variables were kiln rotation rate (0.25 rpm or 0.1 rpm), and turbulence air addition (on or off). An additional variable is the location of the sampling probe near the kiln exit (upper or lower sampling region). For each combination of independent variables, the system was allowed to equilibrate for at least 30 minutes while blank packs containing only sorbent were fed into the kiln. Then a series of 6 toluene-charged packs were fed into the system, one every 10 minutes, providing one hour of data at that condition. The experimental test matrix, shown in Table 1, was duplicated on two consecutive days with the kiln sampling probe in the upper kiln location on the first day and in the lower kiln location on the second day. All other measurement locations remained the same; therefore, for all measurements other than those from the kiln probe, the experiment was replicated on the second day.

In the unaveraged oxygen data presented by Leger et al. [11], the effects of the independent variables were difficult to discern from the variation of individual packs. The same is true of the other continuous variables in their unaveraged form. Thus, an average response to a pack during each experimental condition is more useful for comparisons because the variation between individual packs is averaged out while the primary features of the data are retained. Also, since the ultimate goals of this work include performing mass balances and characterizing toluene evolution rates for each experimental condition, the use of averaged data reduces the individual pack variation in these calculations as well.

Results

The procedure for ensemble averaging the data is discussed here and illustrated in Fig. 3. To generate an average transient response of a given data channel to a single pack, an appropriate time base must first be generated. The time at which each pack dropped into the kiln was recorded during the experiment. This time provides the reference for the transient response of that pack, i.e. for each data point, the time relative to the most recent pack insertion is calculated. Then the ensemble average of the data for each pack at the same relative time is calculated. Figure 3 shows examples of the CO_2 data in the unaveraged form, the relative time based form, and

Fig. 3. Carbon dioxide data as (a) recorded, (b) in the time-based form, and (c) in the averaged form.
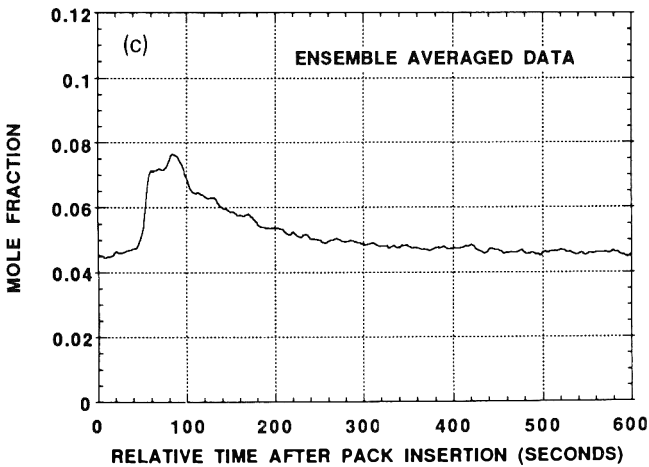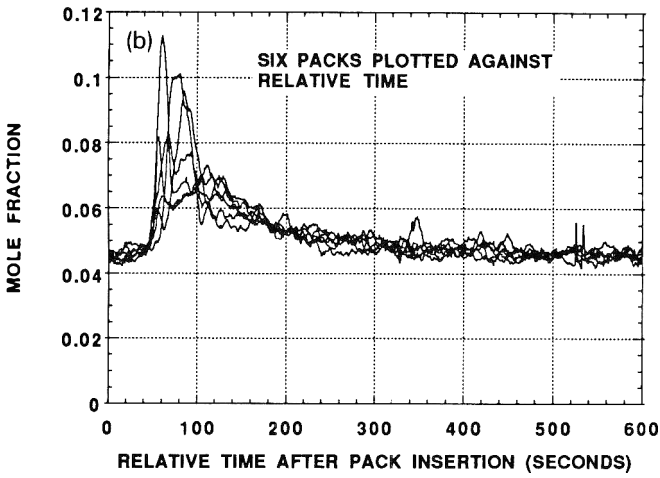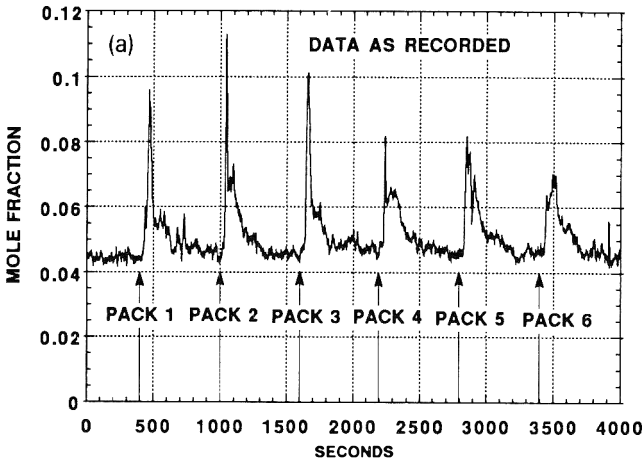
the ensemble averaged form. The ensemble averaging process tends to smooth the data, yielding a result that is easier to compare between experimental conditions.

Data presentation

The averaged data are shown in Figs. 4 through 8. In general, the graphs show continuous measurements taken during fast kiln rotation rate with turbulence air off, fast rotation rate with turbulence air on, slow rotation rate with turbulence air on, and slow rotation rate with turbulence air off. Figure 4 shows the O_2, CO_2, gas temperature, CO, and total hydrocarbon measurements obtained from the upper and lower kiln exit locations. In Fig. 5, graphs of similar afterburner data are shown for each day of experiments. The graphs for both days should replicate each other since the afterburner probe remained in the same location. Figure 6 shows the stack data, which should also replicate over the two-day period. Figure 7 presents the bed temperatures, and typical facility temperatures and pressures are shown in Fig. 8.

Each of the figures is discussed next. One general observation common to all figures is that there was no clearly discernible effect of kiln rotation rate on any of the measured parameters.

Kiln O_2 — Fig. 4(a) and (b)

In the upper kiln, the magnitude of the oxygen response to the waste containing packs is roughly the same regardless of operating conditions. In the lower kiln, however, the response is considerably increased when the turbulence air (TA) is on, Fig. 4(b). The baseline oxygen values are very low in the upper kiln when the turbulence air is off, Fig. 4(a). The oxygen values are quite high in the lower kiln regardless of operating conditions.

Kiln CO_2 — Fig. 4(c) and (d)

The addition of turbulence air, Fig. 4(d), lowers the overall levels of CO_2 in the upper kiln and increases the magnitude of the CO_2 response in the lower kiln. The levels of CO_2 observed in the lower kiln are substantially lower than those in the upper kiln, particularly with the turbulence air turned off, Fig. 4(c).

Kiln gas temperature — Fig. 4(e) and (f)

The addition of turbulence air lowers the overall gas temperature levels in the upper kiln and increases the magnitude of the temperature response (compare Fig. 4f with 4e). In the lower kiln, the turbulence air does not clearly change the overall temperature levels, but it does increase the magnitude of the temperature response. The gas temperatures in the upper kiln are much higher than those in the lower kiln.
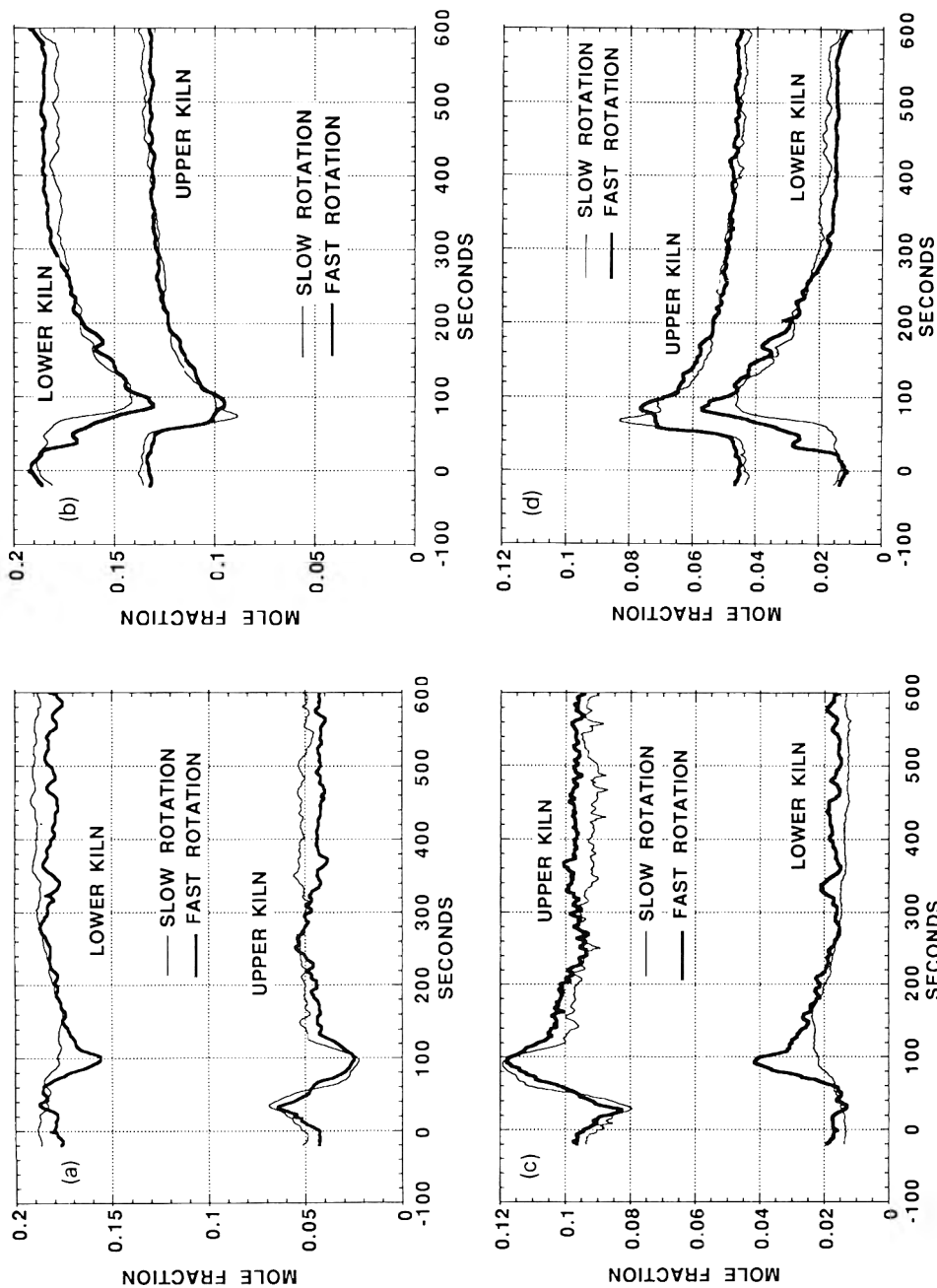
Fig. 4. Parameters measured by the kiln probe, with and without turbulence air (TA). Oxygen dry mole fraction (a) without, and (b) with TA; carbon dioxide dry mole fraction (c) without, and (d) with TA; gas temperature (e) without, and (f) with TA; and carbon monoxide (g) and total hydrocarbon (h).
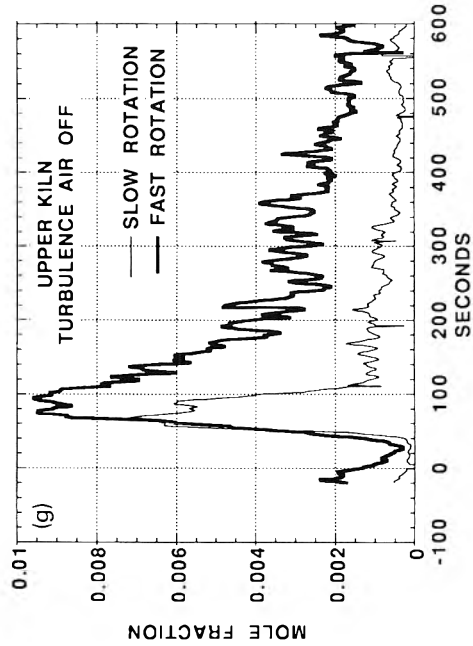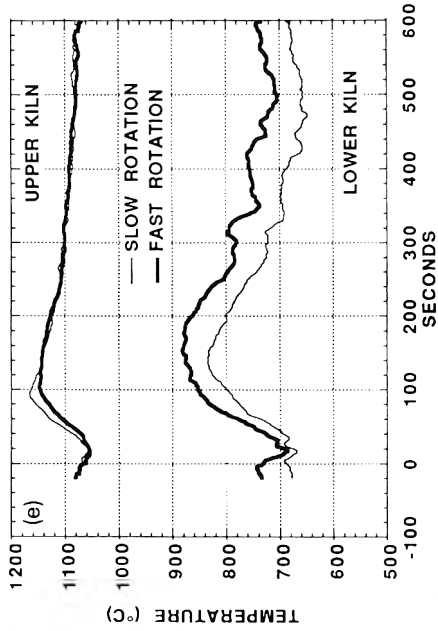
Fig 4. Continued.
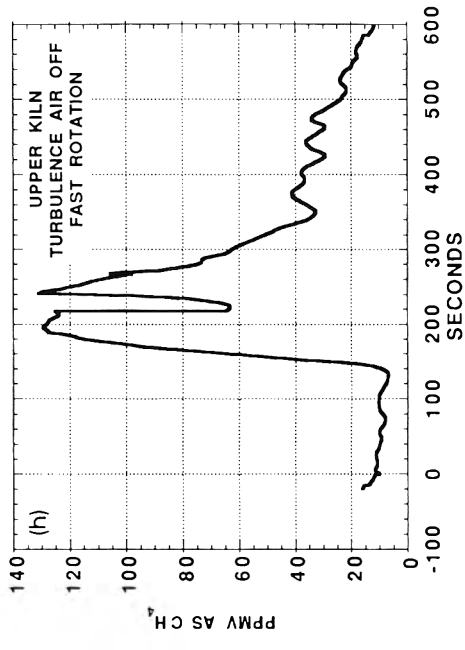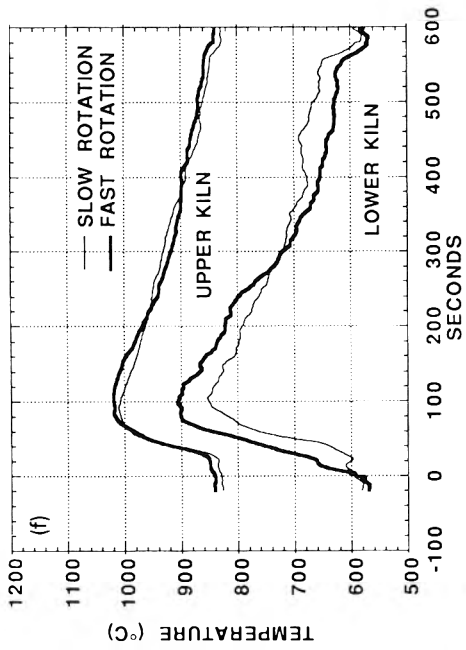
Kiln CO and THC — Fig. 4(g) and (h)

In the upper kiln, relatively large amounts of CO were observed only during operation with turbulence air off. The addition of turbulence air reduced the observed CO values to near zero so these data were not plotted in the figure. Very little CO was observed in the lower kiln under any conditions; hence, these data also were not plotted. In the upper kiln with turbulence air off, it appears that the fast rotation rate caused a greater CO response than did the slow rotation rate. However, it should be noted that the CO concentration should be rather sensitive to oxygen levels, and the baseline oxygen level was almost one percent higher during the slow rotation rate conditions. Since the baseline conditions are not a result of the waste combustion and should be independent of rotation rate, this difference in CO response may result from slightly different support flame feed settings.

Before discussing the total hydrocarbon (THC) data, an operational aspect must be considered. To prevent the loss of hydrocarbons from the sample gas, the THC sample stream was split from the main sample stream before passing through the sample chiller, secondary condensate trap, and desiccant dryers. Unfortunately, excessive condensation in the sample line extinguished the flame ionization detector on a few occasions and greatly reduced the sample flow rate at other times. As a result, the kiln THC data are generally suspect. The THC analyzer appeared to be operating properly during the first set of data obtained in the upper kiln with turbulence air off and fast kiln rotation rate as shown in the figure. A substantial THC response was observed during that operating condition, corresponding with high CO levels observed at the same time. For slow rotation rate with turbulence air off in the upper kiln, the THC response was suspiciously flat even though high CO levels were observed. We attribute this behavior to the THC sampling problems discussed above. All the other operating conditions showed low THC levels corresponding to low CO levels. Although this seems reasonable, the sampling problems preclude confirmation of this observation.

Afterburner O_2 — Fig. 5(a) and (b)

For the afterburner data, one sees good reproducibility from one day to the next, although the overall oxygen levels are about 1% higher on the second day. On both days, the addition of turbulence air reduced the magnitude of the oxygen response, Fig. 5(b). Since turbulence air addition is accompanied by an increase in overall gas flow rate while the amount of toluene burned remains the same, the response to pack combustion is diluted by the increased flow.

Afterburner CO_2 — Fig. 5(c) and (d)

The reproducibility of the CO_2 data appears very good. Again, the addition of turbulence air, Fig. 5(d), appears to decrease the response from a pack due to dilution.

(a)

(c)
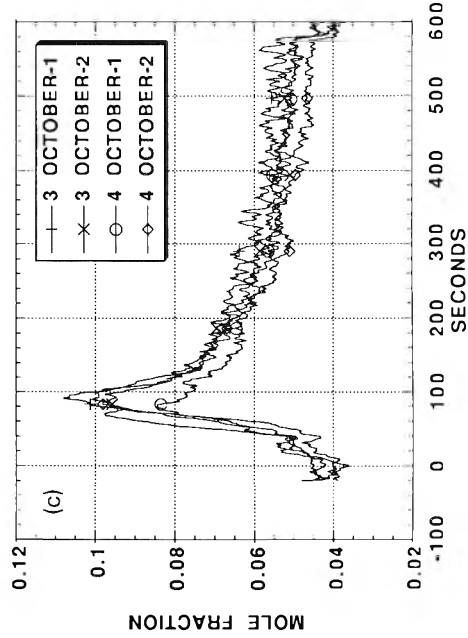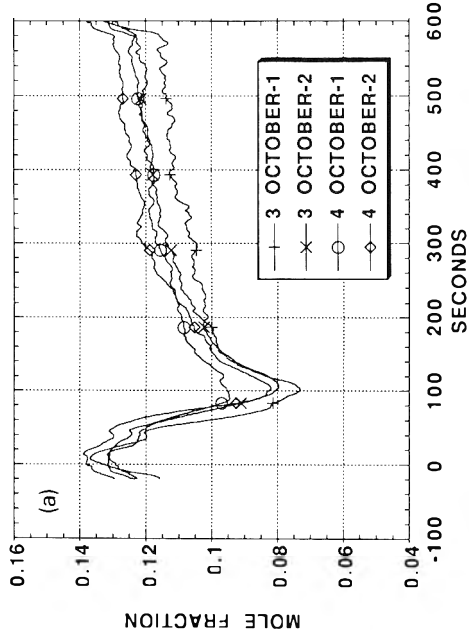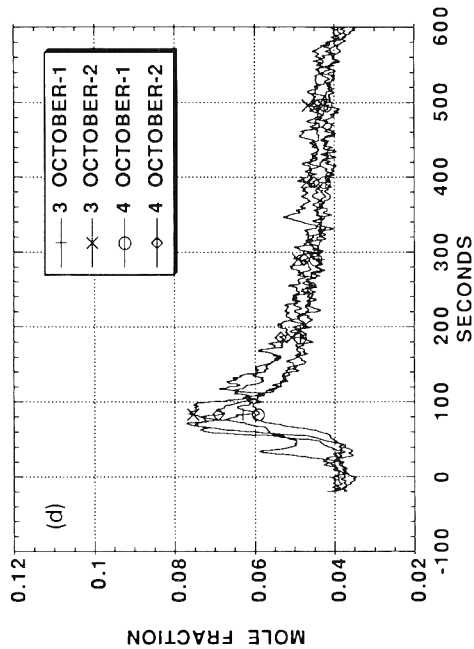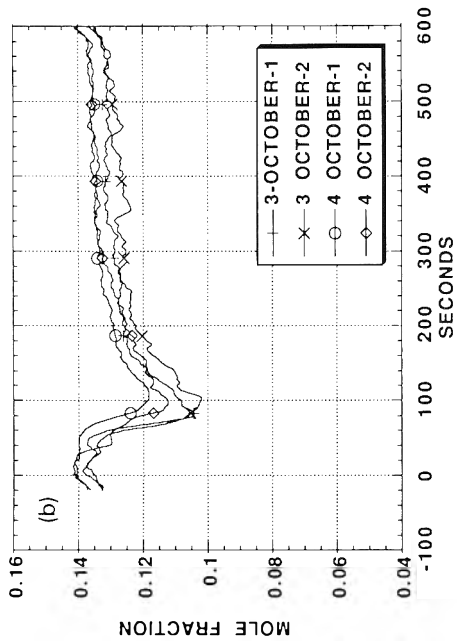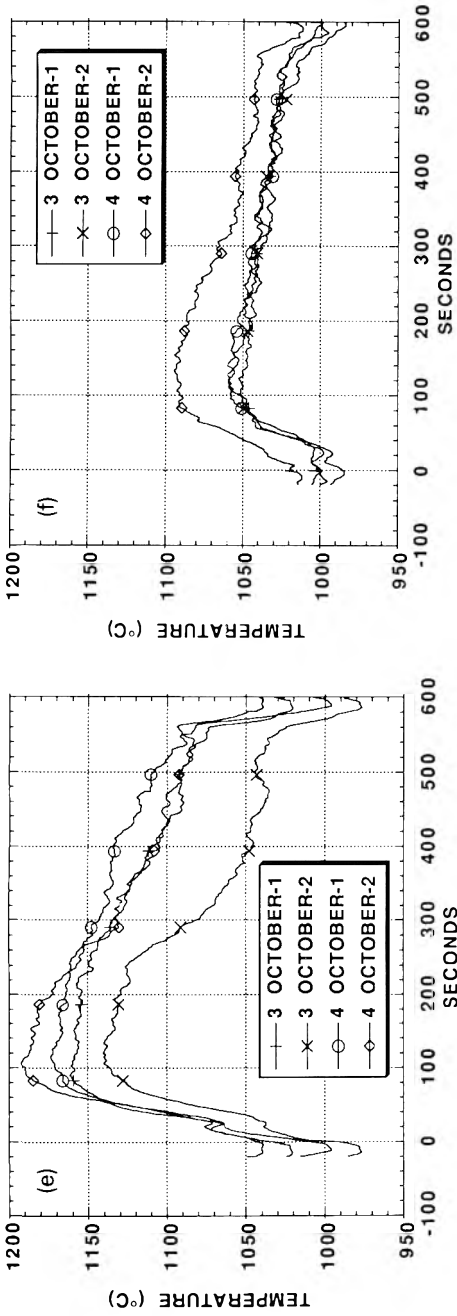
Fig. 5. Parameters measured by the afterburner probe. Plot symbols are used intermittently to identify data sets only. Key symbols − 1 and − 2 refer to slow and fast kiln rotation rates, respectively. Oxygen dry mole fraction (a) without, and (b) with TA; carbon dioxide dry mole fraction (c) without, and (d) with TA; and gas temperature measured (e) without, and (f) with TA.

Afterburner gas temperature — Fig. 5(e) and (f)

Overall, the afterburner gas temperature response appears to be quite reproducible. It clearly shows the effect of opening the loading chute door for pack insertion into the kiln. This is seen as the sudden drop in temperature at the end of each curve, which results from additional air entering through the kiln loading chute door during pack loading. Sometimes, the temperature level is seen to return momentarily to the baseline value after the door closes but before the pack begins to burn. Notice that the magnitude of the effect due to the loading chute door is reduced when turbulence air is added, Fig. 5(f). This is also true of the peak temperature response due to pack combustion. This is, in both cases, thought to be due to dilution by the higher gas flow under turbulence air addition.

Afterburner CO and THC

In contrast to what was observed in the kiln, very little CO is seen in the afterburner under any conditions. In fact, for discussion purposes, the afterburner CO never rose above baseline. The THC analyzer used with the afterburner probe suffered from the same operational problems as the THC analyzer for the kiln probe. In addition, problems with the sample flow rate caused a very long lag in the instrument response. The observed THC levels were low (< 15 ppmv), which corresponds to the low levels of CO observed in the afterburner on both days. In general, both the CO and THC measurements taken from the afterburner never rose appreciably above baseline.

Stack O_2 — Fig. 6

The stack oxygen response tends to be very smooth, with the minimum occurring later than for kiln or afterburner measurements, as expected. The delay may be due to stack oxygen analyzer response or to the time required for the combustion gases to flow through the pollution control equipment. The data are quite repeatable, showing only a slight dilution effect with turbulence air turned on, Fig. 6(b). One should note that the oxygen levels measured in the stack generally match those measured in the afterburner, indicating little or no air infiltration downstream of the afterburners in the pollution control equipment. Measurements with turbulence air off on the first day are an exception, showing stack oxygen levels approximately 1% higher than those measured in the afterburner.

Stack CO

We were able to monitor two redundant facility CO analyzers in the stack. For the operating conditions in these experiments, the CO levels in the stack were so low that all we could observe was instrument noise.

Kiln bed temperature — Fig. 7

The kiln bed temperature measurements presented here were measured by a thermocouple probe inserted axially through the kiln's front rotary seal and
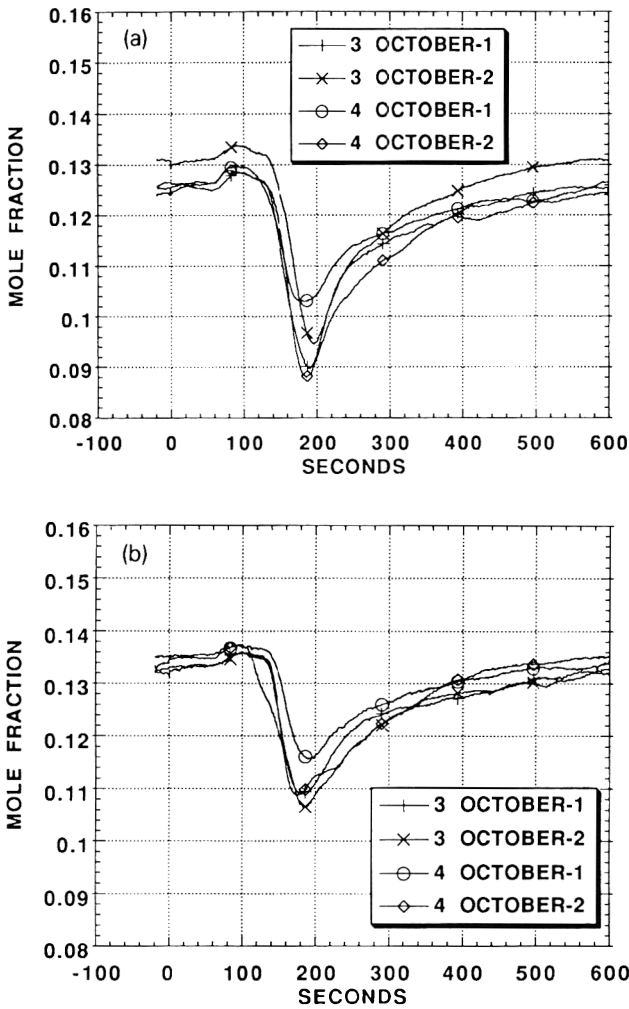
Fig. 6. Oxygen dry mole fraction measured in the stack. Plot symbols are used intermittently to identify data sets only. Key symbols –1 and –2 refer to slow and fast kiln rotation rates, respectively. (a) Without, and (b) with TA.

into the solids bed. Unfortunately, even though the probe consisted of a 19 mm diameter heavy wall stainless steel tube, it was bent substantially during the experiments each day. When one considers the forces acting on the probe due to the drag of the sorbent bed and the occasional pack bumping into it, together with the high temperatures, it is not too surprising that the probe was bent. The data obtained, although somewhat erratic, bear a strong resemblance to the gas temperature data obtained by the kiln probe. The "bed" temperature is seen to drop off before a pack is loaded, as if it were measuring
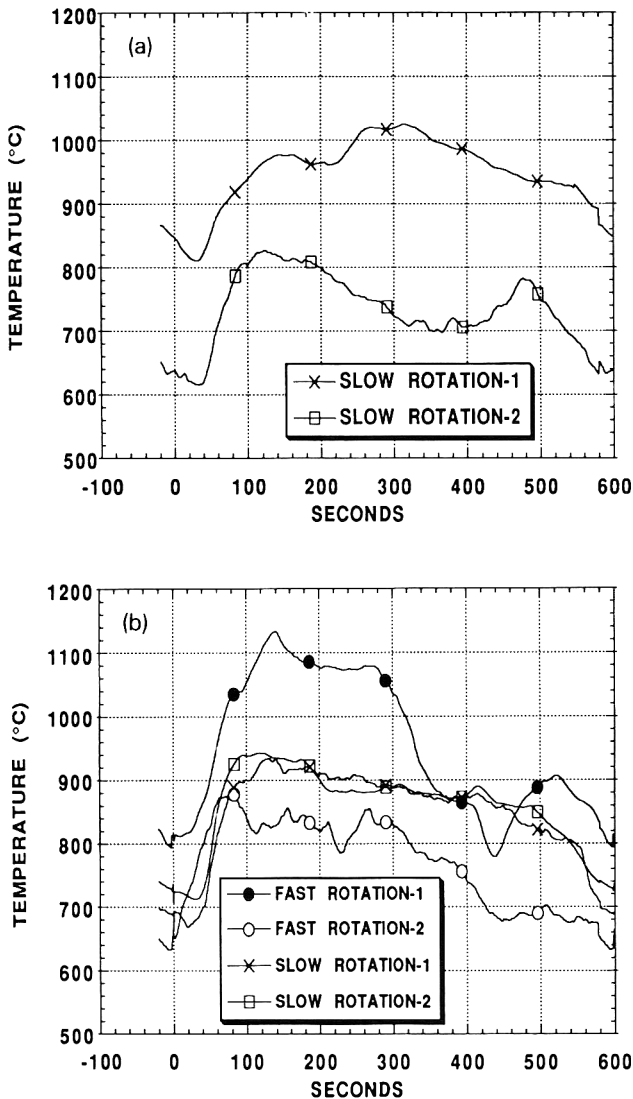
Fig. 7. Temperature measured by the bed thermocouple probe. Plot symbols are used intermittently to identify data sets only. Key symbols −1 and −2 refer to operation on 3 and 4 October, respectively. (a) Without, and (b) with TA.

the effect of cold leak air entering from the loading chute door. As a result, we believe that the thermocouple tip was protruding from the solids. This could not be verified visually because a number of steel lid-retaining rings from the plastic packs collected where the end of the probe should have been, as if they were hung on the probe tip. They may have contributed to the bending of the probe. No clear observations can be drawn from these data, except that the

temperatures measured with this probe may represent a very rough measure of the bed and kiln wall surface temperatures in this general location.

Facility temperatures and pressures — Fig. 8(a) and (b)

Two facility thermocouples were monitored during these experiments. One was located near the top of the kiln exit in the transition section, while the other one was located in the afterburner. Under all conditions, the afterburner thermocouple gave the higher reading of the two. Typical traces for the experiments are shown in Fig. 8(a). Notice the smooth, gentle response of each facility thermocouple compared to the gas temperature responses measured by the kiln and afterburner probes (Figure 4e and f, and 5e and f). One explanation for this smooth response is that each facility thermocouple is inside a heavy wall 19 mm Monel thermowell, resulting in fairly long thermal time constants. A second explanation is that neither thermowell is radiation shielded. At the temperatures indicated, radiation heat transfer between the refractory walls and the thermowell may be the dominant mode of heat transfer. If this is the case, then the thermocouples are indicating the rise and fall of the refractory surface temperature in the region around the thermocouple. The refractory itself has a long thermal time constant, thus the measured response will be slow and gradual, as was observed. In the afterburner, where the temperatures are higher, the refractory to thermowell radiation exchange should be even more dominant. Indeed, the afterburner temperature response is very small in magnitude and it lags the pack insertion considerably more than does the kiln exit temperature response. The temperature measured by the afterburner thermocouple is always substantially lower than the gas temperature measured by the afterburner probe, again consistent with radiation heat exchange with the refractory walls. The temperature measured by the kiln-exit thermocouple is substantially lower than the gas temperature measured by the kiln probe in the upper kiln exit region. This may be due to the radiatively cool ash quench area below the facility thermocouple acting as a radiant heat sink, or it may be due to a non-homogeneous temperature field at the kiln exit. Overall, the temperatures measured by the facility thermocouples are remarkably repeatable and the overall temperature levels do not vary in response to experimental conditions. This is expected because the input air and gas flow rates were set to provide the same facility temperature for each operating condition.

The facility pressure transducers at the feed end of the kiln and in the transition section were monitored, and typical traces are presented in Fig. 8. The transition section pressure (Fig. 8b) is always the higher of the two. The data appear noisy compared to the other monitored variables, even though they have been ensemble averaged like all the other data. The responses measured at each end of the kiln by different pressure transducers, even after averaging, show almost exactly the same "noise" down to the smallest fluctuation. This would be unlikely if the fluctuations were originating in the
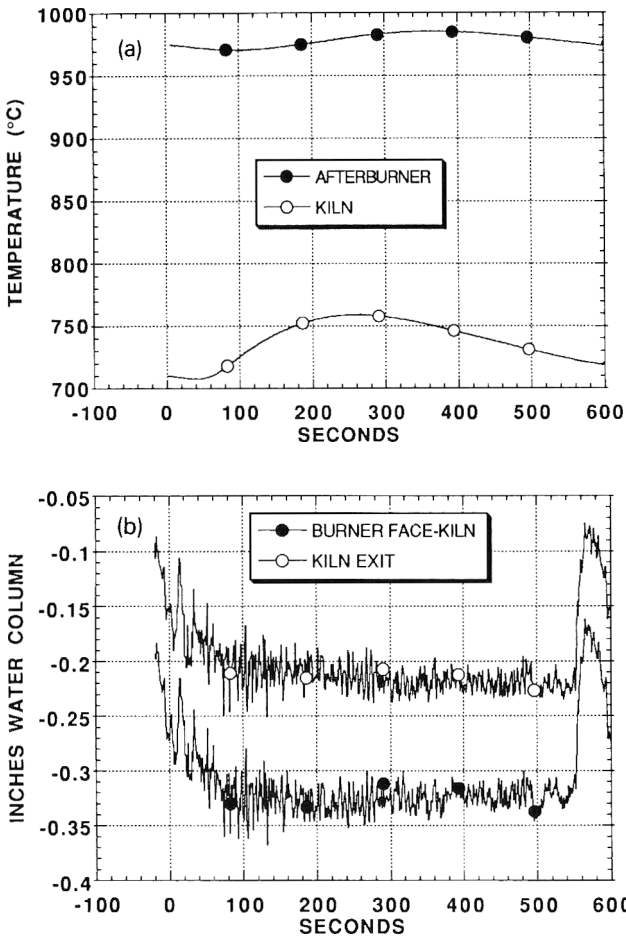
Fig. 8. (a) Temperature and (b) pressure measured by the facility probes. Plot symbols are used intermittently to identify data sets only. For temperature, the higher reading is from the top of the afterburner and the lower reading is from above the kiln exit. For pressure, the higher reading is from the exit end of the kiln and the lower reading is from the burner end of the kiln.

instruments, so these rapid fluctuations in pressure are evidently present in the kiln and are not instrument noise.

One prominent feature of the pressure response is the dramatic rise before pack insertion associated with air entering through the loading chute. One may notice that the pressure is somewhat more erratic during the first 100 to 200 seconds after pack insertion. This may be the result of toluene combustion in the kiln. It is important to note that the toluene combustion did not cause a net pressure rise of the sort that could lead to a positive pressure excursion. Finally, since the pressure was a controlled parameter, it shows little variation across operating conditions.

Gas chromatographic data

The gas chromatographic (GC) methods used in these experiments are identical to those used in previous experiments [7, 14]. The sampling procedure is slightly modified. The gas stream from the sampling probe in the kiln is drawn through a one liter glass sampling bomb with teflon stopcocks. The bomb is purged with the sample gas for approximately 30 s, then the stopcocks are closed, isolating the sample. A second sample bomb is then purged and filled, and so on for a total of six samples all obtained in series during the combustion of a single pack. The sample bombs are contained in boxes of three bombs each, so between the third and fourth samples the lines are disconnected from one box and connected to the next. Samples were taken in the same fashion from the afterburner probe simultaneously with the kiln samples. The continuous monitors were used for the first six packs during the operating condition and then were disconnected. The grab samples were taken immediately afterward, during the seventh pack under the same operating condition. Because of time constraints, grab samples were obtained only during slow rotation rate with no turbulence air addition. The samples were obtained at the end of the experiment on both days and were immediately transported to the laboratory and analyzed within several hours.

The results of the GC sample analyses are shown in Figs. 9 through 12. The GC methods quantified N_2, O_2, CO_2, CO, CH_4, C_2H_2, C_2H_4, C_2H_6, C_6H_6, and C_7H_8. The hydrocarbon concentrations measured by the GC were multiplied by the number of carbon atoms in each species and then summed to give a total hydrocarbon measurement in methane equivalents (only for comparative purposes). The GC data are plotted as a function of sample time together with the averaged continuous data (heavy line in the figures) obtained on the same day for the same operating condition. In these figures, the 95% confidence intervals (the lighter lines) are included for the continuous data to show the relative variability of the continuous data for each pack. The confidence interval is defined as:

$$\text{Confidence interval} = \bar{y}_i \pm t_{n-1} \sqrt{\frac{\Sigma y_i^2 - (\Sigma y_i)^2}{n(n-1)}} \tag{1}$$

where $\bar{y}_i$ denotes the mean value of the samples at time "i"; t_{n-1} is the two-tailed student t statistic for $n-1$ degrees of freedom, $\alpha = 0.025$; y_i is the value of a sample at time "i"; and n is the number of samples to be averaged at time "i". The sample size, n, in each case was 6, one for each pack, at a given relative time.

Upper kiln GC data — Fig. 9

The graph of oxygen in the upper kiln (Fig. 9a) shows good agreement between continuous data and the GC data points. The same behavior is seen for the CO_2 data (Fig. 9b). Other questionable GC samples taken from the second box of three sample bombs are not shown on the graph. It appears likely that an

Fig. 9. GC data (circles) and average continuous data (heavy line) obtained from the upper sampling location in the kiln during slow rotation rate and operation without turbulence air addition. The 95% confidence interval on the continuous data is shown by the two light bracketing lines. (a) Oxygen and (b) carbon dioxide measurements, (c) carbon monoxide and (d) THC measurements.

air leak occurred somewhere in the connection of the second sample box, causing the last three samples to be diluted with air. Figure 9(c) shows the CO data and again there is very good agreement with the continuous data. While the continuous THC analyzer showed little or no response, the GC samples (Fig. 9d) clearly show a large response. From this we conclude that the kiln THC analyzer was in fact malfunctioning during that operating condition. This means that large amounts of hydrocarbons were present in the upper kiln during both fast and slow kiln rotation rates when the turbulence air was turned off. This corresponds with the high CO levels that were present during these operating conditions. The hydrocarbon species measured in the upper kiln showed that methane was predominant, and no toluene was detected. This is consistent with results obtained during processing of xylene [6].

Lower kiln GC data — Fig. 10

In the lower kiln, the oxygen data points (Fig. 10a) agree fairly well with the continuous O_2 data, although the second data point is below the continuous data. Since the low value is backed up by a correspondingly high CO_2 data point and no likely mechanism exists to cause this type of error in the GC samples, we accept it as a valid measurement. The CO_2 data (Fig. 10b) show reasonable agreement for the three data points shown. The CO data of Fig. 10(c) agree well, all registering low levels. The GC THC data points (Fig. 10d) indicate a small spike in the hydrocarbon concentration that was not registered by the continuous THC analyzer. Again one may conclude that the continuous analyzer was not functioning at that time. The GC analyses showed small quantities of toluene in these samples, and relatively low concentrations of methane. Again these measurements are consistent with those obtained during xylene experiments [6].

Afterburner GC data on 3 October 1990 — Fig. 11

In the afterburner on the first day of experiments, the O_2, CO_2, and CO data (Figs. 11a–c) show good agreement. The THC data (Fig. 11d) show an interesting behavior although the levels shown in the figure are quite small. The GC registered 14 ppmv of hydrocarbons at 30 s and the continuous analyzer registered essentially zero until the spike noted at 200 s. The maximum level registered by the continuous monitor was only approximately 12 ppmv which agrees quite well with the GC value at 30 s. We feel that the continuous analyzer was operating properly and registering the correct concentrations; however, the sample flow rate may have been reduced, causing a three minute delay before the sample reached the analyzer. This reduced flow rate could be attributed to the already long sample line and build up of condensate interfering with the flow control valve and rotameter.

Afterburner GC data on 4 October 1990 — Fig. 12

On the second day of experiments, the afterburner O_2 and CO_2 data again show very good agreement (Figs. 12a and b, respectively). The CO analyzer
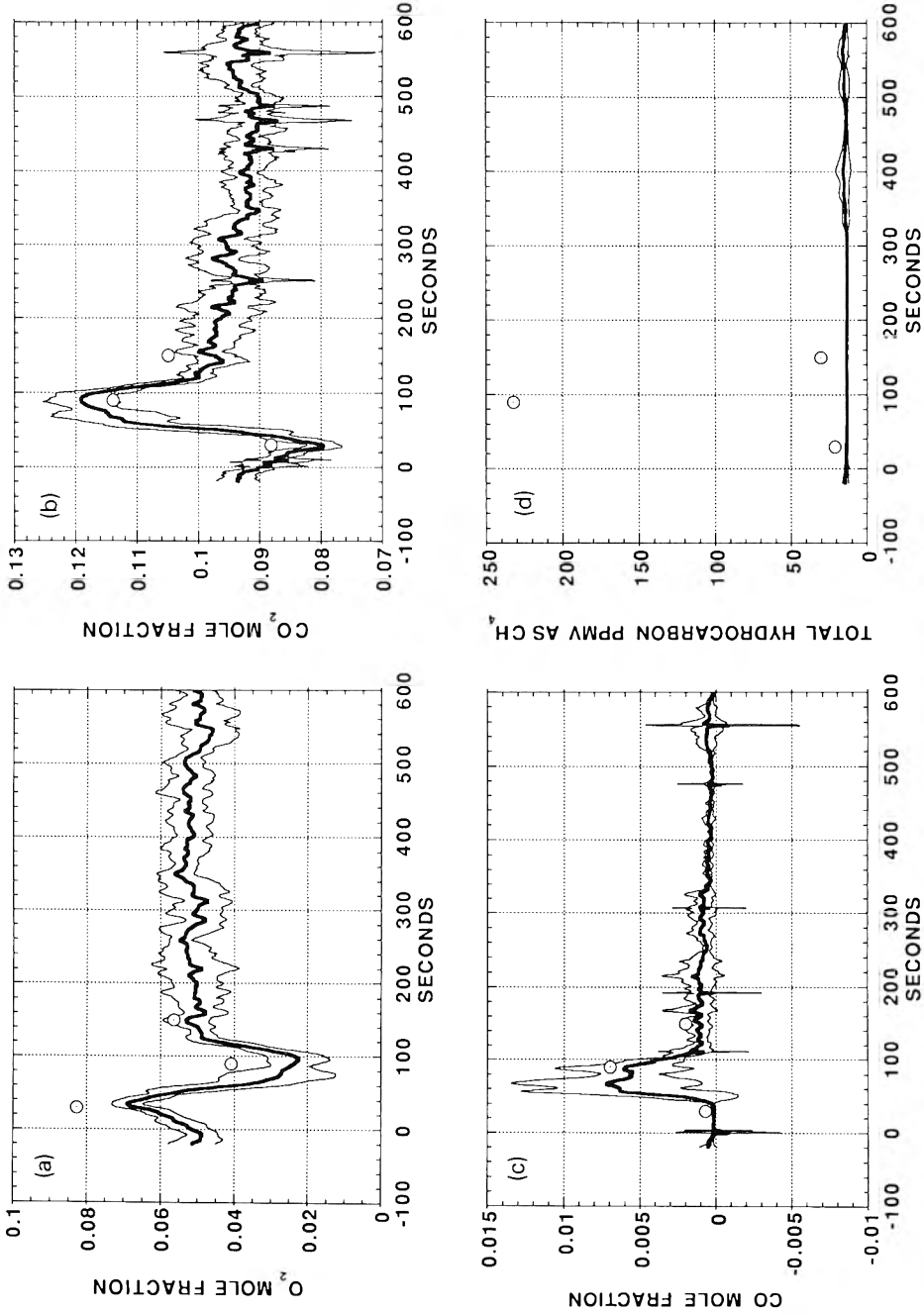
Fig. 10. GC data (circles) and average continuous data (heavy line) obtained from the lower sampling location in the kiln during slow rotation rate and operation without turbulence air addition. The 95% confidence interval on the continuous data is shown by the two light bracketing lines. (a) Oxygen and (b) carbon dioxide measurements, (c) carbon monoxide and (d) THC measurements.
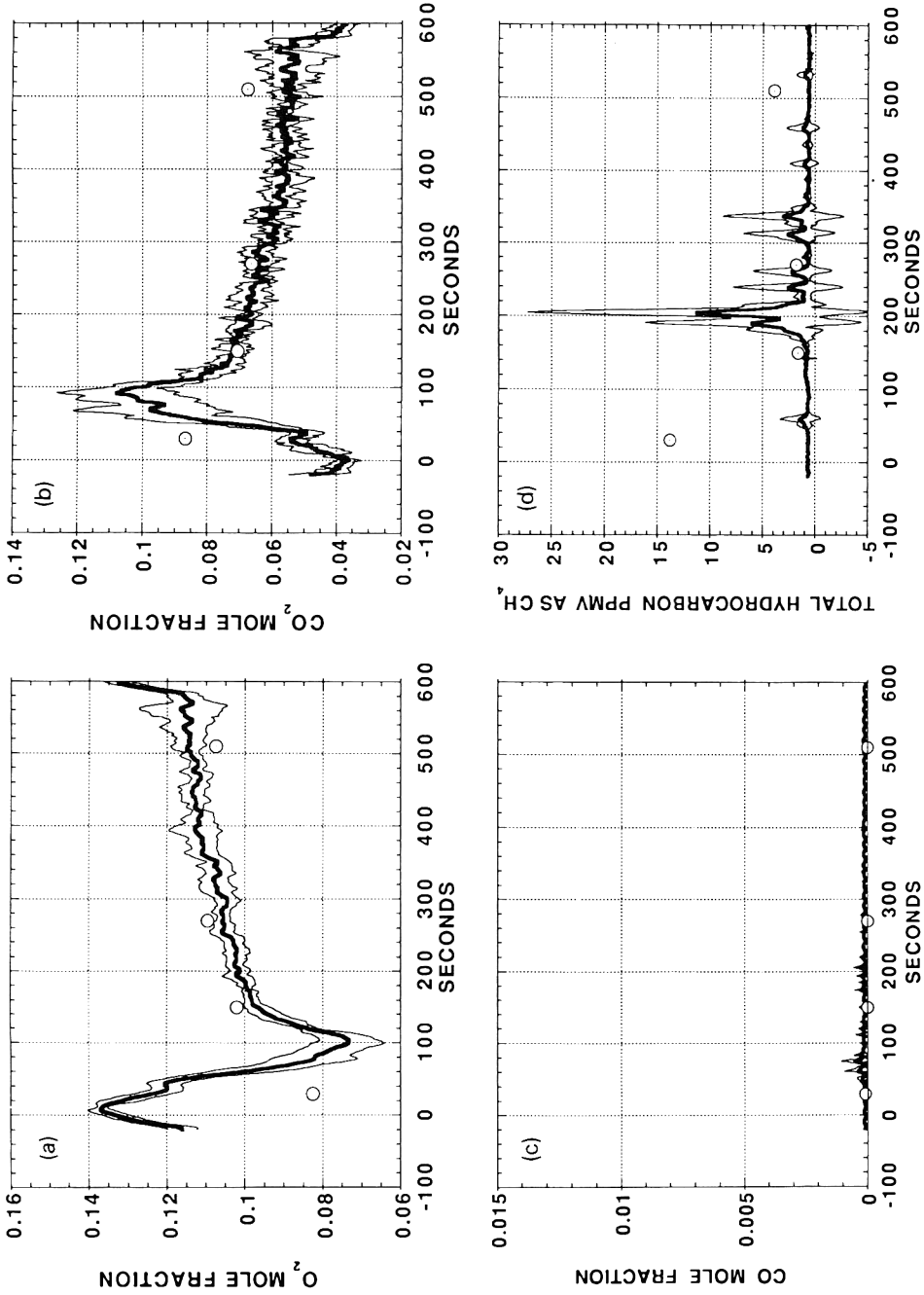
Fig. 11. GC data (circles) and average continuous data (heavy line) obtained from the afterburner on 3 October 1990 during slow rotation rate and operation without turbulence air addition. The 95% confidence interval on the continuous data is shown by the two light bracketing lines. (a) Oxygen and (b) carbon dioxide measurements, (c) carbon monoxide and (d) THC measurements.
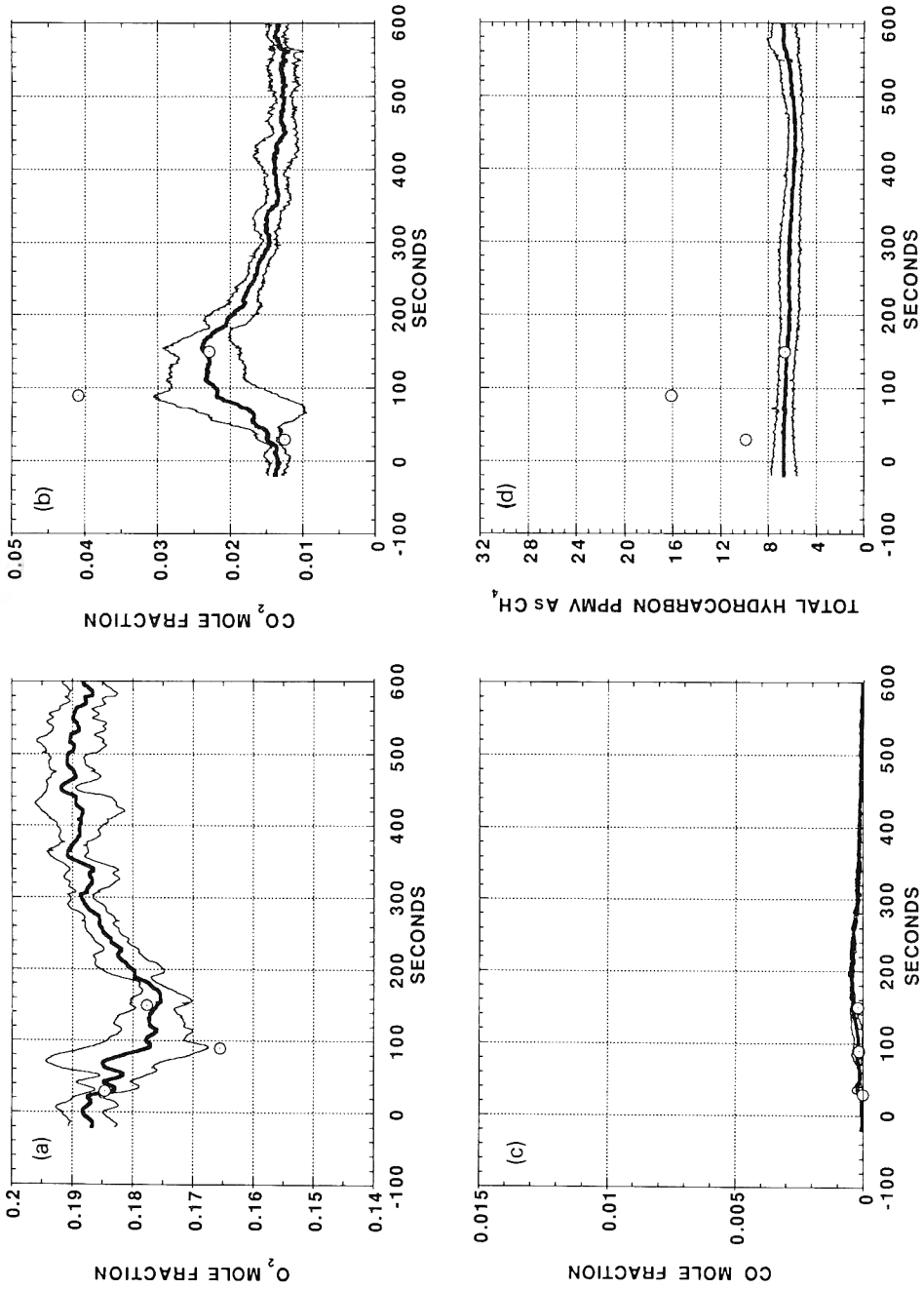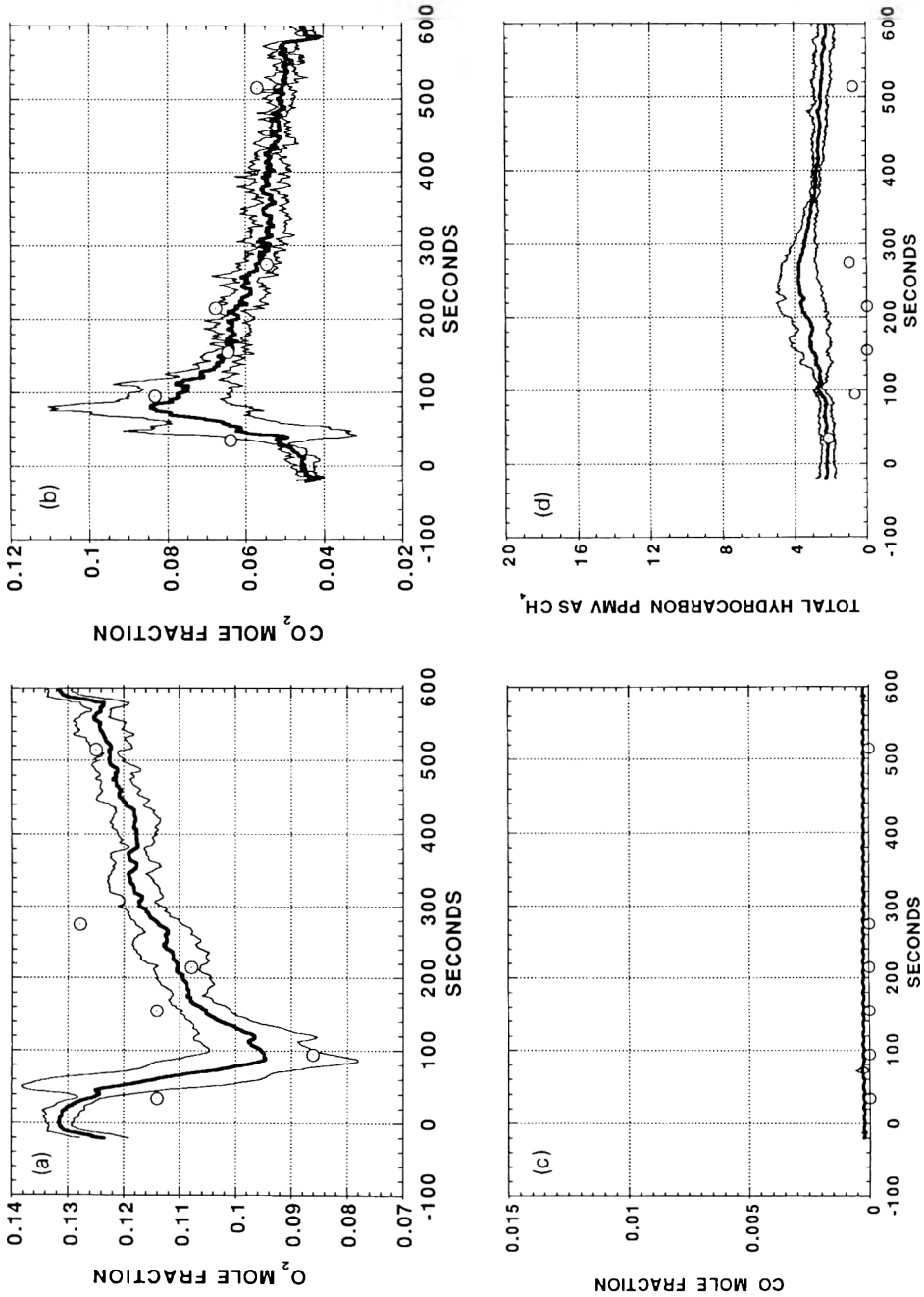
Fig. 12. GC data (circles) and average continuous data (heavy line) obtained from the afterburner on 4 October 1990 during slow rotation rate and operation without turbulence air addition. The 95% confidence interval on the continuous data is shown by the two light bracketing lines. (a) Oxygen and (b) carbon dioxide measurements, (c) carbon monoxide and (d) THC measurements.

shows no response due to pack combustion, nor do the GC samples (Fig. 12c). Both the GC and the continuous THC analyzer indicate low levels of hydrocarbons and little or no response from pack combustion (Fig. 12d).

Overall, although there were problems with some of the GC samples and with sample conditioning for the THC analyzers, the data agreement is generally very good. The confidence intervals show that the data, particularly the O_2 and CO_2 responses, were quite repeatable from pack to pack. Considering the difficulties inherent in this type of study in the field, the overall quality of the data is thought to be quite good.

Discussion

This set of experiments was designed to be experimentally similar to earlier experiments that were conducted using packs of xylene and dichloromethane [6, 7]. The only major differences were to be the use of toluene and the more extensive instrumentation and data acquisition in the latter experiments. Data taken during the xylene experiments and these toluene experiments should be similar because the two compounds are quite similar in their combustion properties. The stratification between the upper kiln exit and lower kiln exit is seen with both toluene and xylene, as well as during all other experimental studies on this system [2–4, 6, 7]. The changes associated with the introduction of turbulence air, particularly the dilution effect and the effect on CO and THC in the upper kiln, were also seen during the xylene experiments.

During the xylene experiments, rotation rate was seen to have a substantial effect on the response to a pack in the kiln. The faster rotation rate was associated with greater magnitude and shorter duration responses for all the measured variables. This effect was totally absent during the toluene experiments. In addition, the xylene experiments often yielded multiple-peaked responses from each pack. The toluene data showed no such tendency for multiple peaks and, in fact, tended to show a very repeatable response characterized by a rapid rise in the measured variable followed by a gradual decay.

Clearly some difference between the toluene and xylene experiments affected the way in which the waste evolved from the sorbent and thus affected the dependence of evolution rate on kiln rotation rate. Observations of the video taken during the experiments have pointed to differences in bed motion as the cause of the difference in evolution rates. The bed motion during the xylene experiments could be characterized as slumping motion. In this motion regime, solids intermittently tumble down the free surface of the bed, and then follow the wall in a layer below the surface before reemerging to tumble across the surface again. This motion causes the solids to mix, and each part of the bed is repeatedly exposed at the surface. During the toluene experiments, however, the bed exhibited a slipping motion. With this type of motion, the entire bed slips relative to the wall, and it moves as if it were a solid piece, with the same particles remaining on the surface. In this type of bed motion, the solids mix

very slowly. The reason for the different bed motions in the two sets of experiments is not entirely clear. The packs were identical except for the type of liquid contaminant added to each, they were fed at the same 10-minute intervals, and the kiln was rotated at the same rates. This should have resulted in the same type of bed motion.

The bed motion is, among other things, dependent upon the roughness of the kiln wall. Since the kiln wall refractory is usually coated with a layer of hardened slag of variable thickness and texture, it is quite possible that the surface was smoother during the toluene experiments, resulting in the slipping motion. Another possible influence is the presence of the bed thermocouple probe during the toluene experiments. Some of the steel lid retaining rings were observed collecting in the area of probe. If these rings were actually looped over the end of the probe, as we suspect, the probe could have held the conglomeration of barrel pack rings and sorbent together. This would have given the bed some structural integrity, causing it to slip as a whole rather than mixing and slumping. Even the drag of the thermocouple probe alone may have triggered slipping before the bed could rise high enough for a slump to occur.

The presence of slipping motion of the bed during the toluene experiments at first appears unfortunate. Our previous work has led to a scaling model for predicting waste evolution based upon measurements taken in a system of a different size [1]. The scaling model was lacking in the area of field-scale data; these toluene experiments were to provide additional field-scale data for use in testing the scaling analysis. Unfortunately, these data cannot be used because the scaling analysis requires similarity of bed motion. There may be a seren-dipitous side to this story, however. First, the bed motion was most likely influenced by the temperature probe, although unintentionally, even though all other parameters remained the same. This opens up the possibility that the bed motion may be intentionally modified by inserting fixed structures into the bed, allow one to control the bed motion and the resulting mixing and con-taminant evolution characteristics. Second, we now have data obtained under similar experimental conditions with similar contaminant species (xylene and toluene), the only difference being the motion exhibited by the bed. This is an opportunity to make comparisons and determine the effects of bed motion on contaminant evolution in more detail. These comparisons will be made in the companion to this paper [13].

Summary and conclusions

A detailed study of unsteady conditions inside the field-scale rotary kiln incinerator operated by the Louisiana Division of Dow Chemical USA has been successfully accomplished. Experience gained during earlier studies and the use of more extensive instrumentation has provided a clearer picture of the processes occurring within the incinerator and through the entire system. In

this paper, the ensemble averaged data for each monitored variable are presented as a function of experimental conditions. A list of the conclusions that are drawn from this averaged data follows:

- The bed motion during these experiments was observed to be in the slipping regime, in contrast with slumping bed motion seen in earlier experiments under similar conditions.
- Vertical stratification at kiln exit is inferred through measurements of O_2, CO_2, and gas temperatures. The upper kiln is characterized by lower O_2, higher CO_2, and higher gas temperatures.
- The addition of turbulence air tends to reduce the magnitude of the stratification observed in the kiln.
- Substantial amounts of CO are observed only in the upper kiln and then only during operation with no turbulence air.
- Kiln rotation rate, over the range studied, appears to have no effect on any of the measured variables. This is thought to be a result of the slipping bed motion observed at both rotation rates during these experiments.
- The addition of turbulence air reduces the magnitude of responses to a pack measured in the afterburner and stack, apparently through dilution of the toluene combustion products by the higher gas flow rates.
- Reproducibility of data in the afterburner and stack are quite good. No replicate measurements were taken in the kiln on consecutive days.
- The continuous gas species measurements in the kiln and afterburner agree well with gas chromatographic analyses of grab samples from those locations.
- The measured bed temperatures presented here are probably not accurate because of uncertainty in the location of the thermocouple tip; however, they may be a rough measure of the bed and kiln wall surface temperatures in the front of the kiln.
- The temperature responses to pack combustion measured by the facility thermocouples are sinusoidal, and very smooth in contrast with the measured gas temperatures. Large thermowells and lack of radiation shielding on the facility thermocouples appear to explain the discrepancy.
- During these tests, the incinerator system met all state and federal regulations for each experimental condition.

The data presented in this paper will be used to calculate toluene evolution rates and mass balances in the companion paper [13] in this issue.

Acknowledgements

References

1 T.W. Lester, V.A. Cundy, A.M. Sterling, A.N. Montestruc, A. Jakway, C. Lu, C.B. Leger, D.W. Pershing, J.S. Lighty, G.D. Silcox and W.D. Owens, Rotary kiln incineration: comparison and scaling of field-scale and pilot-scale contaminant evolution rates from sorbent beds, Env. Sci. Technol., 25(6) (1991) 1142–1152.
2 V.A. Cundy, T.W. Lester, J.S. Morse, A.N. Montestruc, C. Leger, S. Acharya, A.M. Sterling and D.W. Pershing, Rotary kiln incineration I. An in depth study — Liquid injection, J. Air Pollut. Control Assoc., 39(1) (1989) 63–75.
3 V.A. Cundy, T.W. Lester, A.N. Montestruc, J.S. Morse, C. Leger, S. Acharya and A.M. Sterling, Rotary kiln incineration III. An in depth study — CCl₄ destruction in a full-scale rotary kiln incinerator, J. Air Pollut. Control Assoc., 39(7) (1989) 944–952.
4 V.A. Cundy, T.W. Lester, A.N. Montestruc, J.S. Morse, C. Leger, S. Acharya and A.M. Sterling, Rotary kiln incineration IV. An in depth study — Kiln exit and transition section sampling during CCl₄ processing, J. Air Pollut. Control Assoc., 39(8) (1989) 1073–1085.
5 T.W. Lester, V.A. Cundy, A.N. Montestruc, C.B. Leger, S. Acharya and A.M. Sterling, Dynamics of rotary kiln incineration of toluene/sorbent packs, Combust. Sci. Technol., 74(1–6) (1990) 67–82.
6 V.A. Cundy, T.W. Lester, A. Jakway, C.B. Leger, C. Lu, A.N. Montestruc, R. Conway and A.M. Sterling, Incineration of xylene/sorbent packs — A study of condition at the exit of a full-scale industrial incinerator, Environ. Sci. Technol., 25(2) (1991) 223–232.
7 V.A. Cundy, C. Lu, C.A. Cook, A.M. Sterling, C.B. Leger, A.L. Jakway, A.N. Montestruc, R. Conway and T.W. Lester, Rotary kiln incineration of dichloromethane and xylene — A comparison of incinerability characteristics under various operating conditions, J. Air Waste Manag. Assoc., 41(8) (1991) 1084–1094.

8   V.A. Cundy, T.W. Lester, C.B. Leger, A.N. Montestruc, G. Miller, S. Acharya, A.M. Sterling, J.S. Lighty, D.W. Pershing, W.D. Owens and G.D. Silcox, Rotary kiln inciner-ation — Combustion chamber dynamics, J. Hazardous Mater., 22(2) (1989) 195–219.

9   J.S. Lighty, R. Britt, D.W. Pershing, W.D. Owens and V.A. Cundy, Rotary kiln incineration II. Laboratory-scale desorption and kiln-simulator studies — Solids, J. Air Pollut. Control Assoc., 39(2) (1989) 187–193.

10 J.S. Lighty, G.D. Silcox, D.W. Pershing, V.A. Cundy and D.G. Linz, Fundamentals for the thermal remediation of contaminated soils — Particle and bed desorption models, Environ. Sci. Technol. 24(5) (1990) 750–757.

11 C.B. Leger, V.A. Cundy, A.M. Sterling, A.N. Montestruc and A.L. Jakway, Rotary kiln incineration of toluene on sorbent contained in plastic packs — System dynamics inferred from continuous O_2 measurements, Remediation, 1(3) (1991) 275–291.

12 C.B. Leger, A Study of Selected Phenomena Observed During Rotary Kiln Incineration, PhD Dissertation, Louisiana State University, Department of Mechanical Engineering, Baton Rouge, LA, August, 1992.

13 C.B. Leger, V.A. Cundy, A.M. Sterling, C.A. Cook, A.N. Montestruc, A.L. Jakway and W.D. Owens, Field-scale rotary kiln incineration of batch loaded toluene/sorbent. II. Mass balances, evolution rates, and bed motion comparisons, J. Hazardous Mater., 34 (1993) 31–50.

14 J.S. Morse, V.A. Cundy and C.B. Leger, Gas syringe sampling at very low pressure, Chromatographia, 32(11/12) (1991) 579–582.

Field-scale rotary kiln incineration of batch loaded toluene/sorbent. II. Mass balances, evolution rates, and bed motion comparisons

Christopher B. Leger[a], Charles A. Cook[a], Vic A. Cundy[a,*],
Arthur M. Sterling[b], Alfred N. Montestruc[a],
Allen L. Jakway[a] and Warren D. Owens[c]

[a] Mechanical Engineering Department and [b] Chemical Engineering Department,
Louisiana State University, Baton Rouge, LA 70803 (USA)
[c] Mechanical Engineering Department, The University of Utah, Salt Lake City,
UT 84112 (USA)

Abstract

A field-scale rotary kiln incinerator is used to obtain data on the processing of toluene contaminated sorbent contained in plastic packs. The solids bed in the kiln exhibited slipping motion during these experiments. Evolution rates for toluene are determined from experimental data, and cumulative evolution curves are generated. These cumulative evolution curves are very nearly approximated by an exponential function, and as such can be characterized by an exponential time constant. The average time constant for toluene evolution is 141 seconds. This time constant is not dependent upon either kiln rotation rate or turbulence air addition. Unmetered air infiltration was calculated to be between 2.8 and 3.5 times the metered air flow rates. Mass balances on the toluene are performed, yielding good results which are also independent of experimental conditions. The data suggest that stack oxygen concentrations and stack flow rates may be the preferred data for these purposes because they are monitored in existing rotary kiln incinerator facilities. A comparison of contaminant evolution during slipping and slumping bed motion is also discussed.

Introduction

An extensive study of an industrial scale rotary kiln incinerator is being conducted by a team of researchers from Louisiana State University and the University of Utah. The focus of the study is a 17 MW rotary kiln incinerator operated by the Louisiana Division of The Dow Chemical Company, in Plaquemine, LA. This facility has been described in several previously reported studies [1–6]. The experimental details of the most recent study

---

*To whom correspondence should be addressed.

described here, as well the entire data set obtained during this study, were presented by Leger et al. [7, 8]. In these experiments the kiln rotation rate was either 0.1 rpm or 0.25 rpm (slow or fast, respectively), and the kiln was operated with or without the addition of turbulence air (compressed air injected in the front of the kiln to induce mixing and swirl). The four experimental conditions (fast, turbulence air off; fast, turbulence air on; slow, turbulence air on; slow, turbulence air off) were repeated on a second day of testing. During each experimental condition, six plastic packs containing toluene-contaminated clay sorbent were incinerated, one every ten minutes. The transient responses measured throughout the incinerator system for the six packs were ensemble averaged to produce an average response for a single pack under each operating condition. These averaged responses are presented in a companion paper [8].

In previous studies [9, 10] continuous gas analyzers were used to monitor conditions only at the kiln exit. Contaminant evolution rates and mass balances were performed using these data, although some very restrictive assumptions were necessary. The primary difficulty was the use of measurements from only two points at the kiln exit to predict the overall species flow rates even though large gradients in species concentrations and temperature are known to exist there. A system of weighting factors was developed to assign a fraction of the overall flow to the concentrations measured at each probe location. Using these methods, mass balances obtained during operation without turbulence air were quite good. When turbulence air was added to the system, however, the mass balances were not as good.

From the previous work it became clear that measurements taken at the kiln exit, although informative, were not sufficient for calculating contaminant evolution rates and closing mass balances without making gross assumptions. The poor mixedness of the gas stream at the kiln exit does not allow one to calculate accurately the total flow rate of a species without measuring both the species concentration and the gas velocity at numerous locations over the exit cross-section. Otherwise, only gross assumptions about the species and flow distribution can be made. The need for better data with which to calculate contaminant evolution rates was one of the motivations for adding continuous measurements of O_2 and CO_2 in the afterburner and O_2 in the stack. The assumption of a well-mixed gas stream characterized by a uniform concentration of each gas species seems much more realistic at these locations. Measurements taken at a single location can then be used to calculate contaminant evolution rates and close mass balances without resorting to complicated weighting factor schemes. Thus, the techniques used in this work are similar to those used in the previous mass balance work, except for the use of different monitored variables and less restrictive assumptions.

In this paper, the averaged data from the companion paper [8] are used, together with input air and natural gas flow rates, to calculate the average leak air flow rates and the time dependent toluene evolution rates. Using these results, mass balances are performed and the characteristic times for toluene

evolution are determined. The first step in this process is to determine the baseline O_2 and CO_2 concentrations in the afterburner and the baseline O_2 concentration in the stack. These, together with the metered natural gas and air flow rates into the system, are then used to calculate the rate of air leakage into the system. The total air and natural gas flow rates, together with the stoichiometric equation for methane and air combustion, are used to calculate the total flow rate of combustion gas through the system (from the afterburners to the stack). Then, using the combustion stoichiometry of toluene and air, and the deviation of the O_2 and CO_2 concentrations from baseline, the time resolved toluene combustion rates are calculated. Integrating the toluene combustion rate over time, a mass balance on toluene is performed for the system. Using the cumulative toluene evolution curve, a characteristic time for the evolution process is determined. The toluene evolution rate curves are compared to the xylene evolution rate curves obtained earlier [9], and the differences, presumably caused by the different types of bed motion, are discussed. Finally, the implications of this work are summarized.

Baseline estimation and flow rate determination

The first step in calculating toluene evolution rates and performing toluene mass balances is to establish the gas flow rates in the system. Incinerator systems operate at a slight vacuum to prevent fugitive emissions; this causes unmetered air infiltration. Because air leakage into the system is not known explicitly, the flow rates must be established from experimental measurements of the baseline combustion products. The term "baseline" refers to the steady conditions existing in the incinerator system without any contaminant or pack combustion. The baseline levels of CO_2 and O_2 measured in the afterburner and stack are produced only by the natural gas and air introduced into the kiln and afterburner. Even when combustion of toluene perturbs these concentrations, they return to the baseline levels before the next pack is inserted. Figure 1 shows a typical ensemble averaged CO_2 trace from the afterburner. The peak in CO_2 due to toluene combustion is seen, as well as a drop in CO_2 mole fraction below baseline shortly before the combustion begins. This drop in CO_2 corresponds with the opening of the loading chute door in the kiln to insert the pack and the resulting inrush of leak air above the baseline flow rate. Although a double-door system is used during the loading process, the seal is imperfect. The CO_2 mole fraction approaches the baseline level before the loading chute door is opened, and it is seen to resume momentarily the baseline value after the loading chute door closes, but before toluene combustion begins. For this work, the baseline mole fraction of CO_2 or O_2 is the average of the values exhibited immediately before the loading chute door opens and immediately before pack combustion begins. This value is determined by first graphing the data, drawing a best estimate horizontal line through the data immediately before and after the loading chute door perturbation, and reading
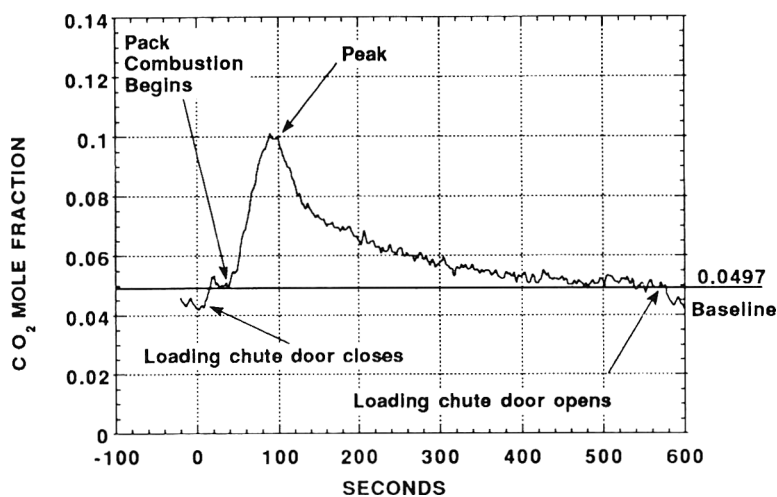
Fig. 1. Typical averaged CO_2 response curve showing important features and baseline. The data were obtained on 3 October 1990 during fast kiln rotation rate with no turbulence air addition.

the coordinate of this line from the vertical axis in terms of mole fraction. This line and the corresponding value are also shown in Fig. 1. Although this is a manual procedure, it is the most reliable method available and it is not entirely arbitrary thanks to the presence of the loading chute door perturbation that is used as a marker.

The following assumptions are made in determining the baseline air leak rate and the total flow rate:
1. The natural gas is assumed to be pure CH_4.
2. The CH_4 undergoes complete combustion with air, providing baseline levels of O_2 and CO_2 against which transients due to toluene combustion can be measured.
3. Combustion of all toluene in a pack is completed before the next pack is inserted 600 seconds later, so that baseline O_2 and CO_2 concentrations may be estimated at the beginning and end of each transient response.
4. No air leakage occurs downstream of the afterburner sampling location.
5. Metered air and natural gas flow rates, together with the calculated air leak rate, yield a total flow rate that is constant under baseline conditions. This assumption is known to be incorrect when the loading chute door is open; however, neither baseline values nor toluene evolution rates are calculated during that period of time.
6. The flow at the afterburner and stack locations is homogeneous with respect to the CO_2 and O_2 concentrations under baseline conditions. Thus, the measured concentrations are representative of the entire flow at these locations.

The following derivation is used to calculate the baseline air leak rate and the total flow rate, and the terms are defined in the glossary. The stoichiometry for complete CH_4 combustion with oxygen is given as:

$$CH_4 + 2O_2 \rightarrow CO_2 + 2H_2O \tag{1}$$

The combustion process for the kiln and afterburner together, under baseline conditions, may be represented by the following stoichiometric equation:

$$M_{CH_4}CH_4 + (M_{air} + M_{leak})(0.208O_2 + 0.792N_2) \rightarrow$$

$$M_{CH_4}CO_2 + 2M_{CH_4}H_2O + (M_{air} + M_{leak})(0.208O_2 + 0.792N_2) - 2M_{CH_4}O_2 \tag{2}$$
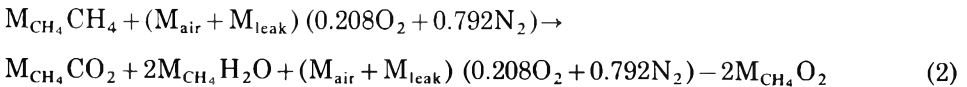
The total molar dry flow rate after the combustion process is obtained from the right hand side of eq. (2) by summing all coefficients except that for H_2O to yield:

$$M_{dry\ flow} = M_{air} + M_{leak} - M_{CH_4} \tag{3}$$

The dry flow rate is of interest because the instruments used to measure the CO_2 and O_2 concentrations required dry gas samples. From the stoichiometric coefficient for the CO_2 produced in eq. (2), and by using eq. (3) for the total molar flow rate of products, the mole fraction of CO_2 in the products on a dry basis is:

$$[CO_2] = M_{CH_4}/(M_{air} + M_{leak} - M_{CH_4}) \tag{4}$$

Here the bracketed species, $[CO_2]$, indicates dry mole fraction. Solving eq. (4) for the air leak rate yields:

$$M_{leak} = M_{CH_4}(1 + 1/[CO_2]) - M_{air} \tag{5}$$

An alternative approach for determining the air leak rate is to solve eq. (2) in terms of the O_2 mole fraction on a dry basis. The result is:

$$[O_2] = (0.208(M_{air} + M_{leak}) - 2M_{CH_4})/(M_{air} + M_{leak} - M_{CH_4}) \tag{6}$$

Equation (6) is then solved for the air leak rate as:

$$M_{leak} = M_{CH_4}(2 - [O_2])/(0.208 - [O_2]) - M_{air} \tag{7}$$

Equation (5) may be used to calculate the baseline leak rate of air using metered flow rates and the baseline CO_2 mole fraction measured at the afterburner. Equation (7) will also yield the baseline leak rate of air; it can be applied using either the baseline O_2 mole fraction measured in the afterburner or measured in the stack. Regardless of the method used to calculate the leak rate of air, eq. (3) gives the total dry molar flow rate through the system at either the afterburner sampling location or the stack.

Table 1 shows the metered air and natural gas flow rates, as well as the measured baseline mole fractions of CO_2 and O_2 at the afterburner and stack, for each operating condition and date. In the table, the experimental conditions are abbreviated, so that the condition of "fast kiln rotation rate with

TABLE 1

Natural gas and air flow rates, and measured baseline mole fractions of O_2 and CO_2 as a function of experimental conditions (fast or slow kiln rotation rate, turbulence air on or off, data taken on 3, 4 October 1990)

Experimental condition	Natural gas M_{CH_4}[a]	Metered Air M_{air}[a]	$[O_2]$[b] Afterburner	$[CO_2]$[b] Afterburner	$[O_2]$[b] Stack
Fast off 3	840	4200	0.123	0.050	0.132
Fast off 4	870	4480	0.130	0.045	0.127
Fast on 3	1060	6610	0.133	0.043	0.134
Fast on 4	1060	7450	0.136	0.044	0.136
Slow off 3	870	3920	0.116	0.053	0.127
Slow off 4	860	4480	0.125	0.049	0.127
Slow on 3	1060	6570	0.132	0.039	0.134
Slow on 4	1050	7450	0.137	0.040	0.135

[a] Standard cubic meters per hour. To obtain kmol/s, multiply by 1.24×10^{-5}.
[b] Measured baseline mole fraction.

turbulence air off on 3 October 1990" becomes "Fast Off 3". Notice that when the turbulence air is on, the natural gas flow rate is increased, and the metered air flow (which includes both the burner air and the turbulence air) is also increased. This increase in natural gas input is required to heat the added cool turbulence air to maintain the system operating temperature according to the facility thermocouple located at the kiln exit. The values given in Table 1 are those necessary to solve for leak air flow rates using eqs. (5) or (7).

Table 2 shows the leak air flow rate calculated using each approach, and the resulting total flow rate using each leak rate. These total dry flow rate calculations are based upon:
1. Leak rate estimated from baseline afterburner O_2 mole fraction,
2. Leak rate estimated from baseline afterburner CO_2 mole fraction,
3. Leak rate estimated from baseline stack O_2 mole fraction, and
4. Total flow rate correlated from pressure across the induced draft fan at the stack.
Observe that the calculated leak rates are very large; for operation with turbulence air off the leak air flow rate averaged 3.5 times the metered air flow rate, while for operation with turbulence air on the ratio is 2.8. The total dry flow rates calculated from the three leak air flow rates agree rather well; however, the dry flow rate measured across the induced draft fan, even after correction for density and moisture, is generally higher.

Toluene evolution rates

Once the total flow rates and baseline values for O_2 and CO_2 concentrations have been established, the rate of toluene combustion as a function of time may

TABLE 2

Leak air flow rates and total dry flow rates of combustion products as a function of experimental condition and calculation method

Experimental condition	Calculated leak air flow M_{leak} [a]			Calculated total dry flow $M_{dry\,flow}$ [a]			Measured Dry flow [c]
	AB[b] O_2	AB[c] CO_2	Stack[d] O_2	AB[b] O_2	AB[c] CO_2	Stack[d] O_2	$M_{dry\,flow}$ [a]
Fast off 3	14300	13500	16300	17700	16900	19700	25300
Fast off 4	16200	15600	15500	19900	19200	19100	24900
Fast on 3	19600	19200	20000	25100	24700	25600	29800
Fast on 4	20000	17700	19800	26400	24100	26200	30500
Slow off 3	13900	13300	16100	16900	16300	19200	25000
Slow off 4	14900	13800	15500	18600	17500	19100	25400
Slow on 3	19300	21200	19900	24800	26700	25400	29600
Slow on 4	20300	20000	19500	26700	26400	25900	30700

[a] Standard cubic meters per hour. To obtain kmol/s, multiply by 1.24×10^{-5}.
[b] Based upon baseline afterburner O_2 mole fraction.
[c] Based upon baseline afterburner CO_2 mole fraction.
[d] Based upon baseline stack O_2 mole fraction.
[e] Total dry flow rate correlated from pressure rise across the induced draft fan.

be calculated. The following additional assumptions are necessary before proceeding:
1. The toluene undergoes complete combustion, forming CO_2 and H_2O, and consuming O_2. Concentrations of incomplete combustion products such as CO, hydrocarbons, and soot are negligible.
2. The perturbation of the measured CO_2 and O_2 mole fractions caused by combustion of the plastic pack itself is negligible [7].
3. The flow at the afterburner and stack locations remains homogeneous with respect to the CO_2 and O_2 concentrations during the combustion of toluene in the kiln.
4. The combustion of toluene has only a negligibly small effect on the dry gas flow rate at the afterburner and stack. In other words, the flow rates calculated from baseline conditions remain representative during the combustion of toluene [10].
5. There is no delay between the evolution of toluene from the sorbent and its subsequent combustion, making the evolution rate of toluene equal to the calculated rate of toluene combustion.

The rate of toluene combustion can be calculated from the measured response of the CO_2 mole fraction in the afterburner or the O_2 mole fraction in the afterburner or the stack. The deviation of the CO_2 or O_2 concentrations from baseline values represents the effect of toluene combustion. The

stoichiometry for complete toluene combustion is:

$$C_7H_8 + 9O_2 \rightarrow 7CO_2 + 4H_2O \tag{8}$$

Thus for every mole of toluene burned, 7 moles of CO_2 are formed and 9 moles of O_2 are consumed. On the basis of measured CO_2 mole fraction, we can then express the toluene combustion rate (in kmol/s) as:

$$M_{C_7H_8} = [([CO_2] - [CO_2]_{baseline})M_{dry\ flow}]/(7 \times 3600) \tag{9}$$

Similarly, the toluene combustion rate based upon measured O_2 mole fraction is:

$$M_{C_7H_8} = [([O_2] - [O_2]_{baseline})M_{dry\ flow}]/(9 \times 3600) \tag{10}$$

Note that since the CO_2 and O_2 concentrations were measured as a function of time, eqs. (9) and (10) can be applied to give toluene evolution rates as a function of time.

As seen in Table 2, there are four ways to obtain the total dry flow rate (calculation based upon measured afterburner CO_2 mole fraction, calculation based upon measured afterburner O_2 mole fraction, calculation based upon measured stack O_2 mole fraction, and direct measurement from pressure drop across the induced draft fan). Similarly there are three ways to calculate the toluene evolution rate (based upon the mole fraction response of the after-burner CO_2, afterburner O_2, and stack O_2) once the total dry flow rate is specified. This yields 12 possible combinations of flow rate and species response to calculate toluene evolution rate. To reduce the number of combinations, the flow rate and species response methods were grouped in a logical manner. The same data that were used for the total dry flow rate calculation were also used for the toluene evolution rate calculation. Ultimately, four toluene evolution calculation approaches were compared. They are:

1. The dry flow rate, obtained from eq. (7) using the baseline afterburner O_2 mole fraction. is used in eq. (10) together with the response of the after-burner O_2 mole fraction to obtain the toluene evolution rate.
2. The dry flow rate calculated using eq. (5) from the afterburner CO_2 baseline mole fraction is used in eq. (9) to obtain the toluene evolution rate.
3. The dry flow rate, obtained from eq. (7) using the baseline stack O_2 mole fraction, is used in eq. (10) together with the response of the stack O_2 mole fraction to obtain the toluene evolution rate.
4. The dry flow rate from the induced draft fan measurement is used in eq. (10) together with the stack O_2 mole fraction response to give a fourth estimate of the toluene evolution rate.

Figure 2 shows the resulting toluene evolution rate calculated using method (1) from the CO_2 mole fraction curve shown in Fig. 1. The toluene evolution rate is normalized by the total amount of toluene initially present in a pack. Notice that the time dependent toluene evolution rate curve is directly related to the CO_2 mole fraction curve. Very similar results are obtained using the O_2 concentrations measured in the afterburner and stack. Since the time
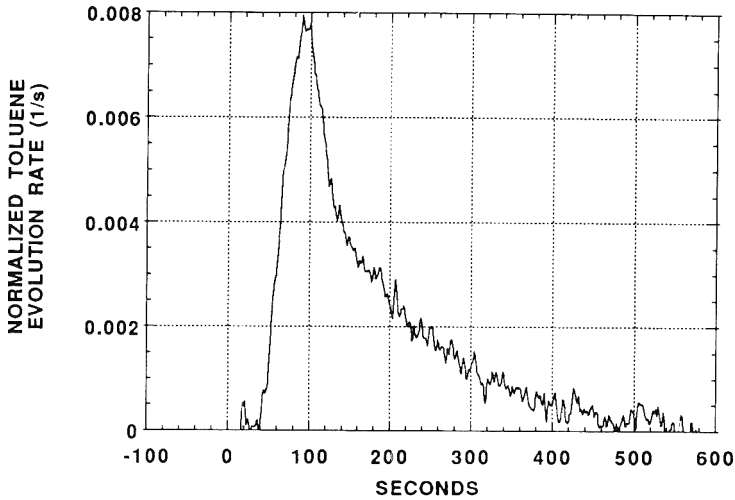
Fig. 2. Normalized toluene evolution rate (with respect to the total amount of toluene initially present in a pack) obtained from the afterburner CO_2 response shown in Fig. 1.

dependent toluene evolution rate curves are intermediate results, they are not all shown. However, the toluene evolution curves obtained from the afterburner CO_2 data are presented later in this paper for comparisons with xylene evolution curves from Lester et al. [9].

Toluene mole closure

Once the instantaneous toluene evolution rates are obtained, the calculation of mole balances on toluene is straightforward. One must simply integrate the toluene evolution rates over time to obtain the cumulative toluene evolution. The toluene evolution rate always return to zero within 600 seconds, so the cumulative toluene evolution should always approach the total moles of toluene initially present in a single pack. The cumulative toluene evolution curves generated from the afterburner CO_2 data and normalized by the total moles of toluene initially present in a pack are shown in Fig. 3. Similar curves were generated based on the afterburner and stack O_2 responses.

Each toluene-laden pack incinerated in the system contained 0.178 kmol of toluene. The final values of calculated cumulative toluene evolution were normalized, dividing by 0.178 kmol to obtain the closure on toluene. This mole closure is expressed as the ratio of calculated toluene evolution to the toluene content of a single pack. The calculated fractional toluene closures are given in Table 3 for each method of calculation and each operating condition. These fractional toluene closures are also shown graphically in Fig. 4 for each calculation method and operating condition. Overall, the toluene closure is
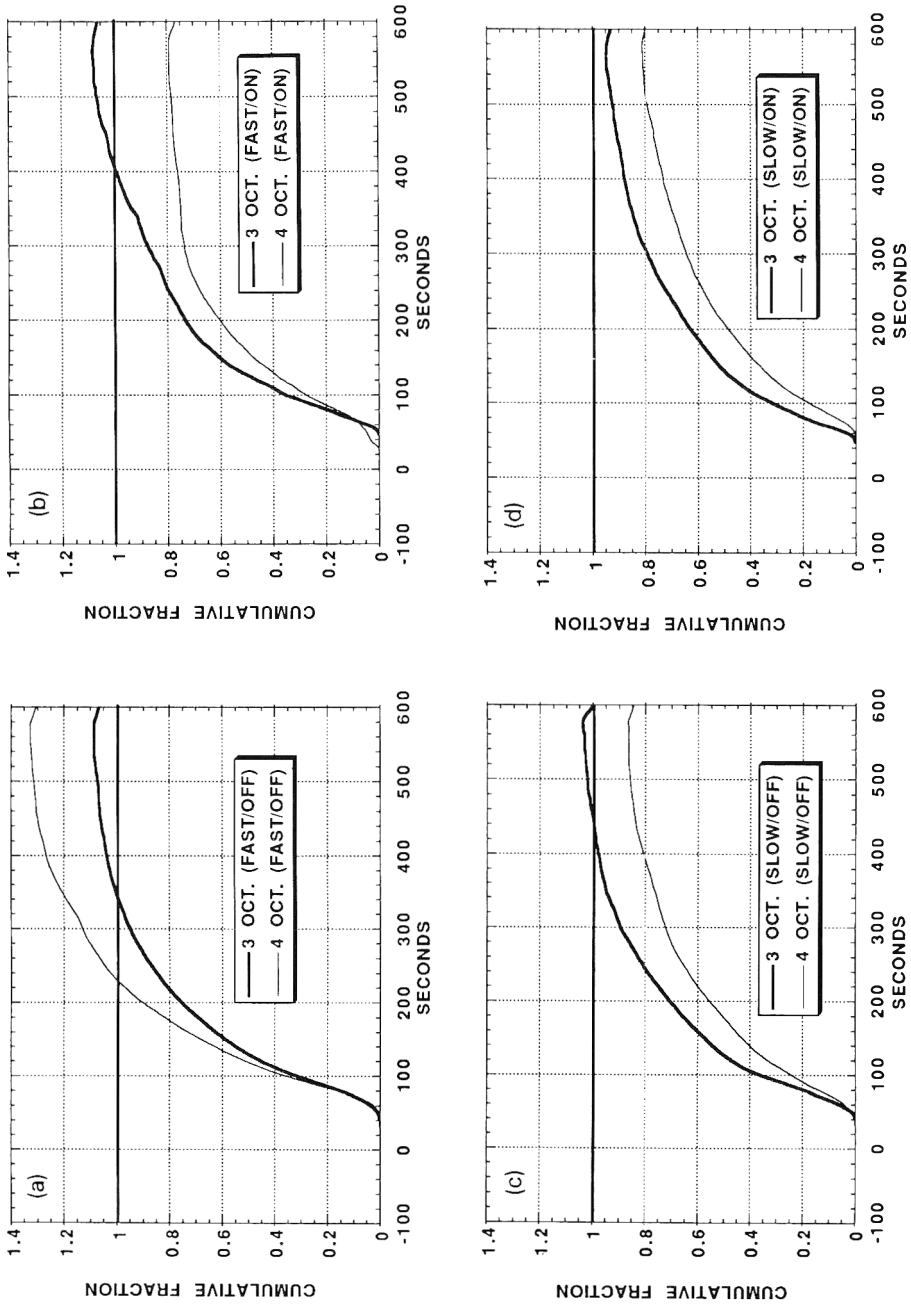
Fig. 3. Normalized cumulative toluene evolution (with respect to the total amount of toluene initially present in a pack) as a function of experimental conditions. Fast kiln rotation (a) without, and (b) with turbulence air (TA); and (b) with turbulence air (TA). Slow kiln rotation (c) without, and (d) with turbulence air (TA).

TABLE 3

Toluene mass closure fraction obtained for each experimental condition for each calculation method. See also Fig. 4

Experimental condition	Toluene closure				Average	Standard deviation
	$AB O_2$[1]	$AB CO_2$[2]	Stack O_2[3]	Stack flow[4]		
Fast off 3	0.90	1.09	0.76	0.98		
Fast off 4	1.13	1.33	0.84	1.10	1.02	0.18
Fast on 3	0.97	1.08	0.88	1.03		
Fast on 4	0.73	0.79	0.92	1.07	0.93	0.13
Slow on 3	0.54	0.95	0.78	0.90		
Slow on 4	0.57	0.81	0.63	0.75	0.74	0.15
Slow off 3	0.80	1.04	0.73	0.95		
Slow off 4	0.79	0.87	0.59	0.79	0.82	0.14
Average	0.80	0.99	0.77	0.95	0.88[a]	
Standard dev.	0.20	0.18	0.12	0.13		0.18[a]

[1] Using the afterburner O_2 mole fraction for total flow rate and toluene evolution rate.
[2] Using the afterburner CO_2 mole fraction for total flow rate and toluene evolution rate.
[3] Using the stack O_2 mole fraction for total flow rate and toluene evolution rate.
[4] Using the total dry flow rate measured in the stack together with the stack O_2 mole fraction to get toluene evolution rate.
[a] Average and standard deviation of all 32 values of toluene closure.
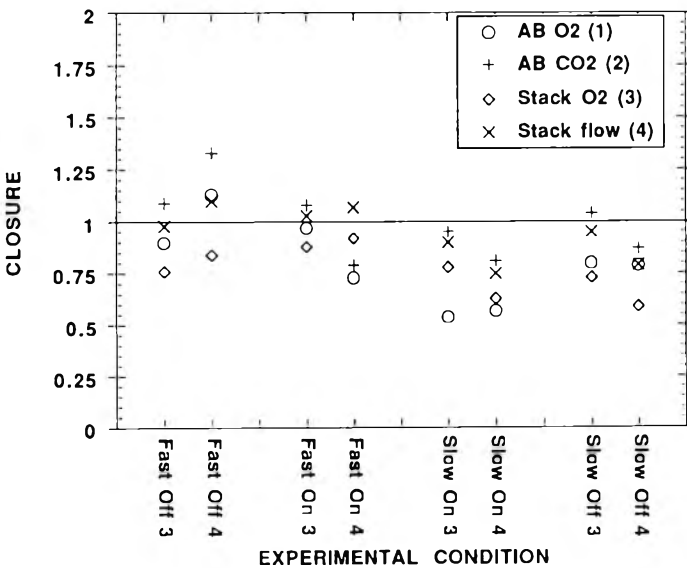
Fig. 4. Mole closures on toluene as a function of operating condition and calculation method. Parenthetical numbers in key correspond with those in Table 3.

quite good considering the nature of these experiments. Table 3 also shows the average toluene closures for each calculation method and experimental condition, and the standard deviation of these values. Based on the data of Table 3, the overall average toluene closure is 88% and the overall standard deviation of the data is 18%. An analysis of variance (ANOVA) test showed that the variation of toluene closure between consecutive days was not statistically significant (99% significance level). The variation in toluene closure as a function of turbulence air addition was also not statistically significant. The variation between calculation methods was significant as was the influence of rotation rate. Although the calculation methods influence closure, the results of one method can not be selected over another. While we intuitively agree that calculation method will have an influence on calculated mass closure, it was unexpected that kiln rotation rate would influence mass closure. Changing the kiln rotation rate from fast to slow caused a decrease in average mass closure from 98% to 78%. The reason for this influence remains unclear.

In earlier studies on xylene and dichloromethane using measurements at the kiln exit only [9, 10], closure was not good during operation with turbulence air addition. Since this dependence was not observed in the current experiments, poor closure with turbulence air addition in previous work may have occurred because the turbulence air influenced the quality of the assumptions used in the analysis and not because the ultimate evolution of each species was reduced.

Characteristic time for evolution

In previous work [9, 10] the time necessary for the contaminant to evolve was characterized by the evolution interval, defined as the time required for the middle 80% of the ultimate contaminant evolution to occur. This definition was used because the cumulative evolution curves tended to be irregular, particularly near the beginning and end, due to pack breakdown and bed motion effects. From Fig. 3 one observes that the shape of the cumulative evolution curve for toluene from a slipping bed is very smooth and repeatable for all the data. In fact, the cumulative evolution curves for toluene shown in Fig. 3 can be closely approximated by an exponential function, with the exponential time constant representing the characteristic time for contaminant evolution. If the cumulative evolution curves of Fig. 3 are normalized by their final values, yielding $N_{C_7H_8}(t)$, the resulting curves will begin at 0, approach 1 at the end, and can be readily fit by the expression:

$$N_{C_7H_8}(t) = 1 - \exp(-t/\tau) \tag{11}$$

Figure 5 shows the application of eq. (11) to fit a typical normalized cumulative evolution curve, with a resulting evolution time constant of 120 seconds.

Since the data have been normalized and only the time constant is being extracted, the results are only dependent upon the species response used. In
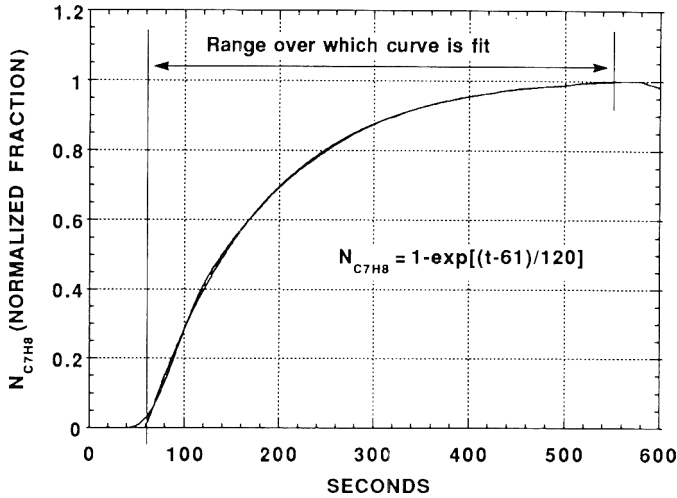
Fig. 5. Typical cumulative evolution curve. The fitted curve follows the data very closely over the range of the fit. Data was obtained on 3 October 1990 from the afterburner CO_2 response at fast rotation with no turbulence air addition (the same data used in Figs. 1 and 2).

other words, differences in the total dry flow rate are normalized out, and there are only three remaining independent normalized evolution rate calculation methods (based upon afterburner O_2 response, afterburner CO_2 response, and stack O_2 response). The cumulative evolution curves obtained from these three methods are fit using eq. (11), and the resulting time constants are given in Table 4 and shown in Fig. 6. Table 4 also shows the averages and standard deviations of the time constants over the four experimental conditions and over the three calculation methods. The overall average time constant for contaminant evolution is 141 seconds, with a standard deviation of 23 seconds. Statistical analysis (ANOVA) showed that the time constants were independent of either the kiln rotation rate or turbulence air addition. This is very different from previous studies on xylene and dichloromethane, where both experimental variables were seen to influence the evolution interval. Figure 6 also shows that the use of stack O_2, afterburner O_2, or afterburner CO_2 in the calculations had no clear effect on the evolution time constant, although the use of afterburner O_2 caused more scatter in the results than did the others.

From the comparisons between calculation methods for obtaining toluene closure and evolution time constants, no single calculation method stands out as clearly better than the others. However, the calculation methods are not equivalent in terms of measurement and calculation difficulty. Measurement of the O_2 and CO_2 concentrations at the afterburner location is far more difficult than at the stack location. Using these measurements to calculate air leak rates is also somewhat troublesome. Furthermore, the total dry flow rate is simply measured at the stack. The simplest method for obtaining toluene

TABLE 4

Evolution time constants for each experimental condition and calculation method. See also Fig. 6

Experimental condition	Time constant (seconds)			Average	Standard deviation
	$AB\,O_2{}^a$	$AB\,CO_2{}^b$	Stack $O_2{}^c$		
Fast off 3	137	120	117		
Fast off 4	141	127	143	131	11
Fast on 3	190	140	155		
Fast on 4	116	103	129	139	31
Slow on 3	95	138	162		
Slow on 4	141	160	153	142	25
Slow off 3	157	130	128		
Slow off 4	183	151	158	151	20
Average	145	134	143	141[d]	
Standard dev.	32	18	17		23[d]

[a] From the afterburner O_2 mole fraction response.
[b] From the afterburner CO_2 mole fraction response.
[c] From the stack O_2 mole fraction response.
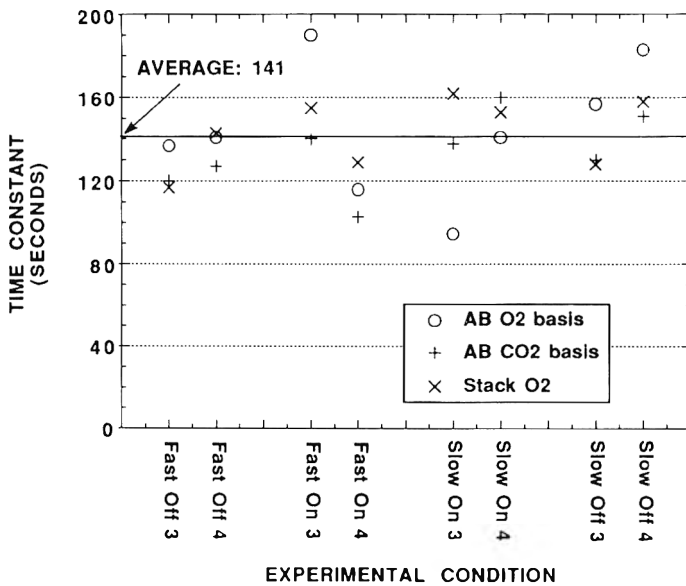[d] Average and standard deviation of all 24 values of the time constant.

Fig. 6. Evolution time constants as a function of operating condition and originating data. (See Table 4.)

evolution rates, therefore, is to use the stack O_2 measurements together with flow rates obtained from the induced draft fan at the stack (calculation method 4). Capability for obtaining both of these measurements (stack O_2 and stack flow rate) is standard on rotary kiln incinerator facilities since these data are routinely used to certify that the system is operating within permit guidelines. Since the waste evolution rates obtained with these measurements (calculation method 4) are equivalent to those obtained with the other methods, future evolution rate characterization studies could make use of existing facility instrumentation for waste evolution rate calculations.

The effects of bed motion on evolution rate

As discussed in the companion paper [8], the bed of solids was exhibiting slipping motion during the toluene experiments, in contrast to the slumping motion observed previously during the xylene experiments [9]. This difference in bed motion regime is a result of either the presence of a thermocouple in the solids bed, or a change in the surface roughness of the slag-coated rotary kiln walls. In the slumping motion regime, solids intermittently tumble down the free surface of the bed, and then follow the wall in a layer below the surface before reemerging to tumble across the surface again. This motion causes the solids to mix, and each part of the bed is repeatedly exposed at the surface. During the toluene experiments, the bed exhibited a slipping motion. With this type of motion, the entire bed slips relative to the wall, and it essentially moves as if it were a solid piece, with the same particles remaining on the surface. In the slipping bed motion regime, the solids mix very slowly. The differences in the bed motion regimes preclude the use of this toluene data in the scaling analysis presented by Lester et al. [9] as was originally intended. It does, however, allow a comparison of evolution characteristics between slipping and slumping beds. Toluene and xylene have similar physical and combustion characteristics, and the experimental conditions were very similar for each contaminant. Since the only major difference between the experiments was the bed motion, comparisons between the xylene and toluene evolution behavior should show the influence of bed motion.

The toluene and xylene evolution rate data are shown in Fig. 7 for the four operating conditions. The normalized toluene evolution rates obtained from the afterburner CO_2 are shown. Each graph also contains the normalized xylene evolution rate obtained from ensemble averaged CO_2 measurements at the kiln exit using CO_2 weighting factors [9]. All the evolution curves are normalized so that the integral of the curve over time is unity.

The toluene data show good overall repeatability between the duplicate tests at each operating condition, although the magnitude of the initial spike in evolution shows some variation. For all operating conditions, the toluene evolution curves show essentially the same behavior: a quick rise to the maximum followed by a gradual decay back to the baseline. In contrast, the
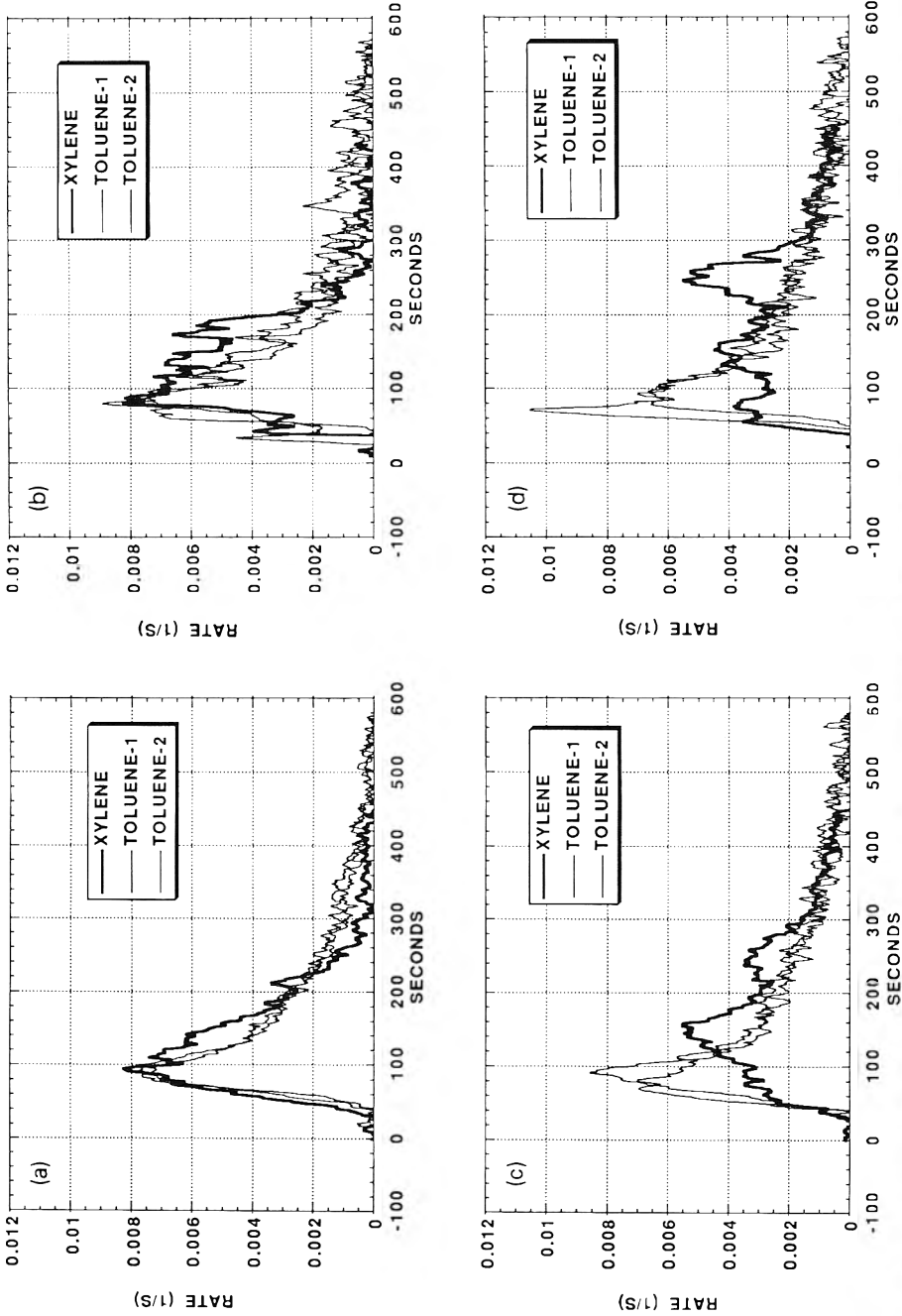
Fig. 7. Comparison of normalized evolution rates for slipping bed (toluene from this study) and a slumping bed (xylene from Lester et al. [9]). For the toluene, replicates obtained from 3 and 4 October 1990 are included (thin lines). Fast kiln rotation (a) without, and (b) with turbulence air. Slow kiln rotation (c) without, and (d) with turbulence air.

xylene evolution curves show a broader maximum followed by a rapid decline. Also, the xylene data show a marked difference between fast and slow kiln rotation rates, with the slow rotation rate resulting in a much broader, less intense period of evolution. The xylene data for the slow rotation rate show three distinct evolution peaks in each case, with a separation of approximately 80 seconds between the peaks. This separation appears to correspond with the time necessary for a particle to circulate through the bed and return to the surface. None of this behaviour is observed in the toluene evolution data.

From the comparisons between evolution for a slipping bed and a slumping bed, some practical observations can be made. First, the evolution behavior observed from the slumping bed is generally better from a kiln operational perspective because of the broader, less intense waste evolution, with less propensity for causing transient "puffs", as defined by Linak et al. [11]. This difference in evolution behavior may be caused primarily by the action of the hot, clean sorbent material present in the kiln from previous packs. During slumping bed motion, the preexisting bed material repeatedly buries the fresh charge from a new pack. This appears to cause an increased resistance to mass transfer from the buried charge, and possibly reduces the rate of heat transfer to the buried charge as well, resulting in a decline in evolution rate. When the fresh charge is reexposed due to circulation of the bed, the evolution rate increases again. This is in contrast to the slipping bed case, where apparently the fresh charge is never buried by preexisting bed materials but rather lies on top of these materials. For volatile wastes such as toluene and xylene, the slipping bed motion is much less preferable because it causes higher peak evolution rates which could, if the magnitude is great enough, lead to a transient "puff". However, if the waste is much less volatile or if it is present in low concentrations, a slipping bed motion may be acceptable because rapid evolution of the waste is unlikely. For these wastes, a slipping bed motion may even be advantageous because the contaminated solids do not become buried in the bed, and so could theoretically be cleaned of their hazardous components more rapidly.

Leger et al. [8] observe that the type of bed motion exhibited may be controllable by the drag exerted by stationary protuberances extending into the bed, or by controlling the roughness of the kiln's inner walls. In addition to hazardous waste, this has important implications in remediation of contaminated soil in rotary-type units. Depending on the level of contamination, moisture content, and the soil type, one bed motion may be preferred to another. This study has shown that, to some degree, control over the bed motion may be possible using techniques not previously considered. More extensive work is needed to better characterize the controllability of bed motion and its effects on a variety of waste/soil materials in field-scale rotary units.

Summary and conclusions

In this study, a field-scale rotary kiln incinerator is used to obtain data on the processing of toluene contaminated sorbent contained in plastic packs. The

incinerator is probed in several different locations with instruments which continuously monitor species concentrations, temperatures, and pressures. Visual observations indicate that the bed exhibited slipping motion during these experiments. Evolution rates for toluene are determined from experimental data, and cumulative evolution curves are generated. These cumulative evolution curves are very nearly approximated by an exponential function, and as such can be characterized by an exponential time constant. The time constants for toluene evolution average 141 seconds and are not dependent upon either kiln rotation rate or turbulence air addition. Air leak rates into the system are calculated to be between 2.8 and 3.5 times the metered air flow rates. Mass balances on the toluene yielded good results, although slower kiln rotation rate appears to decrease the mass closure. Evolution time constants and toluene closure calculations were comparable regardless of the calculation method used. This suggests that stack oxygen concentrations and stack flow rates may be the preferred data for these purposes because they are monitored in existing rotary kiln incinerator facilities.

Comparisons with evolution data taken previously suggest that the slipping bed motion exhibited during these toluene tests caused the toluene evolution rate (as measured by the evolution time constant) to be independent of kiln rotation rate. The slumping motion exhibited during earlier xylene tests apparently restricted mass transfer thus causing the xylene evolution to occur over a longer time with lower peak evolution rates. From an operational perspective, the slumping motion may be preferable for high concentration volatile wastes because it results in a more steady waste evolution. However, for low volatility wastes or low concentration wastes, the slipping bed motion may be advantageous by reducing the mass transfer resistance thus reducing the time to remove the waste from the solids. More work needs to be done to address these possibilities.

Acknowledgements

Nomenclature

$CH_4, O_2, CO_2,$ H_2O, C_7H_8	methane, oxygen, carbon dioxide, water, and toluene species, respectively, used in stoichiometric equations.
$[O_2], [CO_2]$	measured mole fraction of oxygen and carbon dioxide on a dry basis as a function of time.
$[O_2]_{baseline},$ $[CO_2]_{baseline}$	measured mole fraction of oxygen and carbon dioxide on a dry basis under baseline conditions (no waste combustion).
M_{CH_4}	metered molar flow rate of methane into the kiln and afterburner. (kmol/s)
M_{air}	metered molar flow rate of air into the kiln and afterburner. (kmol/s)
M_{leak}	molar flow rate of air leaking into the kiln and afterburner. (kmol/s)
$M_{dry\,flow}$	total molar flow rate of all product species except water. (kmol/s)
$M_{C_7H_8}$	molar flow rate of toluene evolution from the sorbent. (kmol/s)
$N_{C_7H_8}(t)$	molar evolution rate of toluene at time t, normalized by 0.178 kmol. (1/s)

References

1 V.A. Cundy, T.W. Lester, J.S. Morse, A.N. Montestruc, C. Leger, S. Acharya, A.M. Sterling and D.W. Pershing, Rotary kiln incineration I. An in depth study — Liquid injection, J. Air Pollut. Control Assoc., 39(1) (1989) 63–75.
2 V.A. Cundy, T.W. Lester, A.N. Montestruc, J.S. Morse, C. Leger, S. Acharya and A.M. Sterling, Rotary kiln incineration III. An in depth study — CCl₄ Destruction in a full-scale rotary kiln incinerator, J. Air Pollut. Control Assoc., 39(7) (1989) 944–952.
3 V.A. Cundy, T.W. Lester, A.N. Montestruc, J.S. Morse, C. Leger, S. Acharya and A.M. Sterling, Rotary kiln incineration IV. An in depth study — Kiln exit and transition section sampling during CCl₄ processing, J. Air Pollut. Control Assoc., 39(8) (1989) 1073–1085.

4   V.A. Cundy, T.W. Lester, C.B. Leger, A.N. Montestruc, G. Miller, S. Acharya, A.M. Sterling, J.S. Lighty, D.W. Pershing, W.D. Owens and G.D. Silcox, Rotary kiln incineration — Combustion chamber dynamics, J. Hazardous Mater., 22(2) (1989) 195–219.

5   V.A. Cundy, T.W. Lester, A. Jakway, C.B. Leger, C. Lu, A.N. Montestruc, R. Conway and A.M. Sterling, Incineration of xylene/sorbent packs — A study of conditions at the exit of a full-scale industrial incinerator, Environ. Sci. Technol., 25(2) (1991) 223–232.

6   V.A. Cundy, C. Lu, C.A. Cook, A.M. Sterling, C.B. Leger, A.L. Jakway, A.N. Montestruc, R. Conway and T.W. Lester, Rotary kiln incineration of dichloromethane and xylene — A comparison of incinerability characteristics under various operating conditions, J. Air Waste Manag. Assoc., 41(8) (1991) 1084–1094.

7   C.B. Leger, V.A. Cundy, A.M. Sterling, A.N. Montestruc and A.L. Jakway, Rotary kiln incineration of toluene on sorbent contained in plastic packs — System dynamics inferred from continuous O_2 measurements, Remediation, 1(3) (1991) 275–291.

8   C.B. Leger, V.A. Cundy, A.M. Sterling, A.N. Montestruc, A.L. Jakway and W.D. Owens, Field-scale rotary kiln incineration of batch loaded toluene/sorbent-I: Data analysis and bed motion considerations, J. Hazardous Mater., 34 (1993) 1–29.

9   T.W. Lester, V.A. Cundy, A.M. Sterling, A.N. Montestruc, A. Jakway, C. Lu, C.B. Leger, D.W. Pershing, J.S. Lighty, G.D. Silcox and W.D. Owens, Rotary kiln incineration: Comparison and scaling of field-scale and pilot-scale contaminant evolution rates from sorbent beds, Environ. Sci. Technol., 25(6) (1991) 1142–1152.

10 C.A. Cook, V.A. Cundy, A.M. Sterling, C. Lu, A.N. Montestruc, C.B. Leger and A.L. Jakway, Estimating dichloromethane evolution rates from a sorbent bed in a field-scale rotary kiln incinerator, Combust. Sci. Technol., 85(1–6) (1992) 217–241.

11 W.P. Linak, J.D. Kilgore, J.A. McSorley, J.O.L. Wendt and J.E. Dunn, On the occurrence of transient puffs in a rotary kiln incinerator simulator: I. Prototype solid plastic wastes, J. Air Pollut. Control Assoc., 37(1) (1987) 54–65.

Factors affecting wet air oxidation of TNT red water: Rate studies

Oliver J. Hao[a,*], Kotu K. Phull[a,b], Jin M. Chen[a], Allen P. Davis[a] and Stephen W. Maloney[c]

[a] *Department of Civil Engineering, University of Maryland, College Park, MD 20742 (USA)*
[b] *U.S. Army Toxic and Hazardous Materials Agency, Aberdeen Proving Ground, MD 21010 (USA)*
[c] *Construction Engineering Research Laboratory, U.S. Army Corps of Engineers, Champaign, IL 61826 (USA)*

Abstract

Preliminary experiments have demonstrated wet air oxidation (WAO) to be feasible for TNT red water treatment. This paper presents the results of rate studies for the evaluation of temperature, partial oxygen pressure P_{O_2}, initial red water concentration, salt concentration, and catalyst/initiator addition on WAO performance. Results show the WAO efficiency to be a function primarily of temperature, and to a lesser extent, the initial P_{O_2}. A significant initial (usually <5 minutes) rapid reduction in total organic carbon (TOC) or chemical oxygen demand (COD) is observed in all experiments. The extent of reduction varies with the experimental conditions: the harsher the condition, the higher the initial reduction. At lower temperatures, the subsequent WAO of red water proceeds as a first-order reaction with respect to TOC or COD. Under harsher temperature conditions, the reaction follows two distinct first-order phases. High salt concentrations (Na_2SO_4 and $NaNO_3$) slightly enhanced the overall oxidation. Addition of Cu(II) as a catalyst results in rate enhancement. Several issues regarding application of WAO are discussed.

Introduction

The 2,4,6-trinitrotoluene (α-TNT) is the most widely used military explosive. Crude TNT produced from a three-stage nitration of toluene contains 4 to 5% unsymmetrical TNT isomers, which must be removed in order to meet military specifications. Sodium sulfite is added to crude TNT to produce dinitrotoluene (DNT) sulfonates by selectively reacting with the undesirable TNT isomers (e.g., 2,4,5-TNT). The dinitrotoluenesulfonates (DNTS') so formed (e.g., 2,4-DNT-5-SO_3Na) are water-soluble and are easily separated from the sparingly

---

*To whom correspondence should be addressed.

soluble α-TNT. After phase separation, the wastewater has an intense red color and is commonly referred to as "red water." In addition to the DNTS′, red water also contains products of incomplete nitration (e.g., priority pollutants 2,4-DNT and 2,6-DNT) and complex byproducts formed during the nitration and purification stages. A typical red water composition is shown in Table 1. Currently, red water is classified by the U.S. Environmental Protection Agency (EPA) as a RCRA-regulated hazardous waste based on its reactivity.

Based on a recent report by PEI [1] indicating that WAO (wet air oxidation) was one of the promising technologies for hazardous waste treatment, a study was initiated to evaluate WAO for red water treatment. WAO is the oxidation of soluble or suspended oxidizable materials using air or pure oxygen in an

TABLE 1

Red water composition [2][a]

Parameter	Value
pH, units	7.6
Sp. Gravity	1.0
Solids	
Total	2840
Volatile	1020
Fixed	1820
% Organics	36
Inorganic salts	
$[NaNO_2]$	209
$[NaNO_3]$	0
$[Na_2SO_3]$	55
$[Na_2SO_4]$	514
$[Na_2SO_3 + Na_2SO_4]$	569
Alkalinity	
(as $[CaCO_3]$)	43
Organic content	
COD	685
TOC	544
Nitrobodies	
α-TNT	2.27
2,4-DNT	0.21
2,6-DNT	0.03
1,3,5-TNB	3.10
DNTS′[b]	
2,4-DNT-3-SO_3Na	272
2,4-DNT-5-SO_3Na	228

[a] All concentration results in mg/L based on diluted red water (1:100), unless otherwise noted.
[b] Estimated values.

aqueous phase under high temperatures (150–350 °C) and pressures (5.5–17.5 MPa). Preliminary experiments have demonstrated that WAO is effective for diluted red water treatment [2]. For example, at 320 °C and 0.62 MPa P_{O_2}, only small amounts of COD (8 mg/L; 99% removal), TOC (30 mg/L; 94% removal), acetic acid (HAc, 38 mg/L) and total volatile solids (TVS, 127 mg/L; 91% removal) remained after 1-h WAO of 1:100 diluted red water [3]. The DNTS' were not detectable and only a trace amount of 1,3-dinitrobenzene (DNB) remained in the WAO effluent. As a result of the desulfonation of the S-bearing organic compounds in red water (e.g., DNTS'), a significant amount of inorganic sulfate accumulated in the oxidized wastewater. The HAc accumulated up to a temperature of about 300 °C; thereafter the HAc concentration decreased due to its further oxidation.

Results of the preliminary experiments, however, only describe the system performance after 1-h WAO. The transient fate of contaminants during WAO is unknown. Contaminant removal efficiencies under different operating conditions (e.g., longer contact time at lower temperatures), therefore, must be quantified in order to initiate practical and cost-effective engineering applications. Consequently, rate studies were performed to examine WAO efficiencies under different conditions of temperature, oxygen pressure, red water concentration, salt concentration, and catalyst/initiator addition. The results provide additional insight as to the fate of organic compounds, measured either as a gross parameter (i.e., COD) or as a specific compound, under WAO conditions. The results of this study should be useful in the future pilot-scale WAO evaluation for red water treatment.

Materials and methods

Experiments

TNT red water was obtained from ICI-explosives, Canada. A schematic of the apparatus used for the rate studies is shown in Fig. 1. Initially, distilled water was added to the 2-L stainless steel reactor (Parr Instrument) and the 50-mL rinse water cylinder. The raw red water was added to the 50-mL sample cylinder. The amounts of distilled water and sample depended on the red water concentration to be studied. For example, for a 1:25 dilution of red water, the volumes of distilled water, raw red water, and rinse distilled water were 910, 40 and 50 mL, respectively, in the reactor, sample cylinder, and rinse water cylinder.

After sealing the reactor, a prescribed amount of O_2 was discharged into the reactor and the contents were heated to the desired temperature. The stirrer speed was maintained at 200 rpm to minimize mass transfer limitation [3]. Once the desired temperature was reached, the raw red water sample was discharged into the reactor via helium backpressure. Subsequently, the distilled water was charged into the sample cylinder for rinsing and finally to the reactor for a total liquid volume of 1 L. After the introduction of the sample and distilled
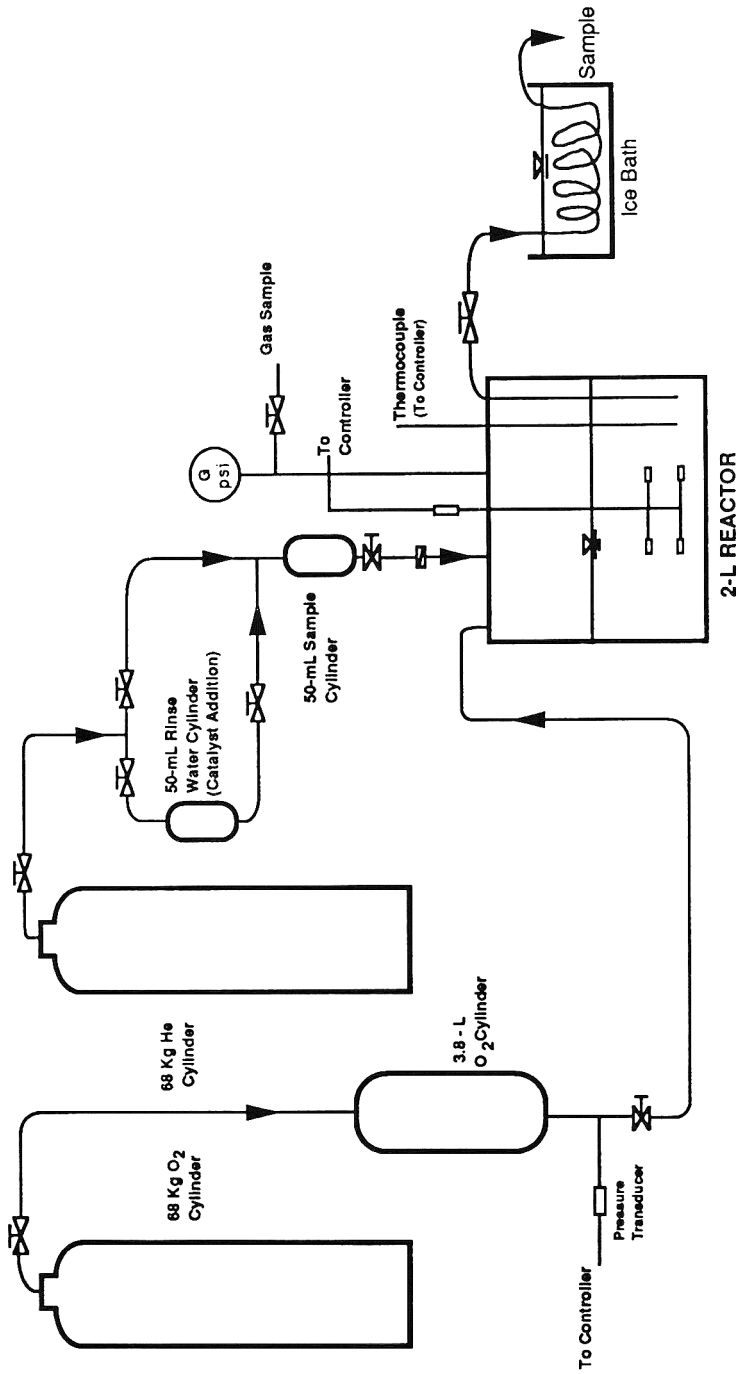
Fig. 1. Schematic of WAO apparatus used for rate studies.

water into the reactor, the temperature dropped slightly and the pressure increased somewhat; both stabilized within 2–3 minutes. The total run time for each experiment was approximately 2 h. An experimental mass balance check has demonstrated that the sample injection technique is reliable [3]. The final pressure after the experiment was slightly less than the initial oxygen pressure.

A radical initiator (H_2O_2) and two different homogeneous catalysts [Mn(II) and Cu(II)], were used to assess their effectiveness for enhancing contaminant removals. The initiator or the catalyst was added to the 50-mL distilled water cylinder and discharged into the reactor as described above.

Samples were withdrawn from the reactor periodically through a stainless-steel coil that was submerged in an ice–water bath. The first sample (10–15 mL) was obtained within 5 min of sample injection. 10–15 mL liquid from the reactor was discarded prior to each sampling event. All samples were analyzed for pH, COD and TOC; some for inorganic salts (sulfite, sulfate, nitrite, and nitrate), solids (total and volatile), HAc, DNTS', six nitroaromatics (nitrobenzene (NB), 1,3-DNB, 2,4- and 2,6-DNT, 1,3,5-TNB, and α-TNT), and UV/VIS absorbance.

The experimental conditions for evaluating the effects of temperature, P_{O_2}, initial red water concentration, salt concentration, and catalyst/initiator addition are summarized in Table 2.

TABLE 2

Experimental conditions for rate studies of WAO of TNT red water

Run No.	Dilution	Temperature (°C)	Initial P_{O_2} (MPa)
1	1:100	260	1.21
2	1:100	300	1.21
3	1:50	260	1.55
4	1:25	260	0.31
5	1:25	260	0.62
6	1:25	260	1.21
7	1:25	260	1.93
8	1:25	260	1.55
9	1:25	260	2.19
10	1:25	230	0.62
11	1:25	280	0.62
12	1:25	300	0.62
13[a]	1:25	260	1.55
14[a]	1:25	260	1.55
15[b]	1:100	260	0.55

[a] With addition of $NaNO_3$ and Na_2SO_4.
[b] With addition of catalyst/initiator.

Analytical methods

A detailed description of analytical methods is presented elsewhere [3]. Briefly, TOC was measured using acid digestion and IR detection of the CO_2 produced. Gas chromatography was used for the analysis of the six nitroaromatics and acetic acid. The DNTS concentrations were estimated using reverse phase ion-pairing chromatography. Ion exchange chromatography was used for sulfite, sulfate, nitrite, nitrate, and acetic acid. Standard Methods [4] were used for COD and solids.

Results and discussion

Typical profiles for TVS, TOC, and COD as a function of WAO reaction time (Fig. 2; $T = 260\,°C$ and $P_{O_2} = 0.31\,MPa$, dilution ratio $= 1:25$) showed similar trends. There was a significant initial reduction of TOC, COD, and TVS immediately after sample injection (within the first sampling event, usually $< 5\,min$). After the initial "flash" destruction, the reaction proceeds as a first-order reaction:

$$r = -\,\mathrm{d}C/\mathrm{d}t = kC \tag{1}$$
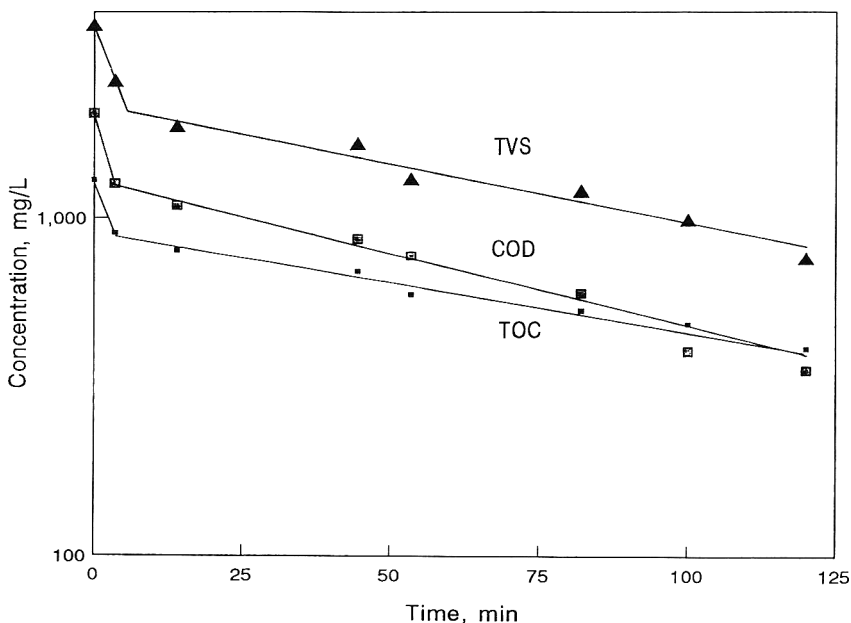

Fig. 2. Typical COD, TOC and TVS removal profiles at $260\,°C$, $0.31\,MPa$ P_{O_2}, $1:25$ dilution.

where r is the rate of reaction, and C and k are the concentration (TOC, COD or TVS) and the apparent (observed) first-order rate constant, respectively. From the semi-log plots, the rate constants were determined to be 6.5×10^{-3} ($R^2 = 0.98$), 1.1×10^{-2} ($R^2 = 0.97$), and 8.5×10^{-3} min^{-1} ($R^2 = 0.91$), respectively, for TOC, COD, and TVS. The first-order rate dependence with respect to a gross parameter, such as COD or TOC, has also been reported by Baillod et al. [5] for WAO of phenol and nitrophenol; Freeze and Rolinski [6] for coal gasification wastewater; Foussard et al. [7] for paper-mill black liquor; Joglekar et al. [8] for phenol; and Phull [3] for 5-nitro-o-toluenesulfonic acid.

Effect of red water concentration

At a constant temperature of 260 °C, three different red water dilutions (1 : 25, 1 : 50 and 1 : 100) were used to observe the effects on the reaction rates. The COD, TOC, and UV absorbance (@200 nm) results (e.g., Fig. 3 for COD) indicate essentially the same phenomena — the initial rapid contaminant destruction and a subsequent first-order contaminant removal rate. The semi-log plots had identical slopes, thus confirming a first-order reaction with respect to the monitored parameter.
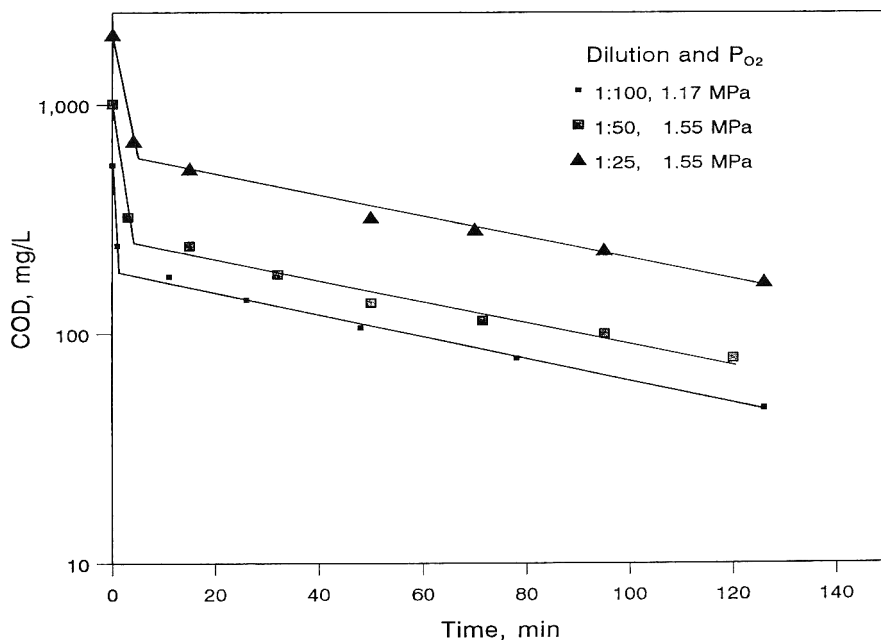

Fig. 3. Effect of red water concentration on WAO rate at 260 °C: COD.

Effect of partial oxygen pressure

For a 1:25 sample dilution ratio at a constant temperature of 260 °C, several different oxygen pressures were used to evaluate the effect on the reaction rates. As shown in Fig. 4a, the initial COD was significantly reduced within the first 5 minutes (e.g., from 2020 mg/L to 580 mg/L in 4 min at 260 °C and 2.19 MPa P_{O_2}). The initial rapid COD reduction is apparently due to the presence of easily oxidizable compounds in red water. The degree of the initial "flash" destruction depends on oxygen pressure, as can be easily seen from the two extreme pressure cases (Fig. 4a). After the initial COD reduction, the removal of slowly oxidizable compounds follows the first-order reaction rate (slopes are all parallel, except for the 2.19 MPa case) and P_{O_2} has no further effect on the COD destruction rate constant. The first-order rate constant is approximately 1.1×10^{-2} min^{-1}. Eckert et al. [9], in their WAO studies of p-chlorophenol, also reported that O_2 (varied by a factor of 11) did not exert any effect on the first-order reaction rate with respect to p-chlorophenol. Although the P_{O_2} did not affect COD destruction rate, the oxygen pressure influenced the extent of overall COD removal due to its effect on the initial COD reduction.

At the highest oxygen pressure (2.19 MPa) used, however, there appear to be two distinct first-order removal phases (Fig. 4a), with a rate constant of 2.2×10^{-2} min^{-1} with respect to COD for the second phase, and 5.7×10^{-3} min^{-1} for the slower phase. The presence of two or more phases of WAO reaction has been reported by others. For example, Foussard et al. [7] divided the organic loading in WAO of biological sludge into two parts: easily oxidized and not easily oxidized. They proposed first-order rate expressions with respect to organic concentration for both parts. A two-phase reaction, first-order in each phase, was also presented by Joglekar et al. [8] for WAO of substituted phenols. Other reactions with two distinct first-order phases include BOD and nitrification in streams [10], chlorine disinfection [11], and endogenous nitrate respiration of activated sludge [12].

The observed TOC destruction with time (Fig. 4b) is similar to that of COD: initial rapid TOC removal dependent on oxygen pressure [e.g., from 1260 to 600 mg/L within 4 min (260 °C and 2.19 MPa)]; a first-order rate with respect to TOC for the subsequent reaction with no effect exerted by the initial P_{O_2} on rate constants for this phase; and two distinct phases under the harshest condition.

Effect of temperature

At a constant pressure of $P_{O_2} = 0.62$ MPa and a dilution factor of 1:25, the effect of WAO temperature on COD destruction is substantial (Fig. 5a). Again, it appears that after the initial COD destruction, slowly oxidizable compounds follow first-order removal and the apparent rate constants are 5.4×10^{-3} and 1.1×10^{-2} min^{-1}, respectively, at 230 and 260 °C. However, at higher temperatures, two distinct phases are present as previously observed in Fig. 4a with the highest P_{O_2}. The rate constants for the first phase were calculated to be 2.3×10^{-2} and 4.2×10^{-2} min^{-1}, respectively, at 280 and 300 °C. For the slower
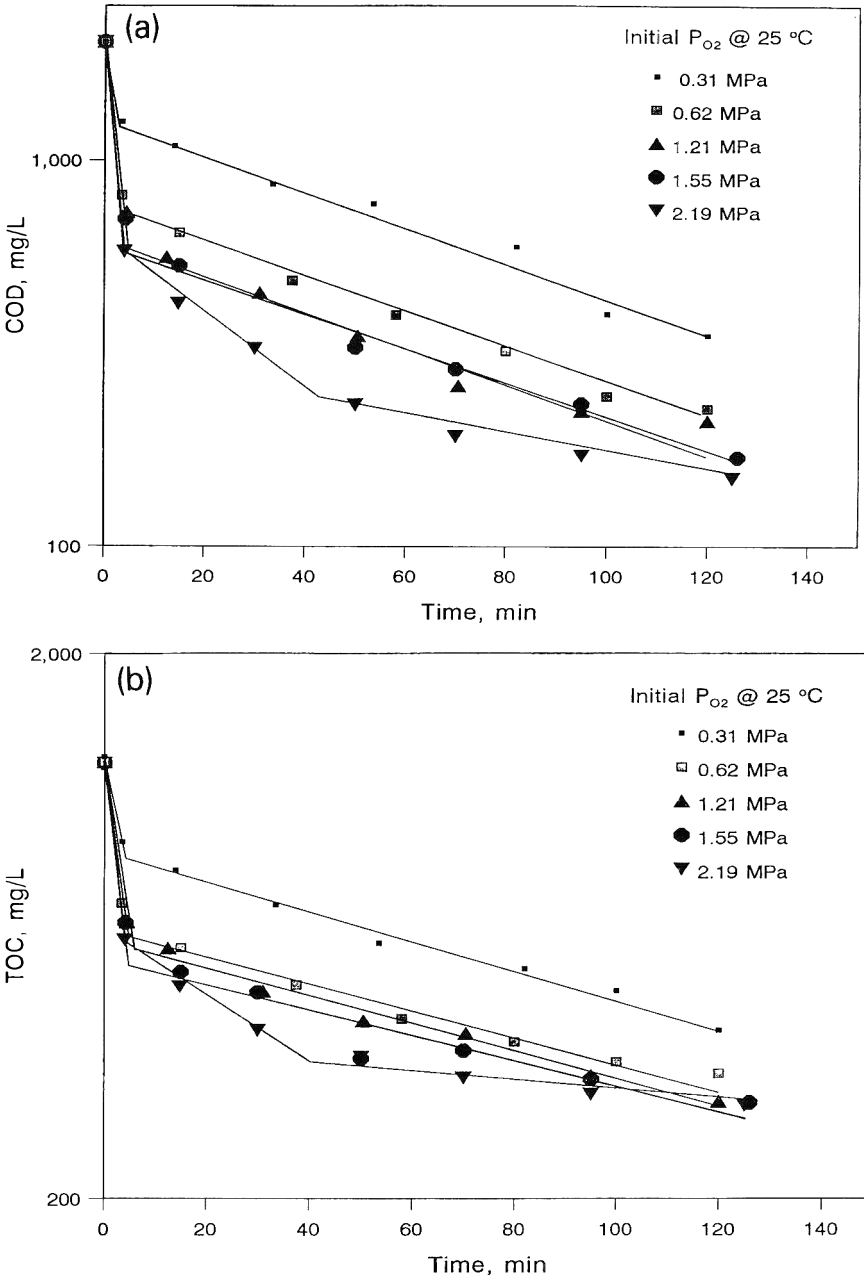
Fig. 4. Effect of initial P_{O_2} on WAO rate at 260 °C, 1:25 dilution. (a) COD, and (b) TOC.

step, the rate constants at 280 and 300 °C were determined to be 9.8×10^{-3} and 1.0×10^{-2} min^{-1}, respectively.

The pattern for TOC reduction (Fig. 5b) as a function of temperature is similar to that for COD. Similar observations were made for UV absorbance reduction at 200 nm. Arrhenius plots for COD and TOC, using the rate constants for the faster reaction phases indicate activation energies to be 17 and 18 kcal/mol, for COD and TOC, respectively. These values are similar to the values reported by other investigators for WAO of different compounds, e.g., 14 kcal/mol for phenol [13] and 16 kcal/mol for acetone [14].

Effect of salt concentration

Inorganic salts (e.g., Na_2SO_4) are not destroyed as a result of WAO; in fact, their amounts increase due to oxidation of inorganic sulfite and organic sulfo groups. In order to evaluate the effects of high salt concentrations on WAO of red water under continuous treatment conditions, two experiments were performed by adding $NaNO_3$ and Na_2SO_4. In the first experiment 1.56% salt solution (15 g/L Na_2SO_4 plus 0.6 g/L $NaNO_3$) was added to the reactor; 5.2% salt concentration (50 g/L Na_2SO_4 plus 2.0 g/L $NaNO_3$ was employed in the other experiment. The COD results (Fig. 6) indicate that the increased salt concentrations enhanced the extent of COD removal. The exact reasons for this are unclear. The trace metals present as impurities in the large quantities of $NaNO_3$ and Na_2SO_4 added might have catalyzed the WAO reactions, resulting in a slightly better overall COD removal. The effects of salt concentration on TOC removal rates (not shown) are similar to those for COD. The higher salt concentration at 5.2% enhanced the TOC removal rate more noticeably.

Effect of catalyst/initiator

A mild WAO condition was selected to observe any enhancement in rates upon the addition of the catalyst or an initiator (Fig. 7). H_2O_2 dosages at 20 and 150 mg/L appear to have an adverse effect as compared to the control system; Mn(II) at 10 mg/L exhibited little effect. Cu(II) catalyst, however, enhanced the overall TOC removal. The enhanced effect of Cu(II) on WAO of other organics has also been cited, e.g., WAO of nitrotoluenesulfonic acid [3].

Other kinetic data

Typical pH profiles for WAO of red water (1:25) are shown in Fig. 8. As expected, the solution pH after the WAO is altered by the experimental conditions. It was significantly reduced from 7.6 to approximately 3.5 within the first sampling period (<5 min). The red water has little buffer capacity and the reduction in pH indirectly infers that SO_3 groups are rapidly detached from the DNTS', resulting in the formation of H_2SO_4. Additionally, organic acids formed from WAO of the various organic compounds in red water may also depress the pH. Rapid desulfonation within the first sampling period is also confirmed by the increased sulfate concentrations (e.g., from 1510 to 2970 mg/L at 300 °C and 0.62 MPa; Fig. 9). The changes in pH and sulfate concentrations
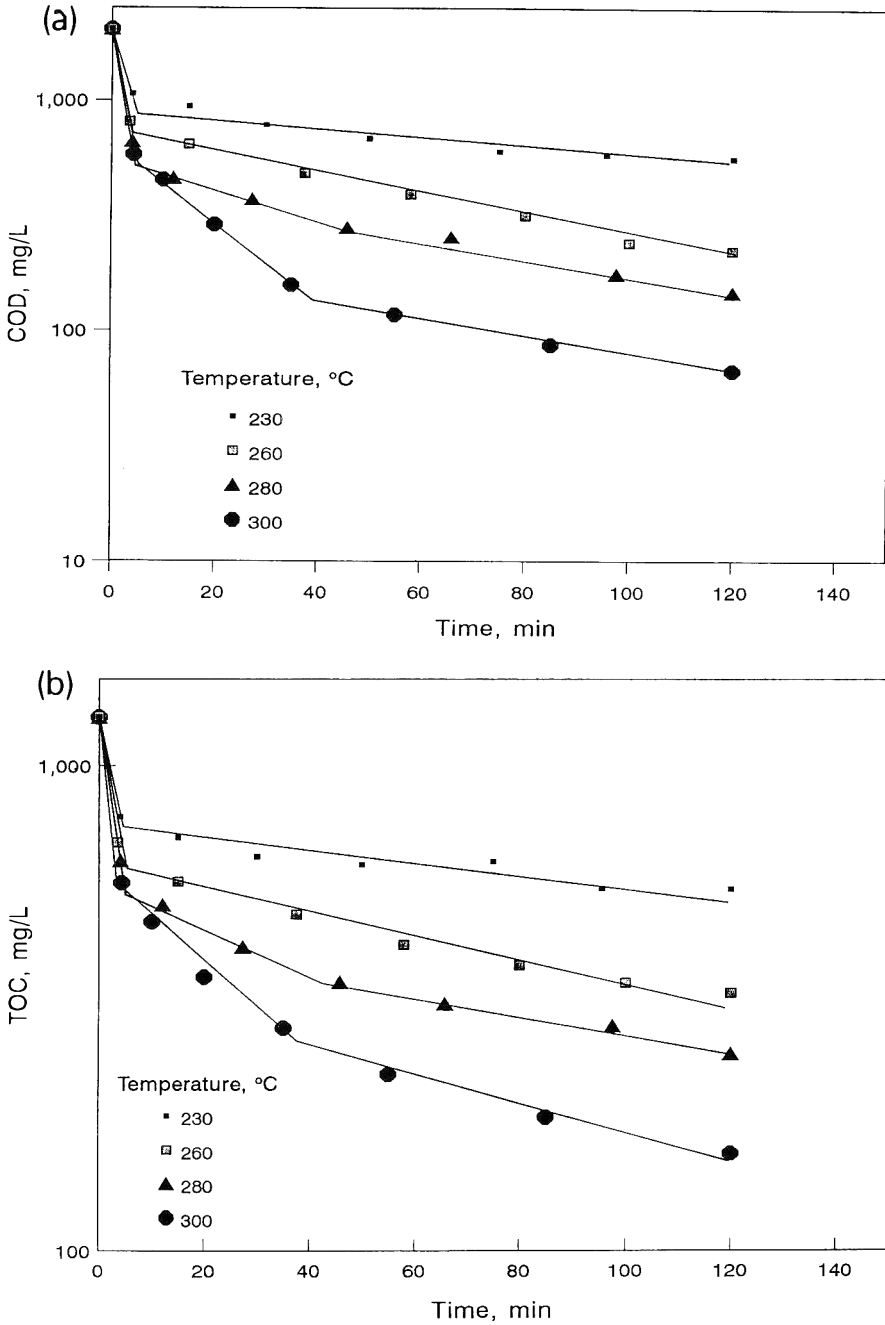
Fig. 5. Effect of temperature on WAO rate at 0.62 MPa P_{O_2}, 1:25 dilution. (a) COD, and (b) TOC.

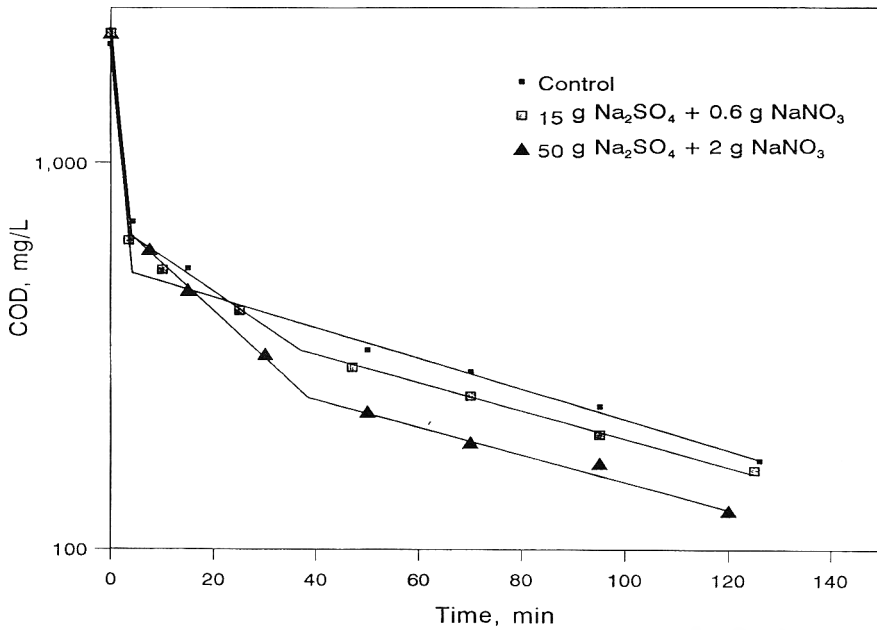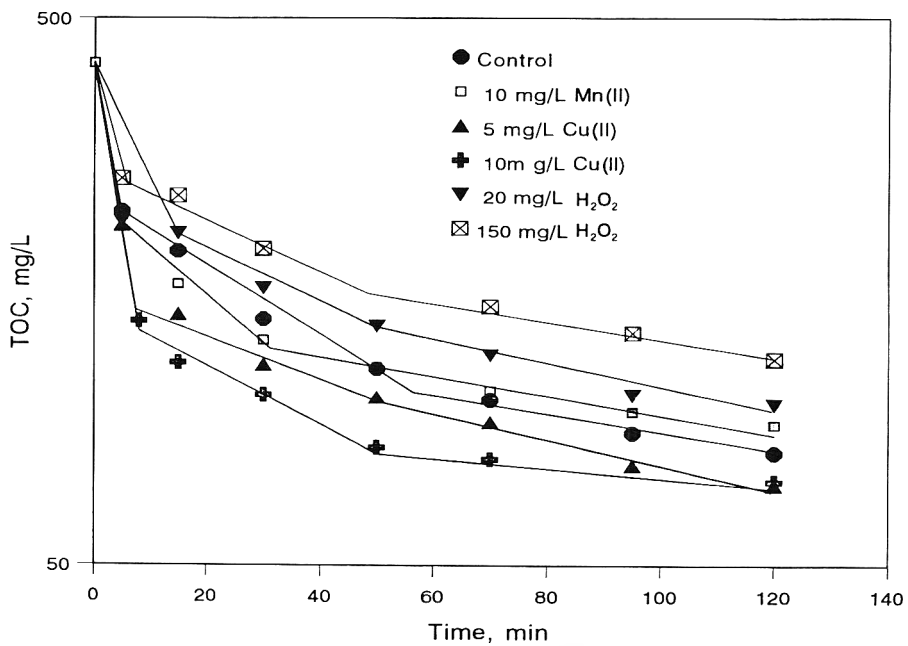Fig. 6. Effect of salt concentration on WAO rate at 260 °C, 1.55 MPa P_{O_2}, 1:25 dilution: COD.

Fig. 7. Effect of catalyst/initiator on WAO rate, 260 °C, 0.55 MPa P_{O_2}.
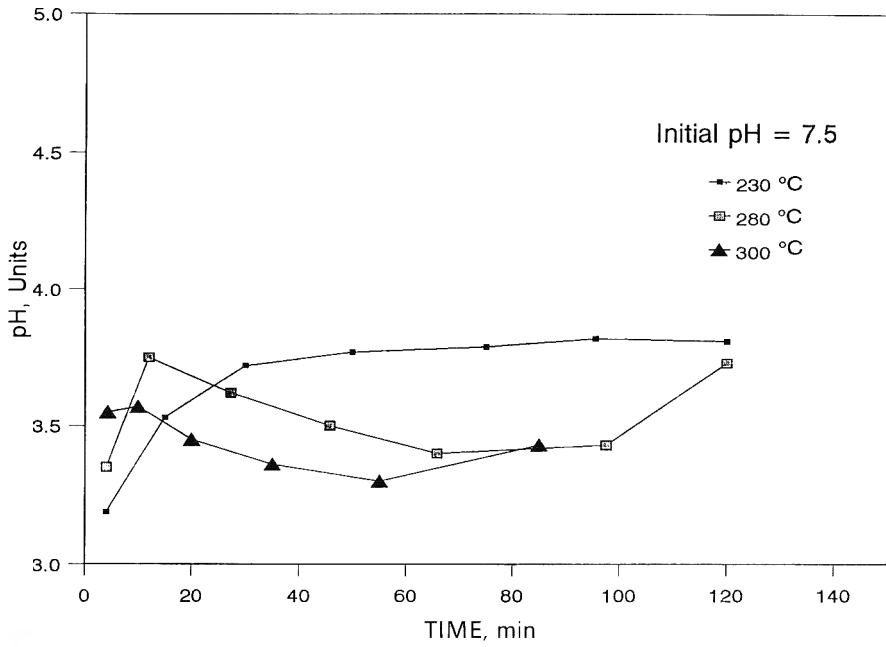
Fig. 8. Typical pH profiles as a function of temperature, 0.62 MPa P_{O_2}, 1:25 dilution.
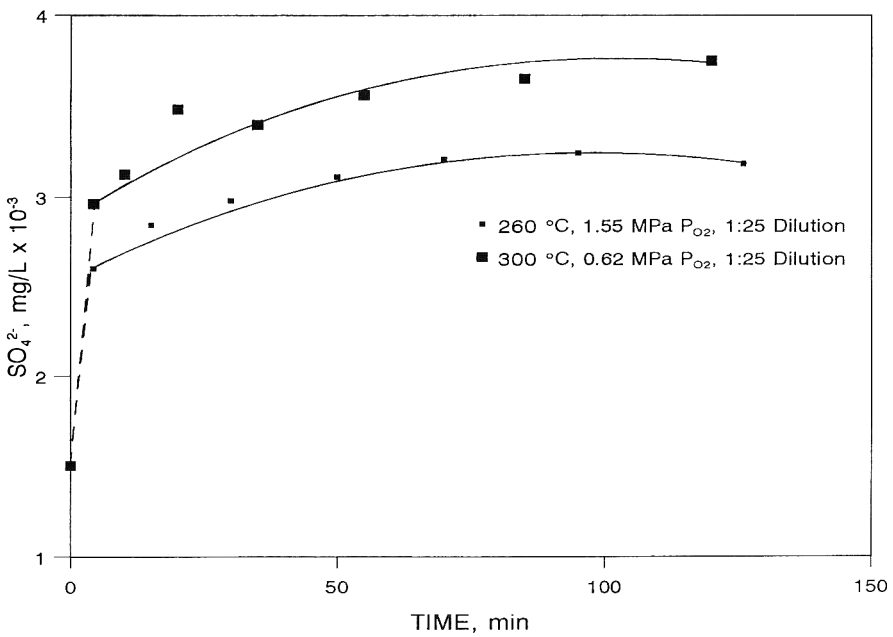
Fig. 9. Accumulation of sulfate during WAO of TNT red water.

correspond well to the initial rapid reduction in COD, TOC, and TVS as discussed earlier. The measured nitrate concentrations were, however, lower than the combined nitrite and nitrate concentrations initially present, without even considering the organic nitro groups present in red water. The unaccounted nitrogen is attributed to the formation of ammonium and N_2 gas [3]. Generation of N_2 from wet oxidation of the nitro group was also reported for other explosives [15, 16].

The data for DNTS removal for two experiments at 260 °C, 1.55 MPa P_{O_2} and 300 °C, 0.62 MPa P_{O_2} (Fig. 10) indicate that 2,4-DNT-5-SO_3Na is more easily oxidized than 2,4-DNT-3-SO_3Na and temperature rather than oxygen pressure exhibits a more significant effect. The results for 1,3-DNB (Fig. 11) compare well with those from 2-h batch experiments [2]. The 1,3-DNB concentration increases with temperature and time, supposedly following DNTS′ → DNT → DNB, and then decreases as a result of further oxidation.

Application

Although WAO may be effective strictly from a technological standpoint, several issues need to be adequately addressed to ensure successful practical application of WAO for the treatment of TNT red water. These issues include cost, energy recovery, corrosion and materials of construction, and toxicity of WAO-treated waste streams.

Fig. 10. Effect of temperature and P_{O_2} on DNTS removal.

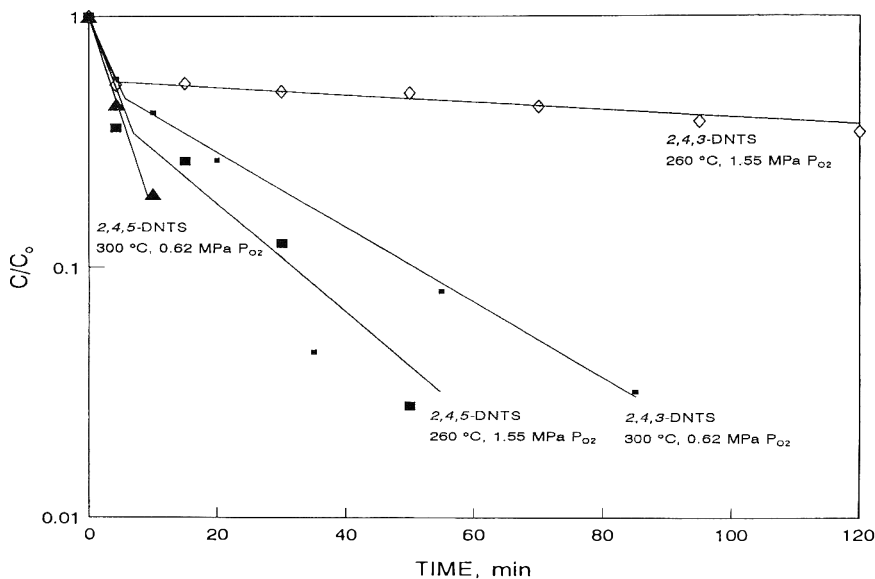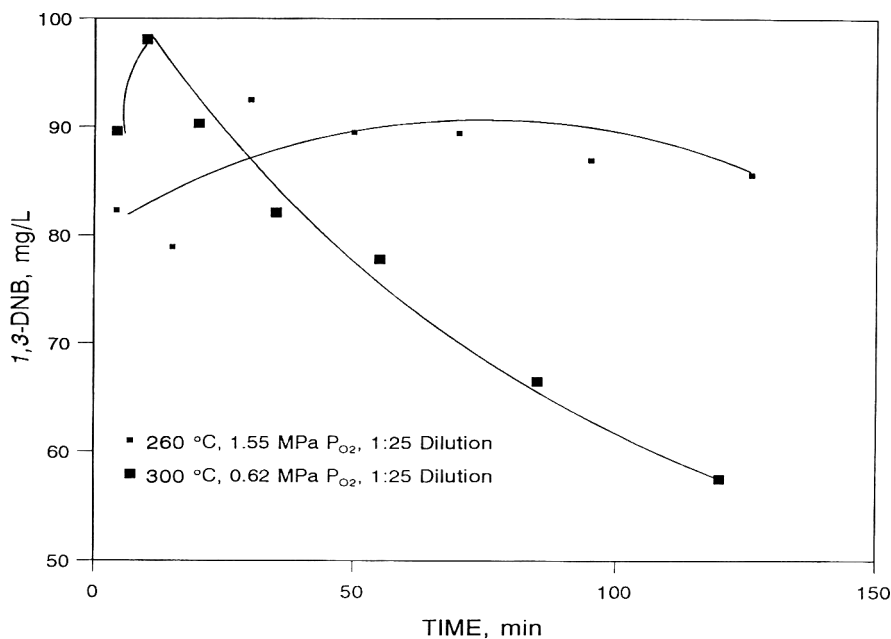Fig. 11. Accumulation of 1,3-DNB during WAO of TNT red water.

Cost and energy

Economics and regulatory compliance are the most important factors influencing the choice of a waste treatment method. The selected method must provide the desired treatment, while keeping capital and operational/maintenance/repair costs to a minimum. The capital cost of a WAO unit is related to the capacity (reactor size) and the desired system pressure (miscellaneous high pressure pumps and air compressors). The major operational cost is the amount of air used, which depends on the degree of oxidation and system conditions.

Generally speaking, full-scale WAO plants require higher capital investment compared to the equivalent treatment alternatives. Other factors, such as minimal "cross-media" pollution, however, may still render the WAO process more desirable. As an alternative, WAO may be used as a pretreatment step to enhance the biotreatability of red water at milder WAO conditions than required for complete mineralization of the waste. Such an operation would result in significantly lower operational costs.

The WAO process offers an opportunity for energy recovery in the form of thermal (steam generation or heating the waste influent), mechanical (expansion of hot offgas), and electrical energy. Recovery of WAO reaction enthalpy for supplementing heat input or even for attaining a self-sustaining process has been reported by several investigators. The minimum concentration of organics required for the process to become self-sustaining depends on temperature and pressure (e.g., $8 \, g/L$ COD at $271 \, °C$, $10.4 \, MPa$ [17]; $10–20 \, g/L \, \Delta$COD at

275 °C [18]; and TOD > 15 g/L at T > 300 °C [7]) based on a heat of reaction of 12,500–13,000 kJ/kg. Some full-scale WAO plants currently in operation are, in fact, used to generate steam [19].

For simplicity, the entire amount of the heat of reaction is assumed to be available for heating the influent and the heat loss from the system is considered to be insignificant. The minimum concentration of organics (C_{min}) for a WAO system to become self-sustaining can be roughly estimated:

$$C_{min} = (\Delta T \times C_p)/H_R \tag{2}$$

where, C_{min} is the minimum organic concentration for self-sustainment, wt%; ΔT the temperature difference between waste influent and the reactor temperature, °C; C_p the heat capacity of water (4.1 kJ/kg °C); and H_R the heat of reaction, kJ/day.

For red water, the heat of reaction in terms of joules per kg of organics must be estimated in order to calculate C_{min}. Based on the reported heat value of 7430 kJ/kg for TNT red water [1], C_{min} is approximately 14% for a ΔT of 260 °C. Because the heat losses may be quite significant, C_{min} determined from reaction (2) may be underestimated. Thus, an initial concentration step may be required for a dilute waste stream for an effective energy recovery. On the other hand, if heat recovery is considered for a given ΔT between the influent and heat exchange effluent, C_{min} should be much lower than that from reaction (2).

Corrosion

WAO is generally more effective at both high and lower pHs [3], however, it is more desirable for COD removal at low pHs. Additionally, the process itself results in a low effluent pH due to the generation of mineral acids and low molecular weight organic acids, as well as the high concentration of aqueous CO_2 at elevated system pressures. For example, the pH of WAO-treated propellants and explosives ranged from 0.7 and 2.9 [15, 16]. The pH of TNT red water decreased from 7.5 to about 3 after WAO; oxidized 5-nitro-o-toluenesulfonic acid had a pH of less than 2 [3].

The design of full-scale WAO reactors must take into account the unique operational conditions of high temperatures and pressures in addition to the low pH of the oxidized solutions, since the corrosivity of the waste is enhanced under such conditions. Furthermore, red water is expected to be more corrosive when subjected to WAO due to the formation of inorganic sulfate. Stainless steel may not be the preferred material of construction for such wastes; special alloys or metals (e.g., Inconel 600, Hasteloy C-276, titanium) may be needed. The proper choice of the material of construction should include bench-scale corrosion tests as well as pilot studies.

Toxicity

A general review of previous WAO studies [3, 20, 21] indicates that the WAO-treated wastes may exhibit higher inhibitory effects on microbial species than the starting material(s). Some literature results further indicate that,

although the WAO process was more efficient in destroying the starting material(s) under harsher conditions, the treatment under these conditions also produced byproducts with higher toxic effects [3]. It is quite clear that the toxicity of the oxidized material should be determined to ensure that direct discharge of treated red water would not pose any environmental problems.

Conclusions

Rate studies of WAO of red water revealed several interesting points. First, a major portion of the COD, TOC, and TVS was destroyed immediately after the injection of the sample into the reactor, due to the oxidation of easily oxidizable compounds present in red water. The degree of this "flash" COD, TOC, or TVS reduction is related to the operating conditions. The higher the temperature and/or pressure, the more the contaminant reduction. After this initial fast activity, P_{O_2} had little effect, and reaction of the slowly oxidizable compounds proceeded at a typical first-order rate with respect to COD (TOC or TVS). Under harsher conditions, however, two distinct first-order rate phases appear. Temperature, as expected, significantly affects the first-order rate constants with an activation energy of approximately 17 kcal/mol for COD. Catalyst Cu(II) and high salt concentrations produced slight enhancements in the WAO rate of red water.

Acknowledgements

References

1   PEI Associates, Technological Evaluation for Treatment/Disposal of TNT Red Water, Report No. CETHA-TE-CR-90048, US Army Toxic and Hazardous Materials Agency, Aberdeen Proving Ground, MD, 1990.
2   O.J. Hao, K.K. Phull, A.P. Davis. J.H. Chen and S.W. Maloney, Evaluation of wet air oxidation of TNT red water, Proc. 24th Mid-Atlantic Ind. Waste Conf., Morgantown, WV. Technomic, Lancaster, PA, 1992, pp. 110–119.
3   K.K. Phull, Wet Air Oxidation of TNT Red Water, Ph.D. Dissertation, Department of Civil Engineering, University of Maryland, College Park, MD, 1992.

4 Standard Methods for the Examination of Water and Wastewater, 16th edn., American Public Health Association, Washington, DC, 1985.
5 C.R. Baillod, B.M. Faith and O. Masi, Fate of specific pollutants during wet oxidation and ozonation, Environ. Prog., 1 (1982) 217–226.
6 R.A. Freeze and E.J. Rolinski, Wet air oxidation studies of coal gasification wastewaters, J. Hazardous Mater., 8 (1984) 367–375.
7 J.-N. Foussard, H. Debeilefontaine and J. Besombes-Vailhe, Efficient elimination of organic liquid wastes: wet air oxidation, J. Environ. Eng., ASCE, 115 (1989) 367–385.
8 H.S. Joglekar, S.D. Samant and J.B. Joshi, Kinetics of wet air oxidation of phenol and substituted phenols, Water Res., 25 (1991) 135–145.
9 C.A. Eckert, G.W. Leman and H.H. Yang, Homogenous catalysis for wet oxidation: design and economic feasibility of a mobile detoxification unit, Haz. Mat. Control, 3 (1990) 20–33.
10 A.K. Deb and S.D. Bowers, Diurnal water quality modelling — a case study, J. Water Pollut. Control Fed., 55 (1983) 1476–1488.
11 C.N. Haas and S.B. Kana, Kinetics of microbial inactivation by chlorine — II. Kinetics in the presence of chlorine demand, Water Res., 18 (1984) 1451–1454.
12 M.H. Kim and O.J. Hao, Comparison of activated sludge stabilization under aerobic and anoxic conditions, J. Water Pollut. Control Fed., 62 (1990) 160–168.
13 J.R. Katzer, H.H. Ficke and A. Sadana, An evaluation of aqueous phase catalytic oxidation, J. Water Pollut. Control. Fed., 48 (1976) 920–931.
14 J.E. Taylor and J.C. Weygandt, A kinetic study of high pressure aqueous oxidations of organic compounds using elemental oxygen, Can. J. Chem. Eng., 52 (1974) 1925–1933.
15 W.M. Fassel and D.W. Bridges, Wet oxidation destruction of propellants and explosives, Proc. Natl. Conf. on Management and Disposal of Residues from the Treatment of Ind. Wastewaters. Information Transfer, Rockville, MD, 1975, pp. 87–97.
16 W.M. Copa and T.L. Randall, Wet Air Oxidation of Propellants and Propellant Wastewater. Zimpro Passavant Report No. TA-97, Rothschild, WI, 1990.
17 C.L. Chou and F.H. Vernhoff, Process for power generation from wet air oxidation with application to coal gasification waste water, Ind. Eng. Chem. Process Res. Dev., 20 (1981) 12–19.
18 H.N. Akse, M.M.G. Senden, M. Tels and J.H.O. Hazewirkel, Detoxification and energy recovery by wet air oxidation of waste streams, Resources and Conservation, 14 (1987) 351–364.
19 W.M. Copa, Personal Communication, Zimpro Passavart, Rothschild, WI, 1992.
20 T.L. Randall and P.V. Knopp, Detoxification of specific organic substances by wet oxidation, J. Water Pollut. Control Fed., 52 (1980) 2117–2130.
21 R. Keen and C.R. Baillod, Toxicity to *Daphnia* of the end products of wet oxidation of phenol and substitute phenols, Water Res. 19 (1985) 767–772.

Plume rise of smoke coming from free burning fires

C. Zonato[a], A. Vidili[c], R. Pastorino[b] and D.M. De Faveri[a,*]

[a] *Department of Physical Chemistry, University of Venice, Calle Larga S. Marta 2137, 30123 Venice (Italy)*
[b] *ISTIC, University of Genova, Genova (Italy)*
[c] *Montefluos SpA, Ausimont Group, Milan (Italy)*

Abstract

In this paper, attention is focussed on the plume rise of smoke arising from free burning fires. Free burning fires have both geometric and emission characteristics quite different from common industrial emission sources. Experimental runs have been carried out in a wind tunnel in order to derive a simple expression to assess the plume rise of smoke arising from free burning fires. Moreover, the experimental expression has been compared with two models available from the literature. The presented experimental expression shows good agreement with these models, in particular for moderate wind speeds, showing a maximum difference of about 10%.

1. Introduction

Previous papers have presented various expressions to assess the plume rise of industrial emissions, most of which are semiempirical being derived from experiments carried out either at a large scale in the field or in wind tunnels. Only a few expressions have been derived from theoretical models.

However, none of these previously derived expressions can be applied generally, because the equations would lead to unrealistic estimates of plume rise if applied either to sources with characteristics different from those tested experimentally or systems that fall outside the assumptions used in deriving theoretical models.

The larger the difference between the situation modelled and the phenomenon responsible for the generation of the smoke, the more unrealistic will be the estimate of plume rise. This is indeed the case for a smoke plume that arises from free burning fires, the characteristics of which are very different from those of a common industrial source plume.

---

*To whom correspondence should be addressed.

In fact, in the case of free burning fires, the heat produced by the flames partly is radiated [1–3], instead of being released completely into the plume as for plumes generated by flare stacks [4, 5].

2. Approach to the problem

The assessment of rise of smoke plumes resulting from free burning fires must be done by implementing *ad hoc* models as those suggested by Mills [6] and Carter [7].

In particular, Mills suggests altering the Briggs formula [8] as follows:

$$\Delta h = \left[(\Delta h_B)^3 + \left[\frac{L}{2\gamma} \right]^3 \right]^{1/3} - \frac{L}{2\gamma} \tag{1}$$

This expression, which takes into account the diameter L of the fire, may be altered bearing in mind that:

$$\Delta h_B = 1.6 \, F^{1/3} X^{2/3} u^{-1} \tag{2}$$

where:

$$F = 0.037 \, Q_H \tag{3}$$

and assuming an ambient temperature $T_a = 293$ K.

Moreover, Mills assumes that the 30% of the heat released in the combustion is dispersed as thermal radiation in the surrounding area, also Mills assumes that the 70% of heat combustion is devoted to the plume rise.

As result of these assumptions the Briggs formula becomes:

$$\Delta h_B = 0.47 \, Q_H^{1/3} X^{2/3} u^{-1} \tag{4}$$

Mills, therefore, modifies the Briggs formula in two ways:
(i) reducing the heat produced in combustion by about 30%, because this portion is dispersed in the environment as thermal radiation, and does not support the plume rise, (i.e. buoyancy of plume);
(ii) inserting in Briggs formula the term $L/2\gamma$ (where $\gamma = 0.6$, entrainment coefficient for buoyant plume rise) in order to take into account the initial diameter of the plume which is considered equal to the extent of the fire.

On the other hand, Carter suggests using Moore's formula [9], modified to exclude momentum.

Therefore Moore's modified formula becomes:

$$\Delta h = 0.512 \, \frac{f}{u} \, \Delta T^{0.125} \left[\frac{gQ}{C_p T_a} X^{*2} (X^* + 27L) \right]^{0.25} \tag{5}$$

where:

$$X^* = XX_t(X^2 + X_t^2)^{-0.5}$$

$$X_t = X_s X_n (X_s^2 + X_n^2)^{-0.5}$$

$$X_s = 120 \ u\varepsilon^{-0.5}$$

$$X_n = 1920 + 19.2 \ Z \qquad \text{or} \qquad 4224 \quad \text{if } Z > 120 \text{ m}$$

$$f = 0.16 + 0.007 \ Z \quad \text{if } Z < 120 \text{ m}$$

$$f = 1 \quad \text{if } Z > 120 \text{ m} \qquad \text{or} \qquad u^{-2}\varepsilon > 2.5 \times 10^{-3}$$

Carter suggested the use of Moore formula on the basis of general considerations without bearing in mind the peculiar characteristics of free burning fires. Equation (5), therefore, is valid for the plume rise assessment for very hot smoke arising from any kind of sources (point or large types). To compensate for area source, Carter estimates the virtual location of an equivalent point source, below the level of the area source.

In any case, however, the plume rise of free burning fires is brought about mainly by the buoyancy force and the height of the plume rise is equal to the real height of the emission because the geometric height of the source (fire) is negligible.

Furthermore, the passage from the flame to the smoke happens continuously, therefore in the assessment of the plume rise it is possible to consider the plume as single element composed by flame and smoke jointly.

Bearing this in mind, in this paper the plume rise assessment has been developed by considering that the heat of combustion is scattered partly in the environment as thermal radiation and the remaining heat of combustion is released to the smoke. The present plume rise assessment uses an expression similar to that of CONCAWE [10] adopted for flare stacks [4], and to Briggs expression as follows:

$$\Delta h = K \frac{Q_h^a X^b}{u^c} \tag{6}$$

The constant K and the exponents a, b, c have been evaluated by experimental measurements in a wind tunnel.

The term Q_h represents the convective heat flow released to the smoke and is evaluated as follows:

$$Q_h = (1 - E) Q_H$$

where Q_H represents the total heat flow while E represents the fraction of heat flux released in the environment as thermal radiation. Therefore E depends on the kind of fuel burning in the fire.

3. Experimental runs

Laboratory-scale tests of free burning pools of liquid were performed in a wind tunnel using diesel fuel and a mixture of lubricant oil with exhausted diesel [11, 12].

The wind tunnel utilized is characterized by a rectangular section, of dimensions $1\,m \times 1.2\,m$ and an overall length of 6 m. Wind simulation has been performed by conveying air into the working chamber through a helical suction fan, which assured an air speed ranging from 0.1 to 1 m/s. Using the lower value of air speed we can expect the concept of Re independence to be valid during the tests [13].

A neutrally stable atmospheric boundary layer was simulated using a 38 mm high fence similar to the one proposed by Castro [14].

Flame buoyancy was varied by using bowls with different diameters and different quantities of fuel inside the containers. Bowls were lain low in a pit, while their upper edges were flush with the bottom of the wind tunnel.

Fuel vapor was lit after preheating the liquid with a bunsen burner, positioned just outside the wind tunnel under the bowl (see Fig. 1).

After reaching the fire point, the warming of the fuel was stopped by shutting off the bunsen burner, the pools were allowed to burn freely afterwards.

The smoke plume centreline was observed and its average height recorded by photography (exposure time 30 s) through the transparent wall of the wind tunnel at different downwind distances.

In order to easily record the plume rise (Δh) a transparent square grid, with sides of 2.5 cm, was fixed onto the transparent wall of the wind tunnel (see Fig. 1).

The main experimental parameters are shown in Table 1 while the results are reported in non dimensionalised variables in Fig. 2.

In particular the experimental results show that the maximum plume rise (Δh_{max}) was observed at a distance from the burning pool 45 times the diameter of the burning pool.
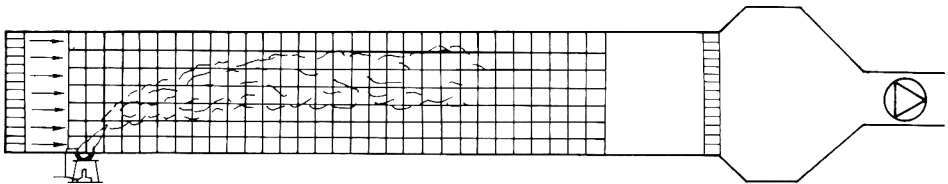

Fig. 1. General view of wind tunnel including the square grid for recording the plume heights.

TABLE 1

Range of the main geometric and operational parameters used for wind tunnel experiments and burning fuel characteristics

| *Wind tunnel characteristics*	
Height	1.00 m
Width	1.20 m
Length	6.00 m
Thermal conditions in wind tunnel:	Neutral to isothermal
Operational parameters	
Wind speed	0.5–0.9 m/s
Diameter of pools	5.4–11.1 cm
Dimensionless number at source	
Froude	0.23–1.53
Reynolds	1807–6673
Burning fuel[a] characteristics	
Mass burning rate	0.015 kg/m^2 s
Low heat value	10800 kcal/kg

[a] Mixture of diesel fuel and lubricant oil.
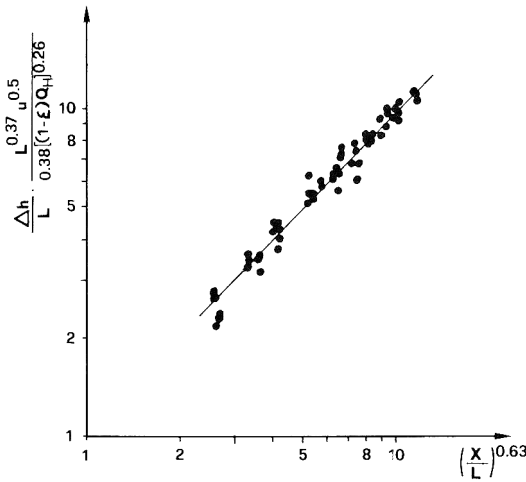
Fig. 2. Experimental results for wind tunnel tests.

By elaborating with the least square method the experimental data the values of the constant K and the exponents a, b and c of eq. (6) can be assessed:

$$\Delta h = 0.38 \frac{[(1-E)Q_H]^{0.26} X^{0.63}}{u^{0.5}} \tag{7}$$

which is valid for $X/L < 45$.

The maximum difference between experimental data and eq. (7) is about 35%. For $X/L = 45$ expression (7) becomes:

$$\Delta h_{max} = 4.2 \frac{[(1-E)Q_H]^{0.26} L^{0.63}}{u^{0.5}} \tag{8}$$

For distances farther than 45 times the diameter of the burning pool the plume heights were steady.

4. Validation of the model

As stated in Section 2, the models to assess the plume rise of a free burning pool must be developed *ad hoc* because the geometric and emission characteristics of the sources (free burning fires) are very different from the common industrial sources (stacks).

Among the expressions presented in the literature only the Mills formula may be applied specifically to the problem examined in this paper, while the Carter formula may also be applied to other emissions.

The Carter formula is, therefore, characterized by a higher degree of uncertainty because of general usefulness, being less specific than the Mills formula.

In this paper, however, both models examined (Mills's and Carter's) will be compared with the experimental data by means of experimental runs carried out in a wind tunnel.

Furthermore, for both the models of Mills and Carter it was assumed that the maximum plume rise (Δh_{max}) is obtained at a downwind distance from the burning pool of $X = 45\,L$, where the smoke plume was fully aligned to the wind direction.

In fact, in the aforesaid models there does not seem to appear a limitation on the plume rise Δh, but it is quite clear that the plume cannot increase indefinitely.

4.1 Mills's model
The Mills model may be rewritten explicitly as follows:

$$\Delta h = \left[(0.47\, Q_H^{1/3} X^{2/3} u^{-1})^3 + \left[\frac{L}{2\gamma} \right]^3 \right]^{1/3} - \frac{L}{2\gamma} \tag{9}$$

where [15]: $Q_H = (\pi L^2/4) m h_c$; $m = h_c\, 1000\, (h_v + C_p \Delta T_0)^{-1}$ for liquid with boiling temperature higher than ambient temperature; and $m = h_c\, (1000\, h_v)^{-1}$ for liquid with boiling temperature lower than ambient temperature.

A comparison between the above mentioned Mills formula and the experimental relation presented in Section 3 may be made if one only considers the term

$$\Delta h_R = 0.47\, Q_H^{1/3} X^{2/3} u^{-1}$$

and comparing with the experimental equation (7), thus examining the following ratio:

$$R = \frac{\Delta h_B}{\Delta h} = 1.34 \, Q_H^{0.073} X^{0.037} u^{-0.5}$$

obtained by considering $E = 0.3$ congruently with Δh_B.

The terms $Q_H^{0.073}$ and $X^{0.037}$ play a negligible role in the plume rise assessment.

In fact by putting $A = Q_H^{0.073} X^{0.037}$ one may consider that the value of the term A is between 2 and 3. Such a range corresponds to a variation of Q_H between 5000 and 20000 kcal/s and to a downwind distance X less than 2000 m.

The trend of the function R is shown in Fig. 3 and a good agreement may be observed between the Briggs equation and the experimental one (eq. 7), above all for wind speeds moderately high ($u > 8$ m/s) the function R is approximately equal to unity ($R \approx 1$).

The difference between the Briggs formula and the eq. (7) is quite high for low wind speeds, less than $2 \div 3$ m/s, which are not significant considering the very high plume rise reached by the smoke.

Furthermore the correction made by Mills in the Briggs expression shifts the curves shown in Fig. 3 downward, in particular those curves which refer to higher values of the term A, i.e., higher Q_H and X values.

This fact makes the R ratio approximatively equal to unity for those wind speeds generally applied in the assessment of atmospheric dispersion of smoke arising from free burning pools.

A more detailed comparison between the Mills model and the experimental model worked out in wind tunnel runs is shown in Fig. 4. For moderate wind speed (5 m/s) the experimental expression is lower than the Mills model
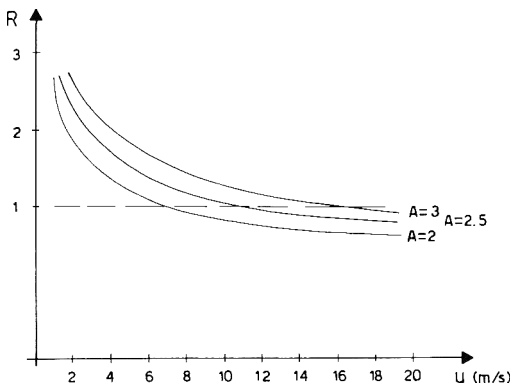

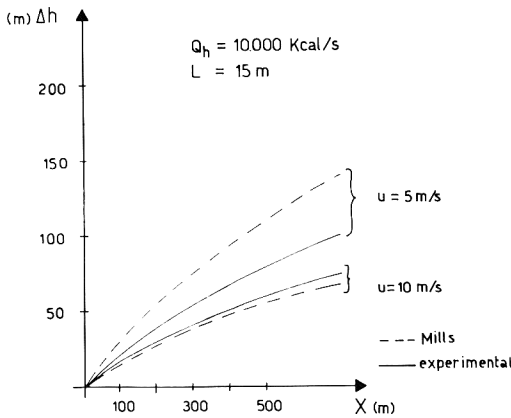Fig. 3. Trend of the ratio $R = \Delta h_B / \Delta h$ vs. wind speed.

Fig. 4. Comparison between the Mills model and the experimental model.

prediction by about 40%, for higher wind speed (10 m/s) the gap, in excess, is only about 9%.

Obviously the aforesaid considerations are valid bearing in mind a medium value of $E = 0.30$. In fact for different emission factor values the Mills equation does not consider different E values.

4.2 Carter's model

A detailed comparison between Carter's formula and the experimental expression (7) derived from wind tunnel runs, is more complicated because the two models are structured in different ways.

Nevertheless, a comparison can be made between the three models, Carter's, Mills's model and the experimental equation (7), on the basis of an example, a fire of carbon disulphide, developed by Carter. The comparison has been done for a wind speed of 10 m/s and for burning pools of different diameters (2, 5, 10, and 20 m). The results of the comparison are shown in Fig. 5.

Despite the general validity of Carter's formula, i.e. not specifically for free burning fires, it shows in the example chosen good accordance with our experimental equation, with maximum difference of about 10%.

On the other hand, Mill's model also shows agreement with the experimental data.

5. Conclusions

The rise of smoke plumes arising from free burning pools should not be assessed by means of analytical expressions reported in the literature for common industrial emissions such as stacks, because of substantial differences between the two types of emissions.
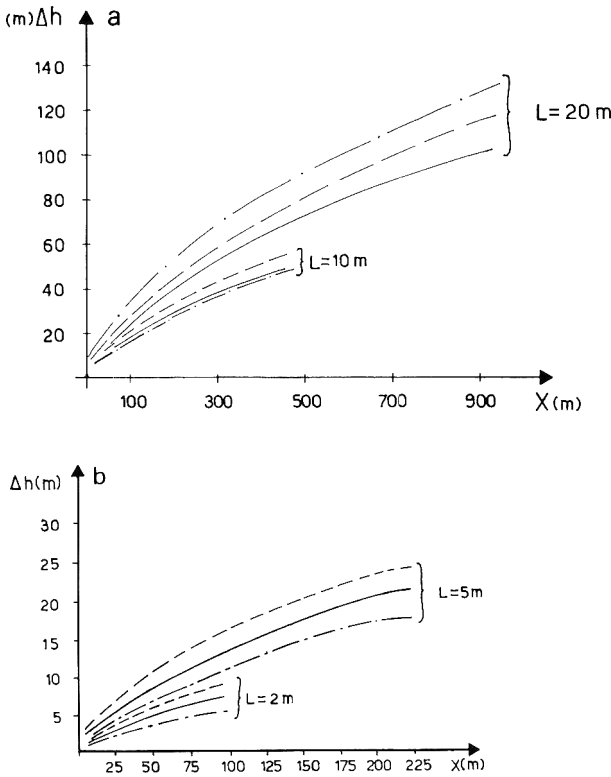
Fig. 5. Comparison among the models of Mills (– – –), Carter (– · –) and that derived from experiments (—). (a) $L = 20$ m and $L = 10$ m; (b) $L = 5$ m and $L = 2$m.

The present paper describes experimental runs carried out in a wind tunnel, which enables the derivation of a simple expression to assess the plume rise from free burning fires.

The experimental model takes into account that, in the presence of flames, the combustion heat is partly dispersed in the environment as thermal radiation and partly transferred to the smoke.

The experimental expression has been compared with two existing models from the literature; that of Mills, specific for the case considered, and that of Carter which is of general validity, not particular to fires, but applicable to very hot smoke.

Good agreement has been noted, with differences of about 9%, between the experimentally derived relation and the Mills model for moderately high wind speed, that is, in the range of wind speeds most significant for reducing the very high plume rise otherwise reached by smokes.

Also the Carter equation, despite its general validity, has shown good agreement with our experimental equation, with maximum differences of about 10%.

Notation

C_p	specific heat of liquid fuel (kcal/kg K)
E	fraction of radiant emission
f	plume rise factor
F	buoyancy flux (m^4/s^3)
g	acceleration due to gravity (m/s^2)
h_c	heat of combustion (kcal/kg)
h_v	heat of vapourisation (kcal/kg)
Δh	plume rise (m)
Δh_B	plume rise calculated by using the Briggs equation (m)
L	diameter (m)
m	mass burning rate ($kg/m^2 s$)
Q	convective heat output ($kcal/m^2 s$)
Q_h	heat rate released to the smoke (kcal/s)
Q_H	total heat rate (kcal/s)
T_a	ambient temperature (K)
T_b	boiling temperature of liquid fuel (K)
T_s	smoke temperature (K)
ΔT	$T_s - T_a$
ΔT_0	$T_b - T_a$
u	wind speed (m/s)
Z	height (m)
X	downwind distance (m)
γ	entrainment coefficient for buoyant plume rise
$\in$	environmental temperature gradient ($K/m \cdot 10^2$)

References

1　G. Fumarola, D.M. De Faveri, R. Pastorino and G. Ferraiolo, Determining safety zones for exposure to flare radiation, In: 4th Int. Symp. on Loss Prevention and Safety Promotion in the Process Industries, Harrogate, 12–16 Sept., 1983.

2　D.M. De Faveri, G. Fumarola, C. Zonato and G. Ferraiolo, Estimate flare radiation intensity, Hydrocarbon Processing, 64(5) (1985) 89.

3　M.G. Zabetakis and Burges, Research on the hazards associated with the production and handling of liquid hydrogen, Ri 5707, US Bureau of Mines, 1961.

4　G. Fumarola, D.M. De Faveri, E. Palazzi and G. Ferraiolo, Determine plume rise for elevated flares, Hydrocarbon Processing, January (1982) 165–166.

5　D.M. Leahey and M.J.E. Davies, Observation of plume rise from sour gas flares, Atm. Environ., 18(5) (1984) 917–922.

6　M.T. Mills, Modeling the release and dispersion of toxic combustion products from chemical fires. In: Int. Conf. on Vapour Cloud Modeling, Boston, MA, November 1987.

7　D.A. Carter, Methods for estimating the dispersion of toxic combustion products from large fires, Chem. Eng. Res. Des., 67 (1989) 348–352.

8　G.A. Briggs, Plume rise, A.E.C. Critical review series, U.S. Atomic Energy Commission, Div. of Technical Information, 1969.

9   D.J. Moore, Atm. Planet. Boundary Layer Phys. (Longhetto), (1980) 339–340.

10 CONCAWE, The calculation of atmospheric dispersion from a stack CONCAWE Publication, Netherlands, 1966.

11 D.M. De Faveri, A. Vidili, E. Palazzi, C. Zonato and G. Ferraiolo, Effect of wind on thermal radiation of flames in uncontrolled, and large, combustion. Preliminary study. In: Proc. XIth World Cong. on the Prevention of Occupational Accidents and Diseases, Stockholm, May 1987.

12 D.M. De Faveri, A. Vidili, R. Pastorino and G. Ferraiolo, Wind effects on diffusion flames of fires of high source momentum, J. Hazardous Mater., 22 (1989) 85–100.

13 D.M. De Faveri, A. Converti, A. Vidili, A. Campidonico and G. Ferraiolo, Reduction of the environmental impact of coal storage piles: A wind tunnel study, Atm. Environ., 24A (1990) 2785.

14 I.P. Castro and W.H. Snyder, A wind tunnel study of dispersion from source downwind of three-dimensional hills, Atm. Environ., 16 (1982) 1869.

15 G.W. Hoftijzer, Methods for the calculation of the physical effects of the escape of dangerous material, TNO, The Hague, 1979 Chaps. 6 and 11.

Computation of natural gas pipeline rupture problems using the method of characteristics

J.A. Olorunmaiye[a,*] and N.E. Imide[b]

[a] *Department of Mechanical Engineering, University of Ilorin, P.M.B. 1515, Ilorin (Nigeria)*
[b] *Department of Mechanical Engineering, Abubakar Tafawa Balewa University, Bauchi (Nigeria)*

Abstract

The flow in a long, high pressure, natural gas pipeline following sudden rupture was modelled as unsteady one-dimensional isothermal flow. The set of hyperbolic partial differential equations were solved with a numerical method of characteristics. The accuracy of the numerical scheme when using linear characteristics with quadratic interpolation was found to be adequate. It was also found that the effect of the curvature of characteristics in isothermal flow was not as pronounced as it was reported in adiabatic flow by Flatt. To assess the hazard of a natural gas pipeline rupture, it is necessary to know the rate of outflow of the gas at the breakpoint as a function of time. The predicted mass flow rate of gas out of the broken end was 18% lower than that predicted using adiabatic flow theory, whereas, there was good agreement with the results of earlier workers who also used isothermal flow theory whose computation method was based on weighted residuals.

1. Introduction

Transient pressure fluctuations in gas pipelines are usually initiated by sudden opening or closure of valves or by compressors. They involve transmittal and reflection of pressure waves in the piping system and may result in pipe rupture from excessive pressure.

The unsteady flow of a gas in a long pipeline after an accidental rupture is of considerable interest to the gas industry because the pipeline contains an enormous amount of flammable gas and a break in it represents a considerable hazard. It is necessary to know the rate of loss of gas from the break to calculate the dispersion range and ground concentration of the air–gas mixture. After rupture, the flow in the low pressure segment of the pipeline is more complex than that in the high pressure segment since the expansion waves entering the pipeline cause flow reversal in the case of the flow in the low

---
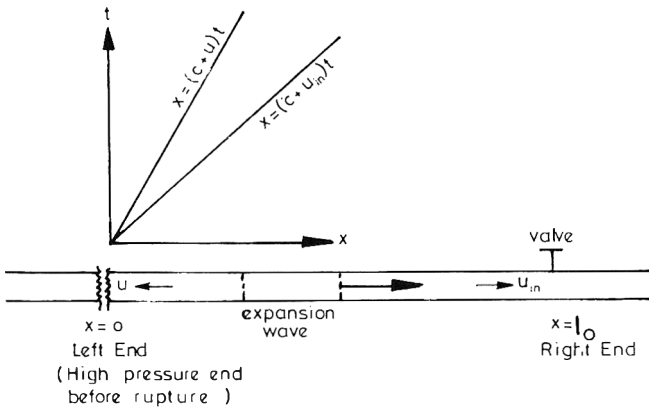
*To whom correspondence should be sent.

Fig. 1. Physical situation of the problem showing an expansion wave entering the pipeline after rupture.

pressure segment. In Fig. 1, it is assumed that the rupture is equal to the pipe cross-sectional area and immediately to the left of the rupture (in the high pressure segment of the pipeline) a valve is closed completely at the instant of rupture.

Fanneløp and Ryhming [1] studied the unsteady flow in a natural gas pipeline in which a break occurred at the high pressure end. They divided the flow into three time regimes. The "early time" regime following the sudden break is dominated by wave processes and the pressure at the open end approaches the ambient value. This is followed by the "intermediate time regime" in which an internal pressure peak occurs, the location of which corresponds approximately with the location of flow reversal where the velocity is zero. By the time the pressure peak gets to the low pressure end of the pipe (the closed end), the "late time" regime starts. In this time regime, the pressure in the pipeline decreases monotonically from the closed end of the pipe to the open end.

They used an integral method to analyse the unsteady flow in the pipeline assuming the flow to be isothermal. They ignored inertia terms in the equations to obtain a set of parabolic equations. Their method could not handle the early time regime and it gave no information on the internal flow because spatial distributions in the range $x = 0$ to $x = l_0$ were assumed for the pressure and pressure–velocity product to obtain solutions.

Lang and Fanneløp [2] improved on this work by using some approximation procedures in the family of weighted residuals. The flow profiles were not specified *a priori* as in the work of Fanneløp and Ryhming but were found as part of the solution. They were able to obtain more accurate results but their methods produced oscillations in the dependent variables predicted during the early time regime.

Ryhming [3] used the method of matched asymptotic expansion to study unsteady isothermal flow in a long pipeline ruptured suddenly. He showed that wall friction caused the velocity derivative along the pipe to become singular at the broken end exit when the flow there was critical. His composite first order solution gave velocity profile in the pipeline at various times. Since his analysis concentrated on predicting the velocity profile and did not include pressure or density variations in the pipe, it could not be used to predict the flow rate out of the pipe during the early time regime.

Flatt [4] developed a method of characteristics to compute unsteady adiabatic flow of natural gas in a long pipeline following a sudden break. Since he used the full set of hyperbolic partial differential equations, his method could handle flows in the three time regimes.

However, with high pressure variations such as occur in pipeline break problems, heat transfer between the fluid and the medium surrounding the pipe will be appreciable unless the pipe is lagged. In fact, the flow process is expected to be closer to isothermal than adiabatic flow due to compensating errors in density and critical velocity that occur in the former. The present effort is directed at developing a numerical method of characteristics to solve the set of hyperbolic partial differential equations describing unsteady isothermal flow following a break in a long pipeline. It therefore compliments the works of Ryhming, Fanneløp and Lang in supplying the missing information in their analysis during the early time regime. It also has the advantage of being applicable to the three flow time regimes.

Flatt [4] did not apply his adiabatic flow model to predict the flow up to the late time regimes because of the long computer time it would take. Since the set of equations for isothermal flow (two equations) is simpler than that for adiabatic flow (three equations) computation time will be less of a problem in this case of the former type, thereby making it less expensive for computing the flow for all the time regimes.

2. Mathematical model

For one-dimensional flow in a pipe of uniform diameter, the conservation equations for mass and momentum are

$$\frac{\partial \rho}{\partial t} + u \frac{\partial \rho}{\partial x} + \rho \frac{\partial u}{\partial x} = 0 \tag{1}$$

$$\frac{\partial u}{\partial t} + u \frac{\partial u}{\partial x} + \frac{1}{\rho} \frac{\partial P}{\partial x} + F = 0 \tag{2}$$

where

$$F = \frac{2f}{d} u |u| \tag{3}$$

and u^2 being expressed as $u|u|$ to ensure that the frictional force shall always act opposite to the direction of motion.

The equation of state for isothermal flow of a perfect gas is

$$P = \rho R T_0 \tag{4}$$

Eliminating density, ρ, from eqs. (1) and (2) using (4), the continuity and momentum equations become

$$\frac{\partial p}{\partial t} + u\frac{\partial p}{\partial x} + P\frac{\partial u}{\partial x} = 0 \tag{5}$$

and

$$\frac{\partial u}{\partial t} + u\frac{\partial u}{\partial x} + \frac{c^2}{P}\frac{\partial P}{\partial x} + F = 0 \tag{6}$$

where the expression for isothermal speed of sound

$$c^2 = R T_0 \tag{7}$$

has been used.

Although the isothermal speed of sound does not change, the expansion wave will fan out as shown in Fig. 1 because the head of the wave travels in fluid particles having positive velocity, whereas the tail travels at velocity c relative to particles having negative velocity.

Choosing the length of the pipe, isothermal speed of sound, the ambient pressure and temperature as the reference parameters, the non-dimensional forms of eqs. (5) and (6) are:

$$\frac{\partial P'}{\partial Z} + P'\frac{\partial U}{\partial X} + U\frac{\partial P'}{\partial X} = 0 \tag{8}$$

$$\frac{\partial U}{\partial Z} + U\frac{\partial U}{\partial X} + \frac{1}{P'}\frac{\partial P'}{\partial X} = -F' \tag{9}$$

3. Numerical method

Equations (8) and (9) constitute a set of quasi-linear hyperbolic partial differential equations which can be solved using the method of characteristics. Hartree's hybrid scheme which was used earlier by Olorunmaiye and Kentfield [5] is also used in this work. In this method, a rectangular grid is imposed on the integration domain and the equations are integrated along the characteristics directions. The dependent variables here are P and U.

The characteristic curves of eqs. (8) and (9) are given by

$$\frac{\mathrm{d}X}{\mathrm{d}Z} = U \pm 1 \tag{10}$$

Equation (10) gives the downstream and upstream propagation directions in the X–Z plane, of a pressure wave travelling at the isothermal speed of sound relative to the fluid.

The compatibility equations along the characteristics having reciprocal slopes $(U+1)$ and $(U-1)$, respectively, are

$$\frac{1}{P'}\frac{\delta_+ P'}{\delta Z}+\frac{\delta_+ U}{\delta Z}+F'=0 \tag{11}$$

$$-\frac{1}{P'}\frac{\delta_- P'}{\delta Z}+\frac{\delta_- U}{\delta Z}+F'=0 \tag{12}$$

The characteristics reaching a grid point for different flow velocities are shown in Fig. 2. The characteristics having reciprocal slopes $(U+1)$ and $(U-1)$ are labelled OV and TV, respectively. The finite difference approximation of eqs. (11) and (12) are

$$U_V-U_O+(\ln P'_V-\ln P'_O)=-F'_{OV}\Delta Z \tag{13}$$

$$U_V-U_T-(\ln P'_V-\ln P'_T)=-F'_{TV}\Delta Z \tag{14}$$

Rearranging eqs. (13) and (14) gives

$$P'_V=\exp\left[\tfrac{1}{2}\{(F'_{TV}\Delta Z-F'_{OV}\Delta Z+U_O-U_T+\ln P'_T+\ln P'_O)\}\right] \tag{15}$$

The double subscripts on a term indicates that the term is taken to be the mean of its value at the end points indicated by the two subscripts (See Fig. 2).

4. Boundary conditions

For flow with velocity $|U|\leqslant 1$, only characteristic OV reaches the grid point at the right end whereas only characteristics TV reaches the grid point at the left end.
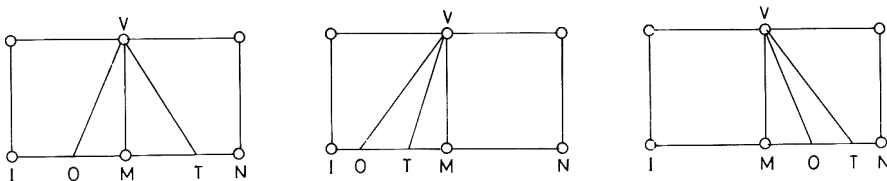
(a) Flow with |u| < 1   (b) Flow to the right   (c) Flow to the left
                                   with |u| > 1   with |u| > 1

Fig. 2. Characteristics reaching an internal grid points.

4.1 Right end

Assuming the change causing unsteady flow in the pipeline happens at the left end as in Fig. 1, the pressure and velocity at the right end is not affected until Z^* when the wave reaches there. Hence,

$$U_V(Z \leqslant Z^*) = U_R \quad (Z=0) \tag{16}$$

$$P'_V(Z \leqslant Z^*) = P'_R \quad (Z=0) \tag{17}$$

where U_R and P'_R are flow variables at the right end at the initial condition.

To simulate the worst case, the valve at the right end is shut instantaneously at the time the wave reaches this position.

$$U_V(Z > Z^*) = 0 \tag{18}$$

This equation and the compatibility equation along OV are solved to obtain the value of P_V at the right end.

4.2 Left end

At the left end, two distinct time sequences are considered. As long as the pressure is sufficiently greater than the external pressure, the flow will be choked and

$$U_V = -1 \tag{19}$$

Treating the outflow at the broken end when choking occurs as isothermal is a rough approximation. A very high heat transfer rate from the ambient to the gas would be necessary to keep the temperature of the rapidly expanding gas from falling. However, the loss of gas when the outflow is choked is small in comparison with the total amount of gas lost during the three time regimes because of its short duration. Therefore the inaccuracy of this assumption does not affect the computation appreciably.

When the pressure falls to the level of external pressure, the condition used is

$$P'_V = P'_A \tag{20}$$

4.3 Other boundary conditions

Other boundary conditions which may be used with the model are:
 (i) prescription of the static pressure as a function of time.
(ii) prescription of the velocity as a function of time. This may be used to simulate valve closure.
The other dependent variable can then be obtained by using the appropriate compatibility equation.

5. Initial conditions

The initial condition is the steady state in the pipeline prior to the initiation of unsteady flow. Neglecting $\ln(P_{IN}/P)^2$ in comparison with $4fx/d$ in long

pipelines (see eq. (6.42) of Ref. [6]), the initial distributions of pressure and velocity in steady isothermal flow are given approximately by

$$P'(X, Z=0) = P'_{IN}\left(1 - \frac{4fU^2_{IN}}{D'} X\right)^{1/2} \tag{21}$$

$$U(X, Z=0) = D_{IN} U_{IN}/P'(X, Z=0) \tag{22}$$

6. Stability and accuracy criteria

The time step was chosen in accordance with the Courant–Friedrichs–Lewy stability criterion which requires that

$$\Delta Z \leqslant \frac{\Delta X}{1+|U|} \tag{23}$$

Eighty percent of this maximum allowable time step was used for the computations.

An accuracy criterion based on the law of conservation of mass, defined by Flatt [4] was used in this work. The accuracy criterion is defined as

$$\varepsilon = \frac{(\text{Mass in pipe at time } t) - (\text{Mass in pipe at time } t + \Delta t)}{(\text{Rate of mass outflow at both ends})\Delta t} \tag{24}$$

The ideal value is 1. Hence, the error is

$$e = \varepsilon - 1 \tag{25}$$

Flatt [4] introduced a factor K_f by which the friction terms of the compatibility equations are multiplied for the boundary grid point when the flow is sonic. Using the value $K_f = 1$ leaves the relations unchanged, whereas $K_f = 0$ indicates that the viscous terms are completely omitted.

He found that the singularity at the broken end during critical flow which was discussed in Ryhming's paper [3] caused greater error in the computation when $K_f = 1$ than $K_f = 0$.

7. Numerical schemes

The equation for the characteristic curves and compatibility relations have been derived following standard procedures. However, the actual numerical implementation of the method of characteristics is not standard. Linear or quadratic interpolation may be used to obtain values of dependent variables at the feet of OV and TV characteristics at the old time level. Also the characteristics may be assumed to be straight or the effect of their curvatures may be considered as suggested by Flatt [7].

Three numerical schemes used in this work are:
 (i) linear characteristics and linear interpolation;
 (ii) linear characteristics and quadratic interpolation; and
(iii) curved characteristics and quadratic interpolation
A more detailed description of the computation can be found elsewhere [8].

8. Results and discussion

FORTRAN programmes written for the three schemes mentioned above were run on a SWAN AT 286/12 IBM Compatible Personal Computer with a math co-processor using a WATFOR 87 compiler.

The physical case to which the programmes were applied is an underwater pipeline of length 145 km, internal diameter 0.87 m, inlet pressure 133 atm, outlet pressure 55 atm, gas temperature $T_0 = 281$ K, and flow rate about 650 kg/s. The outside pressure $P_0 = 6$ atm (corresponding to 50 m depth). The pipeline is filled with natural gas having a ratio of specific heats $\gamma = 1.3$ and specific gas constant $R = 428.2$ J/kg·K. This was the case considered in references [1], [2] and [4]. The flow in the pipeline is initially steady and isothermal until time $t = 0$ when the pipe is completely broken suddenly at the high pressure end. A constant friction factor $f = 0.0018$ which gives a pressure drop of 78 bars for the steady flow before breakage, was used in the computation of the unsteady flow.

8.1 Comparison of the three schemes

Table 1 shows the errors and computing time for various number of grid points when the unsteady flow process had taken place for 100 seconds. The effect of the magnitude of K_f can be seen. When $K_f = 1$, greater magnitudes of error were obtained and the computation time were higher than when $K_f = 0$ as was observed by Flatt [4]. Therefore the viscous term was omitted in the compatibility equation ($K_f = 0$) for the left boundary grid point when the flow there was critical, in subse quent computations as was suggested by Flatt [4].

TABLE 1

Comparison of error and computation time for the time interval $t = 0$ to $t = 100$ s for the three numerical schemes for various numbers of grid points

Number of grid points	Value of K_f	Error, e at $t = 100$ s			CPU Time (s)		
		LCLI[a]	LCQI[b]	CCQI[c]	LCLI[a]	LCQI[b]	CCQI[c]
201	0	0.357	0.429	0.432	69.92	75.74	83.04
	1	0.967	1.033	0.880	89.42	92.71	119.91
401	0	0.228	0.231	0.233	251.40	280.56	309.73
	1	0.837	0.671	0.669	282.64	310.39	342.52
801	0	0.146	0.124	0.124	966.96	1087.74	1202.59
	1	0.437	0.334	0.330	1148.08	1278.04	1296.90
1601	0	0.088	0.066	0.066	3927.39	4289.46	4745.56
	1	0.231	0.170	0.169	4431.55	4564.58	5223.91

[a] LCLI = Linear Characteristic and Linear Interpolation.
[b] LCQI = Linear Characteristic and Quadratic Interpolation.
[c] CCQI = Curved Characteristic and Quadratic Interpolation.

The higher the number of grid points, the smaller the error for each of the three schemes as expected. At a higher number of grid points the two numerical schemes with quadratic interpolation gave lower errors than the scheme with linear interpolation.

The magnitudes of errors shown in Table 1 may not give a fair assessment of the accuracy of the numerical method employed in this work. A global error criterion (in time) rather than the local error criterion given in eq. (24), may be better. Even the numerical evaluation of eq. (24) is in itself sensitive to numerical accuracy.

Figure 3 shows the comparison of mass flow rate at the broken end predicted with the three numerical schemes using 401 grid points. Since the results predicted with the two schemes using quadratic interpolation agree very closely, it is better to use the linear characteristics with quadratic interpolation scheme because the computer time is lower.

The effect of the curvature of the characteristics is not as important in this work as it was in the work of Flatt [4, 7]. Since the value of the isothermal acoustic velocity (c) remains constant for isothermal flow, the changes in the slopes of the characteristics OV or TV ($u \pm c$) are caused only by changes in
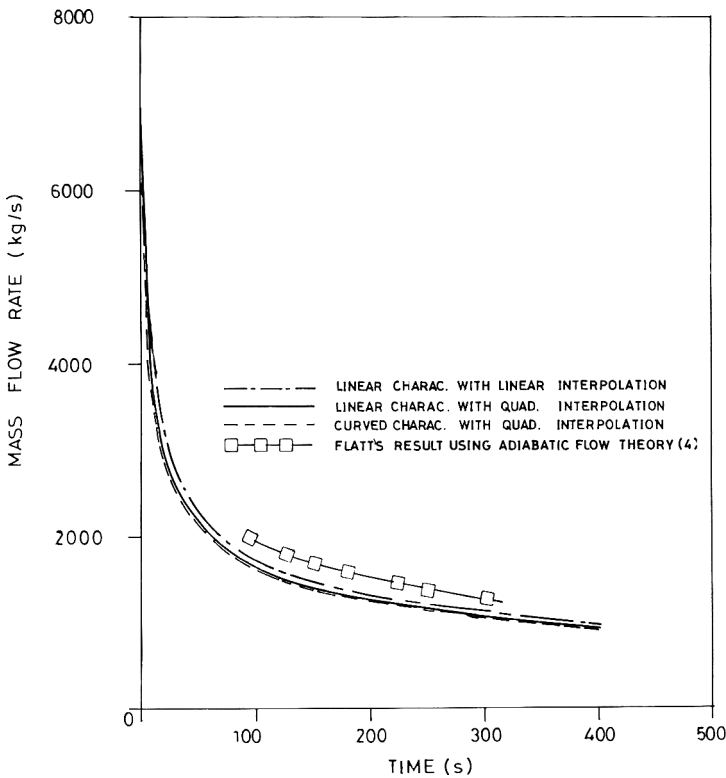
Fig. 3. Comparison of mass flow rate at the ruptured end predicted with the three numerical schemes using 401 grid points. The result obtained by Flatt using adiabatic flow theory is also shown.

magnitude of velocity which are small especially for a fine grid. This is unlike the case of adiabatic flow in which the reciprocal slope of the characteristics are $(u \pm a)$ and both velocity and isentropic acoustic velocity (a) change between T and V and O and V thereby making the slopes vary appreciably.

Secondly an isothermal flow has only two families of characteristics whereas an adiabatic flow has three families of characteristics.

8.2 Test cases

Since a laboratory test of this type of problem cannot be performed in view of the enormous length/diameter ratio, no experimental results are available to test the model. It is necessary to find some other means to assess the model. Ryhming [3] gave the closed form solution of frictionless unsteady isothermal flow obtained during the early time regime when initially there is no flow in the pipe as

$$U = \frac{X}{Z} - 1 \tag{26}$$

for the geometry being considered.
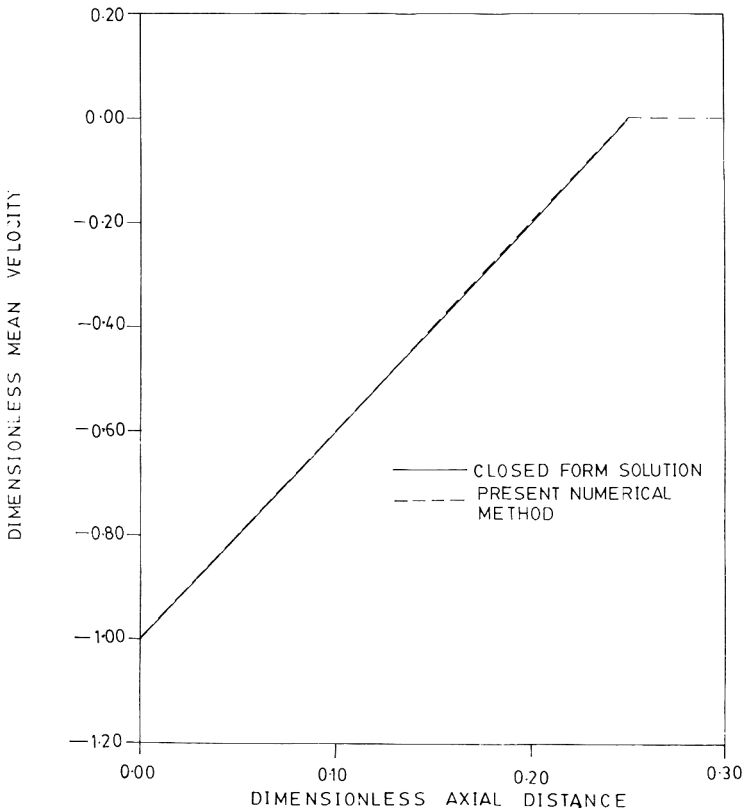
Fig. 4. Comparison of velocity distribution in a pipeline at $Z = 0.25$ predicted with the model for unsteady frictionless isothermal flow following sudden break in the pipeline, with result obtained from closed form solution.
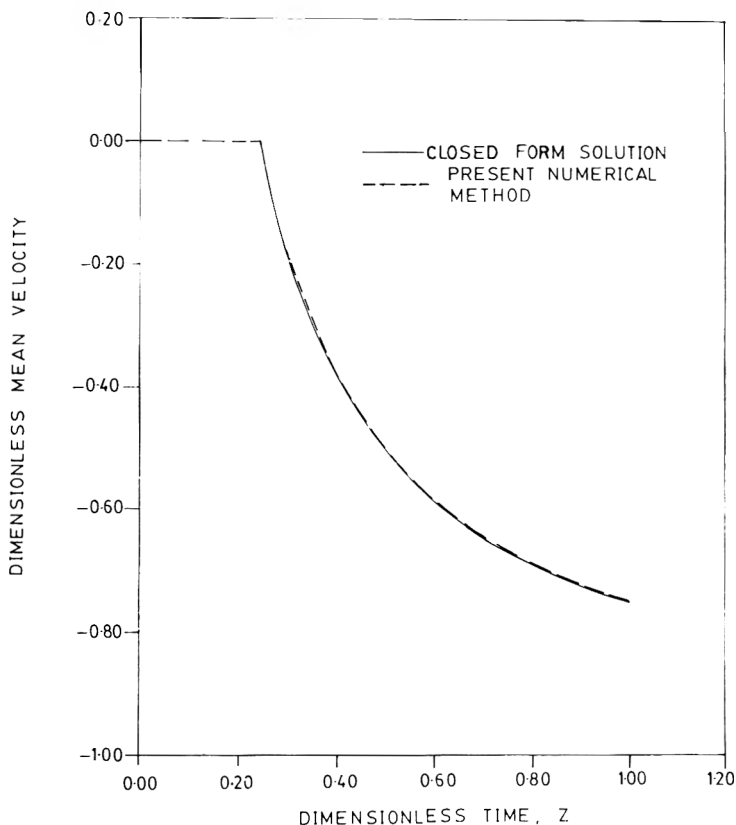
Fig. 5. Comparison of variation of velocity with time at $X = 0.25$ predicted with the model for unsteady frictionless isothermal flow following sudden break in a pipeline, with the result obtained from closed form solution.

This solution is applicable for $X \leqslant Z$. For $X > Z$ the velocity $U = 0$, since the expansion wave causing leftward flow to the ruptured end has not arrived at that point yet. Figures 4 and 5 show comparisons of results predicted with the model with the closed form solution when the pipe was initially filled with natural gas at dimensionless pressure of 22.17. The agreement of the results predicted with the model with the closed form solution is excellent.

In the second test case, the pipeline was loaded to a dimensionless pressure of 22.17 (with reference to ambient pressure of 6 atm at the pipeline depth) and a diaphragm separates the left end from a lower pressure reservoir of pressure 9.05. The diaphragm at the left boundary is punctured suddenly at time $t = 0$. After the transients have died out, the flow obtained should coincide with steady isothermal flow as in eqs. (21) and (22). The pressure and velocity distribution in the pipeline at various times, predicted with the model are shown in Figs. 6 and 7. The pressure and velocity distributions at $t = 10,000$ s agree quite well with the steady state solutions, considering the fact that coarse grids were used in the computation.
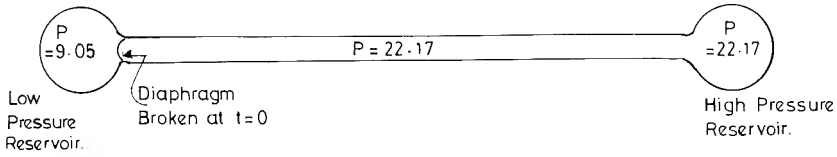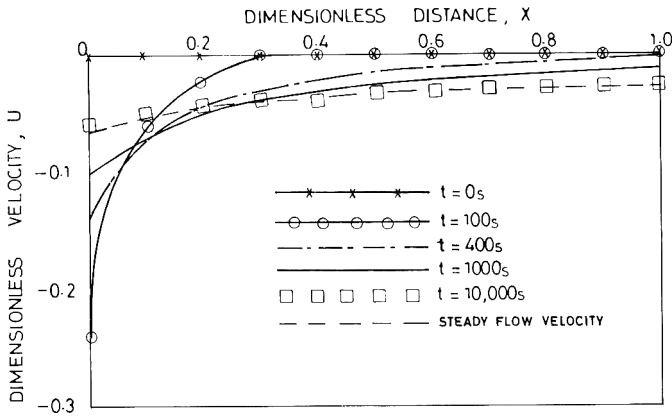
Fig. 6. Velocity distribution at various times for a pipeline linking two reservoirs (101 grid points were used in the computation).
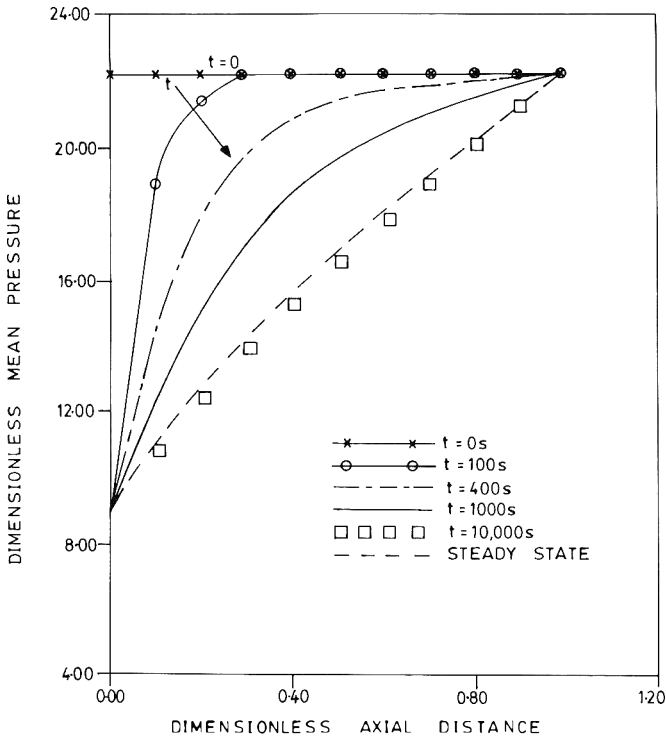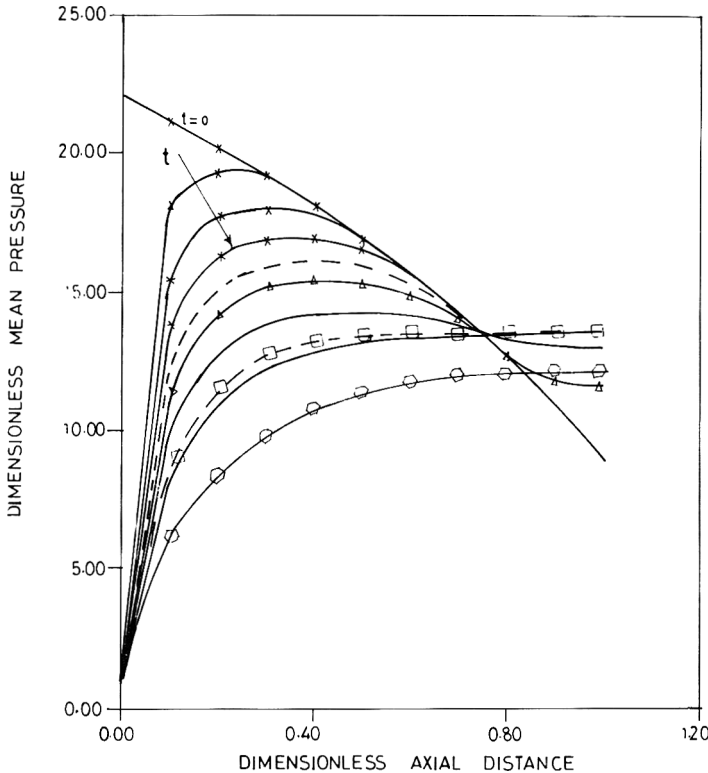
Fig. 8. Pressure distribution in the pipeline after rupture, predicted using 401 grid points, parameter: $t = 0$, 100, 200, 300, 400, 500, 700, 900, 1000, 2000 s.

8.3 More results for the North Sea gas pipeline

The pressure distribution in the pipeline at various times after rupture are shown in Fig. 8. It is interesting to see that the pressure does not change at dimensionless distance of 0.75 from the broken end for a very long time (at least 1000 seconds). In Flatt's result, such a point can be seen at a distance of 0.68 from the broken end in his adiabatic flow analysis for the case in which the valve at the low pressure end was closed at $t = 0$. If the pressure in the pipeline were monitored at such a point there would be no appreciable change in the indicated pressure for a very long time, even after the expansion wave initiated at the rupture has reached that point.

The variation of pressure at the left and right ends with time are shown in Figs. 9 and 10. The pressure starts to rise at the right end as soon as the expansion wave gets there and the valve is shut and peaks at a valve of about 13.7 before it begins to fall.

Shown in Fig. 3 is the mass flow rate out of the broken end between $t = 100$ s and $t = 300$ s obtained by Flatt [4] using unsteady adiabatic flow theory. The

Fig. 7. Pressure distribution at various times for a pipeline linking two reservoirs (101 grid points were used in the computation).
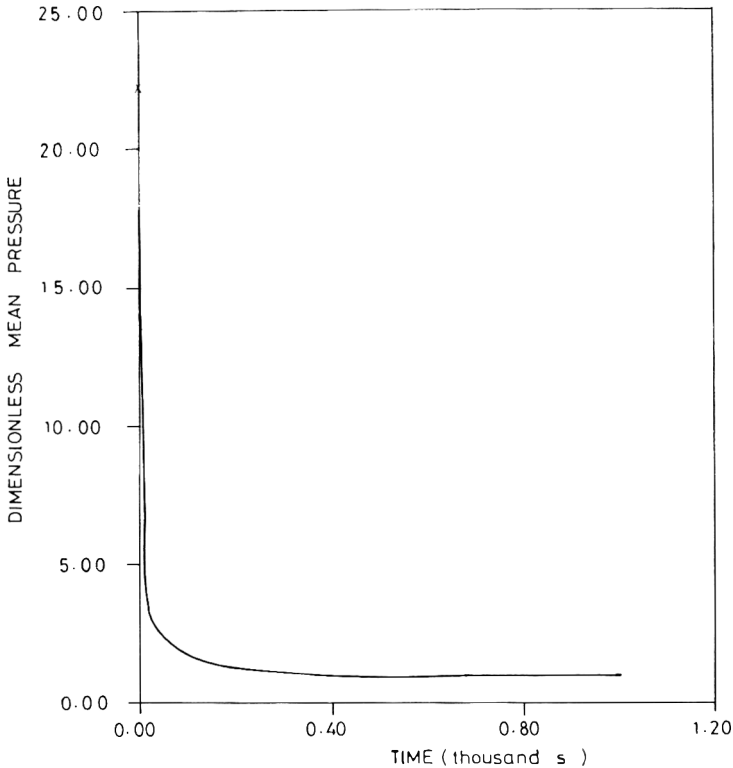
Fig. 9. Predicted pressure variation with time at the break point.

results obtained in this present work using isothermal flow theory are lower than Flatt results by about 18%. This is partly due to the fact that the isentropic sonic velocity is higher than isothermal sonic velocity.

Figure 11 shows the dimensionless mass flow rate predicted using different number of grid points. It took 7 h, 57 min and 17 s to compute the flow for a real-flow time of 2,000 s using 401 grid points. Using 201 and 101 grid points it took 5 h, 54 min and 3 h, 45 min and 61 s to compute the flow for real-flow times of 7,000 and 20,000 seconds, respectively. These results agree quite well with that obtained by Lang and Fanneløp [2] using spectral collocation method with Legendre polynomials, as can be seen in Fig. 11.

From Fig. 3, the mass flow rate out of the broken end was initially 7,550 kg/s. By 100 s the mass flow had reduced to 1630 kg/s. After 5 h and 30 min the mass flow rate was less than 15 kg/s, as can be seen in Fig. 11.

9. Conclusions

A mathematical model based on unsteady isothermal flow theory and solved by the method of characteristics has been presented. The model predicts results consistent with the predictions of other workers.
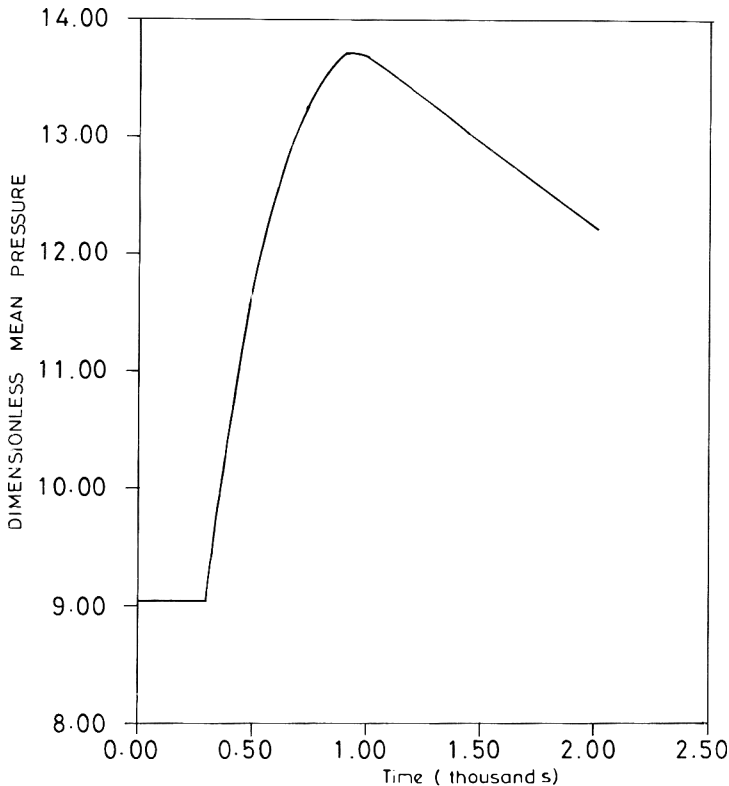
Fig. 10. Predicted pressure at the right hand end of the pipe segment.

Flow rate predicted at the broken end of the pipe is lower than that of adiabatic flow theory by about 18% but it agrees quite well with that of Lang and Fanneløp obtained using a method of weighted residuals to solve unsteady isothermal flow equations.

At a dimensionless distance of 0.75 from the broken end of the pipeline segment, the pressure does not change for a very long time.

The curvature of the characteristics is not as pronounced in isothermal flow as it is in adiabatic flow. Therefore it is not necessary to include the effect of the curvature of the characteristics in the computation of unsteady isothermal flows.

This model is useful in analysing other unsteady flows associated with pipeline operations, such as controlled venting to the atmosphere prior to shutdown or repair, and sudden changes in pressure at either end of the pipeline. The waves generated in these operations cannot be as strong as the waves associated with pipeline rupture. Hence the model can handle such situations easily. All that is necessary is to use appropriate boundary conditions.
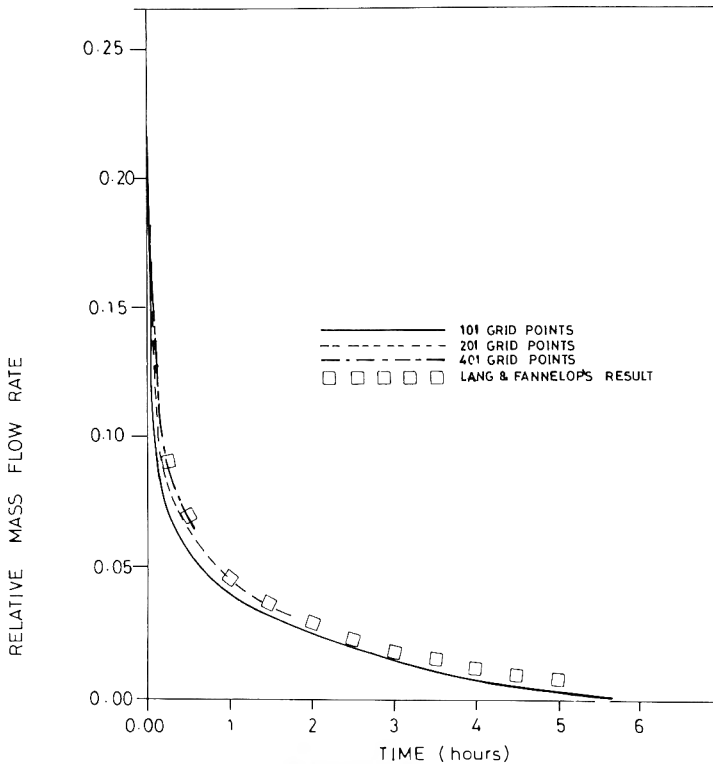
Fig. 11. Relative flow rate ($\dot{m}(0, t)/\dot{m}(0, t=0)$) at the break as a function of time.

Acknowledgements

Notation

Where applicable non-dimensional forms are given.

Roman

c		Isothermal speed of sound
		Reference velocity
d	$D' = d/l_0$	Pipe diameter
e		Error

f		Friction factor
F	$F' = Fl_0/c^2$	Friction force per unit mass
I, M, N, V		Grid points
l_0		Pipe length. Reference length
O, T		Feet of characteristics
P	$P' = P/P_0$	Mean pressure at a pipe cross-section
P_0		Ambient pressure. Reference pressure.
R		Specific gas constant
t	$Z = tc/l_0$	Time
T_0		Ambient temperature. Reference temperature
u	$U = u/c$	Velocity
x	$X = x/l_0$	Axial distance
$Z*$		Non-dimensional time taken for wave to travel from the left end to the right end

Greek

Δt	ΔZ	Time step size
Δx	ΔX	Spatial grid size
ε		Accuracy criterion
ρ	$D = \rho/\rho_0$	Density
ρ_0		Density of gas at the reference pressure and temperature

Subscripts

IN	Initial conditions at left end of pipeline
O	Foot of characteristic OV
OV	Along characteristic OV
R	Dependent variables at right end
T	Foot of characteristic TV
TV	Along characteristic TV
V	Grid point V

Superscripts

Normalized with respect to appropriate reference value

Operators

D/DZ	Substantial derivative
$\delta_+/\delta Z$	Differentiation following characteristic having reciprocal slope $(U+1)$
$\delta_-/\delta Z$	Differentiation following characteristic having reciprocal slope $(U-1)$

References

1   T.K. Fanneløp and I.L. Ryhming, Massive release of gas from long pipelines, J. Energy, 6 (1982) 132–140.

2   E. Lang and T.K. Fanneløp, Efficient computation of the pipeline break problem. 3rd
    Symp. on Fuid-Transients in Fluid Structure Interaction. FED, Vol. 56, ASME Winter
    Annual Meeting, Boston, MA, 1987.
3   I.L. Ryhming, On the expansion wave problem in a long pipe with wall friction, J. Appl.
    Math. Phys. (ZAMP), 38 (1987) 378–390.
4   R. Flatt, Unsteady compressible flow in long pipelines following a rupture, Int. J. Num.
    Methods Fluids, 6 (1986) 83–100.
5   J.A. Olorunmaiye and J.A.C. Kentfield, Numerical simulation of valveless pulsed combus-
    tors, Acta Astronautica, 19 (1989) 669–679.
6   A.H. Shapiro, The Dynamics and Thermodynamics of Compressible Fluid Flow, Vol. I,
    Wiley, New York, 1953.
7   R. Flatt, A singly-interactive second-order method of characteristics for unsteady com-
    pressible one-dimensional flows, Commun. Appl. Num. Methods, 1 (1985) 269–274.
8   N.E. Imide, Computation of Unsteady Isothermal Flow in Long Natural Gas Pipelines.
    M. Eng. Thesis, University of Ilorin, Ilorin, Nigeria, Sept. 1991.

Book Reviews

Hazard Communication Standard Inspection Manual, 3rd edn., by U.S. Department of Labor, Occupational Safety and Health Administration, Directorate of Compliance Programs, Office of Health Compliance Assistance, Government Institutes, Rockville, MD, 1991, ISBN 0-86587-256-2, 198 pp., $55.00.

The Hazard Communication Standard Inspection Manual was developed by the Office of Health Compliance Assistance in OSHA for the following purpose;

"...establishes policies and provides clarifications and ensures uniform enforcement of the Hazard Communication Standard (HCS)."

(HCS is found in 29 CFR 1910.1200 — HAZWOPER). The first 31 pages of the manual convey OSHA's message on the topic with a major focus on Inspection Guidelines, Violations and Interfacing with old standards.

The major share of the book, as with many other compliance manuals is taken up by appendices, several of which are Federal Register page reprints.
  Major appendices include:
- Clarifications and interpretations of the hazard and communication standards.
- Permissible exposure limits (to contaminants)
- Occupational exposure and hazardous chemicals in laboratories — 29 CFR 1910.1450
- Hazardous waste operations and emergency response (HAZWOPER) 29CFR 1910.120

G.F. BENNETT

Emerging Technologies in Hazardous Waste Management II, by D.W. Tedder and F.G. Pohland (Eds.), ACS Symposium Series 4681, American Chemical Society, Washington, DC, 1992, ISBN 0-8412-2102-2, 444 pp., $89.95.

This book is a continuation of a conference session theme begun in 1989. The last volume bearing the same title was published in 1990; in it 22 papers were published. In reviewing the first volume of what appears to be a series, I said the papers were more "innovative" than "emerging" technology. Not so for this one. Many of the papers are truly emerging technologies — biofilters, sequencing batch reactors and stabilization processes.

Twenty papers have been published under four main headings:
1. Thermal treatment and abiotic emissions control
2. Water management
3. Biological treatment
4. Solid waste management

Actually the papers are quite varied, ranging from those dealing with currently utilized technology to basic research.

For example there were papers describing application of sequencing batch reactors, ultraviolet light/ozone/hydrogen peroxide reactor systems and biofilters. All three processes are now utilized industrially for waste treatment. In the emerging stage, I would place a paper from Chicago's Institute of Gas Technology on hazardous material destruction in a self-regenerating combustor-incinerator and in the same category one on detoxification of organophosphate pesticides by an immobilized enzyme system. In the basic research area, I would place papers on the incineration of contaminated soils in an electrodynamic balance and a paper on multicomponent ion exchange-equilibrium Chazabite zeolite. Finally there were two review papers worthy of note, one on contaminant leaching from stabilized waste and another on oxidative techniques for ground water treatment.

GARY F. BENNETT

Controlling Chemical Hazards: Fundamentals of the Management of Toxic Chemicals, by R.P. Cote and P.G. Wells (Eds.), Unwin Hyman, Boston, MA (distributed by Chapman and Hall, London), 1991, ISBN 0-040-60402-1 (hb), 310 pp., £40.00.

In the preface the authors write:

"This book presents environmental protection managers and advanced students in environmental studies programs with an overview of the principles, facts, multidisciplinary approach, and some of the complexities of the management of toxic substances."

To accomplish this task, the editors solicited experts from government, industry, academia, law and environmental groups to write 13 separate but loosely interconnected chapters that deal mainly with toxicology and risk assessment, fate and transport and workplace exposures. In this context, I would rate this book as fair to good.

The editors claim further coverage:

"The text explores critical issues facing managers' responsibilities for preventing and controlling problems associated with the manufacture, transport, use and disposal of chemicals."

In this area I would not rate the book highly.

The obligatory reference to the tragic accident involving methyl isocyanate at Bhopal is noted (about 3400 deaths are claimed, a number that seems to

climb with every new reference). To complete the release scenario, the Love
Canal, Valley of the Drums, and Chernobyl are cited. Not famous, but de-
scribed in detail, is a pesticide warehouse fire in Nova Scotia. Unintentionable
as these problems were, their impact and especially their avoidance/control
were not. However catastrophic these accidents were, the book would have
been much better if the editors (contributors) had stuck to the risk/toxicol-
ogy/transport scenarios — or problems of chronic emissions and left out acute
spills/releases.

Other criticisms include chapters not terribly well written and others that
rambled appearing to be without organization. As is common with multi-
authored texts, great difference is found between the different chapters.
However, the book is very well referenced.

Unfortunately, this is not one book I can recommend. But it could be
improved by, as noted above, a clear focus and much improved editing. Addi-
tionally, I'd begin each chapter with an abstract or preview of what's in the
chapter.

GARY F. BENNETT

The Generator's Guide to Hazardous Materials Management, by L.H. Traverse,
Van Nostrand Reinhold, New York, NY, 1991, ISBN 0-442-00159-2, 420
pp., $59.95.

With a gross understatement Traverse begins his book with the following:

"Today's environmental coordinator faces a full calendar of regulatory responsibilities. The laws
for land, air, and water are challenging and ever-changing as progress continues and our environ-
mental knowledge grows. The subjects and regulations concerning our environment are at times
difficult to comprehend without proper training."

He then continues with a very practical text that outlines for the most basic
user, the essentials of safe and environmentally sound (that means legally
correct) practices of handling, storage and disposing of hazardous chemicals and
hazardous wastes. In doing this, Traverse neatly interwines regulations and
regulatory forms with his explanations of what they mean and how to use them.

His technique is perhaps best illustrated by Chapter 5: Chemistry of the
Material Safety Data Sheet. Traverse begins with the question: How much
chemistry do I have to know? And then he goes through each section of
a Materials Safety Sheet to answer his own question. First he shows an
example section, then he discusses what information is found in that section
and what it means.

When written (1991) the book was current with even a discussion of the new
U.S. EPA land ban regulations. But I noted that one minor section on when the
clock begins running for drum accumulation of wastes has changed (in the
year this reviewer delayed in writing the review) thus emphasizing once again
how dynamic (that means ever changing) regulations are.

The book ends with a short chapter on source reduction. Although not exhaustive, what was written makes a good introduction to a very important topic.

My only major criticism of the book is the lack of reference to other articles and books on this topic. Conversely, reference to government regulations is quite complete.

The book has an excellent (seven-page) detailed table of contents, eight appendices (audit forms, regulations, etc.), and a comprehensive index.

I recommend the book to those newly entering the hazardous wastes arena — which arena unfortunately reminds me of the Roman game when the slaves faced ferocious animals.

G. F. BENNETT

Hazards in the Chemical Laboratory, 5th edn., edited by S.G. Luxon, Royal Society of Chemistry, Thomas Graham House, Science Park, Milton Road, Cambridge CB4 4WF, United Kingdom or CRC Press, Inc., 2000 Corporate Blvd., N.W., Boca Raton, FL 33431, 1992, ISBN 0-85186-229-2, 675 pp., £45.00, or $99.95 + 7.50 delivery.

This is a revised, updated and expanded version of a volume which was first published in 1971. The fifth edition covers the latest regulations of the European Community and United Kingdom relating to chemical laboratories, and even includes a chapter on the American viewpoint. Legal aspects of laboratory work introduce the text, followed by safety planning and laboratory design. Fire protection receives an excellent treatment, while reactive chemical hazards, as reviewed by the previous editor, Leslie Bretherick, are given full attention. Chemical hazards and Toxicology, as well as control of health hazards, are noted in detail, as are; first aid treatments and procedures for chemical exposures. Radiation and also electrical hazards are assessed in terms of the laboratory.

Perhaps the most valuable part of the book is the quick guide to the hazardous properties of nearly 1400 substances, which, along with labeling requirements, give quick and authoritative references in an easy to read form. An index of CAS Registry Numbers is included.

This is a very practical volume, and should be available on a wide basis, in school, college, and industrial laboratories.

HOWARD H. FAWCETT

Hazardous Metals in the Environment (Techniques and Instrumentation in Analytical Chemistry, Vol. 12), edited by M. Stoeppler, Elsevier Science Publishers, Amsterdam, 1992, ISBN 0-444-89078-5, X + 542 pp., $225.50/Dfl 395.00.

The potential human and environmental impact of heavy metals has resulted in significant effort being expended in the study of their source, fate and

transport, analysis and toxicology. Key to these studies is an accurate determination of the metal content of liquids and solids. Thus, the rapid progress in methodology in this area has dictated a need for periodic update and review of the field. That is the purpose of this multi-authored text, and it is well accomplished.

The book has 17 chapters contributed world-wide (with many from Europe) by experts in each area, and each chapter is exceedingly well referenced. The shortest chapter reference list has 31 entries; the longest 445. References in the complete book exceed 3400 in total! One minor point here is even at the expense of adding more pages to the book, I would have liked to have seen titles of all papers cited and not simply author, journal, pages. For me, the title of a cited paper gives a great deal of information. Given the European source of the book, it is not surprising the literature cited leans heavily on their (European) literature. That is excellent for non-European readers, but I note that much U.S. literature has been missed in the one area I was keenly interested in — leaching.

The book offers the reader a general introduction to the problem areas that are currently under study. Following the introduction (by the editor), there are chapters on sampling and sample preservation, strategies and application of the archiving of selected representation specimens for long-term storage in environmental specimen banks.

In this section is an intriguing chapter on the analysis of metals in wine, as a preserved, frequently already historical specimen that clearly reflects technological change over time — this changing technology being the use of different materials in producing and growing grapes over time and the use of different pesticides such as arsenic many years ago. Generally, metal concentrations in wine have fallen, not unexpectedly, with time. I was interested in comparing metal existing and allowable (by German Standards) metal concentrations.

Metal	Century	Mean concentration (μg/L)	Allowable concentration (μg/L)	
			Wine	Water
Cd	18th	5.0	10	—
	19th	3.9		
	20th	1.9		
Pb	18th	2680	300	—
	19th	4320		
	20th	611		
Co	18th	6.8	—	—
	19th	13.9		
	20th	7.9		

The second part of the book provides information on anlaytical methods in determining the levels of a number of toxicologically, ecotoxicologically and ecologically important elements in environmental and biological materials including information on the separation and quantification of chemical and organometallic species.

There are two general chapters in this section:
  (i) Analytical methods and instrumentation — a summary overview
 (ii) Chemical speciation and environmental mobility of heavy metals in sediments and soils

Following these two beginning chapters are separate chapters dealing with the analysis of specific heavy metals: cadmium, lead, mercury, arsenic, thallium, chromium, nickel, cobalt, aluminum, and selenium. The closing chapter treats quality assurance approaches and discusses the paramount importance of appropriate reference materials to avoid incorrect data (results).

GARY F. BENNETT

Environmental Due Diligence Handbook, 2nd edn., by W.J. Denton, D.L. Loos, L.M.A. Hamburg, S.H. Welman, J.C. McDonald and J.C. Mauch of Greg & Tucker (Law firm) and Environmental Audit, Inc. Government Institutes, Rockville, MD. 1991, ISBN 0-86587-245-7, 308 pp., $74.00.

This book is intended for use as a basic guide to the developing process of due diligence, which can reasonably be described as a flexible use of processes and techniques intended to allow an interested party (lender, buyer, fiduciary, etc.) to evaluate the potential environmental risks associated with business transactions involving real estate.

The rapidly developing field of due diligence in the U.S. was spawned by the liability by CERCLA (Superfund), wherein parties who have no involvement with the hazardous substance contamination of the property may be found liable for every expensive cleanup of that property. In response, U.S. Congress provided some relief in SARA by providing an Innocent Landowner Defence which allows parties to avoid liability, if at the time of acquisition, they made every "reasonable" inquiry regarding the property.

The legal consequence of failure to conduct environmental due diligence is that the party acquiring the property cannot make a good faith claim of the innocent landowner defense if the property is later discovered to be contaminated. The practical problem is that the purchaser obtains property without making inquiry into its real value, i.e., is he paying more for the property than it is worth, given the contamination?

Actually the book goes beyond the limited, but important topic stated in its title giving the reader advice on how to assess the property's compliance with all environmental laws and an admonition to assess future environmental compliance problems.

The book contains a plethora of useful information, detailing first the laws affecting due diligence, the sources of information on a piece of property, and very practically how to go about getting that information. Even though the book appears to be written for lawyers, bankers and real estate people it contains much good advice, procedures to be followed and sources of information that will be of great use to environmental auditors.

Some indication of the scope of the book is given by the chapter titles:

1. Impact of Environmental Liability on Business Transactions
2. Sources of Legal Liability
3. What to Look for and Why
4. Public Records Review: What, Where and Why
5. Role of Environmental Assessments and Compliance Audits
6. Lender Risk Management
7. Purchase/Lease Risk Management
8. Fiduciary Risk Management
9. Real Estate Broker, Agent and Appraiser Liability Issue
10. Due Diligence and Contractor Selection

Approximately one-third of the book is devoted to appendices containing supplemental information on:

A. The Weldon Bill – HR 2787 to amend CERCLA to provide specific requirements for the Innocent Landowner Defence.
B. U.S. Environmental Protection Agency's Policy Statement (Fed. Reg. 51 (131) July 9, 1986, p. 25004.)
C. Superfund *De minimis* Landowner Settlements
D. Fannie Mae Procedures for Audits
E. Thrift bulletin — Environmental Risk and Liability, Feb. 6, 1991.
F. Owens Bill – HR 5927 to clarify the liability of lending institutions under CERCLA.

GARY F. BENNETT

Waste Management Guide: Laws, Issues, and Solutions, by D.H. Jessup, BNA Books, Washington, DC, 1992, ISBN 0-87179-713-5, 445 pp., $52.00.

There is no more pervasive and complex law than RCRA (Resource Conservation and Recovery Act) that the U.S. Congress passed in 1976 to completely govern hazardous waste from its generation to its disposal (cradle-to-grave). The law and the comprehensive amendment passed in 1980 (called the Hazardous and Solid Waste Amendment) spawned a formidable body of detailed regulations. To comply with these rules is no simple task.

The book is well written, but in a different style from most texts I have read. I suspect because the author is a journalist formerly on BNA staff and not a scientist or engineer. She discusses aspects of the law but in a most readable style, not slavishly tied to the detailed regulations themselves.

Laws discussed in addition to RCRA, so far as they affect it, include: CERCLA, TSCA, (PCB regulations), Medical Waste Management, the Pollution

Prevention Act (1980), and the Ocean Dumping Law. Also discussed is the management of nonhazardous waste (garbage) and sewage sludge.

Given that Congress is almost always considering new (additional) environmental legislation, I was pleased to see the author discussed bills introduced in Congress and predicted what might be their course of action. The author also pointed out regulations, the U.S. EPA is required to issue under prior legislation and guessed when they might come out and what they might entail.

Chapter 1 contains a brief but well-written description of the Federal laws noted above. Then follows the "meat" of the book.

Chapter 2 concisely reviews (with appropriate citations to the Code of Federal Regulation) the "Rules of Hazardous Waste Management". Chapter 3 lists nonhazardous solid waste management guidelines and rules (including some very interesting data on the comparative costs of landfilling and incineration — with and without energy recovery). Chapter 4 is a follow-on chapter that discusses the trends in state-regulated solid waste management. It includes a recitation of the technical assistance offered by each state for waste minimization/pollution prevention. Concluding this section of the book is a Chapter 5 which describes how RCRA, the Clean Air Act other rules and proposed rules relate to air emissions (or potential emissions) caused by waste management (landfills and incinerators mainly).

The second major theme of the book is comprised of the following four chapters which deal with waste avoidance/waste minimization/pollution prevention:

Chapter 6: Pollution Prevention
Chapter 7: RCRA Hazardous Waste Minimization
Chapter 8: Industrial Waste Recycling
Chapter 9: Municipal Solid Waste Recycling

The next two chapters are more technical. Chapter 10 deals with pretreatment requirements that resulted from the 1980 amendments to RCRA. It goes on to further prevent groundwater from migrating constituents of hazardous waste disposal on land. The amendment directs the U.S. EPA to ban untreated waste from landfills, injection wells, and impoundments. The regulation became known as the "land bans". Chapter 11 discusses disposal facilities, technical standards, issues and guidelines. Items covered in the chapter are solid and hazardous waste incineration, industrial boilers, landfills, and deep injection wells.

The best (or most difficult) topic is saved for the last two chapters: *siting*. It is a key problem because the question "where will we put it?" now totally dominates all discussion of planning for future waste disposal facilities. The discussion here is interesting with some good advice given for handling the public relations aspects of a siting venture but no magic answers to the NIMBY syndrome are found. The good news is that several successful siting ventures are discussed — for solid waste at least. The final chapter discusses the circumstances surrounding one successful hazardous waste facility siting venture in Colorado and two unsuccessful ones in Arizona and North Carolina. NIMBY, NIABY and NOPE are frustrating acronyms that seem to dominate

any siting venture: Not In My Back Yard; Not In Anybody's Backyard; and Not On the Planet Earth. Throughout the book, Jessup cites sources of her information, giving names, addresses and telephone numbers that will allow the reader to pursue his/her interests in that topic more thoroughly.

The last one-third of the text is devoted to appendices, some useful, some not. Appendix A contains directors of U.S. EPA offices, hotlines, and pollution prevention offices. State offices are also listed. So are the major waste exchange — 30 pages well spent. But not the almost 100 pages of hazardous waste (types thereof) tables, I fail to see their relevance to the text.

But let not this perceived "waste of space" at the end of this book deter the potential reader. This is a very useful and well written book, perhaps not for the expert, but certainly for the government planner and/or the consultant/engineer/environmental scientist newly entering the solid waste field.

GARY F. BENNETT

Materials Handling Technologies Used at Hazardous Waste Sites, by M. Dosani and J. Miller, Noyes Data Corp., Park Ridge, NJ, 1992, ISBN 0-8155-1299-6, 213 pp., $45.00.

Written for the U.S. Environmental Protection Agency, this book discusses the types of debris, materials and contaminants found at Superfund and other hazardous waste sites. It then describes materials-handling equipment and general procedures used to perform site restoration and cleanup.

The book has three major chapters:
- Site Characterization
- Materials-handling Equipment and Procedures, such as
  extraction and removal;
  dredging;
  pumping;
  size, volume and reduction;
  separation and dredging;
  conveying systems;
  storage containers, bulking tanks and containment;
  compaction;
  drum handling and removal;
  asbestos remediation;
  emission control;
  low level radioactive waste; and
  equipment decontamination.
- Case Studies which contains 22 case studies with at least two cases cited for each U.S. EPA Region (except for Region 9)
  There are seven appendices.

GARY F. BENNETT,

Announcements

Emerging Technologies in Hazardous Waste Management V, American Chemical Society, 1993 I&EC Division Symposium, Pollution Prevention Subdivision, Atlanta, Georgia, September 27–29, 1993

Aims and Scope

Papers and presentations are invited that describe emerging technologies for treating gaseous, liquid or solid hazardous wastes. Contributors may focus on aspects ranging from fundamental research to demonstration programs for new technologies. Emerging technologies which may be applied to a variety of waste streams are particularly encouraged. Specific applications may include waste treatment for steel and metal manufacturing, oil refining, coal processing, textile, paint and dye production, chemical and pharmaceuticals manufacturing, and nuclear reactor and reprocessing operations. Technologies for water purification or the treatment of leachates from hazardous landfills or contaminated soils are also appropriate. Emerging technologies for other wastes and review articles will be considered.

Call for Papers

Contributors should provide one camera-ready copy of extended abstracts three months prior to the symposium, and five draft copies of full manuscripts two weeks before. Extended abstracts will be published in a Book of Abstracts without review at the symposium. An independent peer review of all full manuscripts will be coordinated by the symposium coordinators and editorial review board to meet ACS standards. One or more books will be published from the full manuscripts after editing and review. (Full manuscripts will also be considered for publication in the *Journal of Environmental Science & Health*).

Abstracts (one paragraph, 150 words or less) should be submitted on the standard ACS abstract form or plain white paper. Fax abstracts to (404) 894-2866. For more information call (404) 894-2856. Contributors will be notified of acceptance by May 1, 1993.

Send abstracts by April 1, 1993 to:
 Dr. D. William Tedder
 I&EC Symposium Chair
 778 Atlantic Drive
 School of Chemical Engineering
 Georgia Institute of Technology
 Atlanta, GA 30332-0100 U.S.A.

Third International Symposium on Hygiene and Health Management in The Working Environment, Ghent, Belgium, 20–22 October, 1993

Aims and Scope

The Symposium is organized by the Koninklijke Vlaamse Ingenieursvereniging (KVIV) (Royal Flemish Society of Engineers), Technologisch Instituut, Genootschap Veiligheid (Technological Institute, Section on Safety) in co-operation with the Belgian Committee "European year of safety, hygiene and health protection at work", and should provide an important contribution to the whole topic of effective management of health risks in the working environment.

Themes will cover such key issues as the regulatory, management and quality approaches to hygiene and health risk controls in the working environment, development of exposure standards and the management of effective communications and information. A combination of review and original papers describing new findings or innovative approaches to some of the issues, will be used to address organizational and technical topics likely to be of practical interest and use to a wide range of health and safety managers, researchers, occupational health physicians and professionals.

Themes

Papers which contribute to the following general themes are invited:
1. Procedures and problems associated with the development and promulgation of occupational exposure limit values for chemical and biological agents.
   The scientific review process, key scientific issues, problems of carcinogens, setting priorities, legal aspects and consultation procedures required within the health and safety legislative framework.
2. Management of exposure to:
   Chemical agents :– toxic substances including carcinogens and those affecting the reproductive system

Physical agents :– including noise, vibration and a range of other poten-
tial hazards.
Biological agents:– in medical, R&D and industrial establishments, etc.
This theme will cover following technical and organizational items: review
of ceiling/treshold and intermediate action levels, assessment of risks,
monitoring, prevention and reduction of exposure, personal protection,
employee information, access to risk areas, training, health surveillance,
new developments on workplace hygiene and occupational health services.
3. Approaches to communication and information on hygiene and health in
the working environment.
Achieving greater awareness, access to and use of specific information,
handling information from exposure and health surveillance programmes,
health education, information on health aspects to be provided to workers.

Organizing committee

President: Ir. E. De Rademaeker (President Safety Division TI/K VIV)
Members: Ir. H. Clerckx (OCB)
        Ir. J. Clerinx (Bayer Polysar Belgium N.V.)
        Ir. H. De Lange (VBO)
        Ms. R. Peys (TI/K VIV)
        Ir. A. Voet (Provincial Safety Institute)

Scientific committee

Provisional list.
President: Ir. J. Clerinx
Members: Dr. sc. R. Bouckaert (Bayer Antwerp N.V.)
        Prof. Dr. ir. E.F. Vansant (University of Antwerp)
        Dr. K. Van Damme (Fund for Occupational Diseases)
        Mr. J.T. Sanderson (FFOM, FIOH, Dip Occup. Hyg. C.I.W.) (Exxon-
Esso)
        M. Tech. J. Bormans (UNICE)
        Lic. R. Grosjean (Ministry of Employment and Labour)
        Dr. L. Quaeghebeur (Belgian Society of Occupational Physicians)

Call for papers

All persons who intend to contribute a paper on one of the themes of the
symposium are requested to send three copies of a 300-word abstract of their
paper together with the attached application card to the Secretariat by *March
31, 1993*. Papers will be selected on the basis of the abstracts by the Scientific
Committee.

Only original papers describing significant new work or innovative approaches to key issues will be accepted. Authors will be notified not later than *May 15, 1993* and will receive instructions for the preparation of their paper.

The final version of accepted papers will be required by *August 1, 1993*.

Contact

3rd International Symposium
"Hygiene and Health Management in the Working Environment"

c/o TI-K VIV
Attn. Ms Rita Peys
Desguinlei 214
B-2018 Antwerpen (Belgium)

Tel. +32 (0)3/216.09.96; Fax +32 (0)3/216.06.89

JOURNAL OF
HAZARDOUS MATERIALS

INSTRUCTIONS TO AUTHORS

JOURNAL OF HAZARDOUS MATERIALS

INSTRUCTIONS TO AUTHORS

General

Review papers, normal papers, project summaries, invited viewpoints and short communications are published dealing with all aspects of hazardous materials arising from their inherent chemical or physical properties. The scope of the journal is wide, ranging from basic aspects of preparation and handling to risk assessment and the presentation of case histories of incidents involving real hazards to employees or the public.

The following list, though not exhaustive, gives a general outline of the scope:

Properties: toxicity, corrosiveness, flammability, explosiveness, radioactivity, information data banks, dose–response relationships
Safety and Health Hazards: manufacturing, processing, transport, storage, disposal, major hazards and hazardous installations
Legislation: international, national, local, codes of practice, threshold values, standards
Incidents: prevention, control, clean-up, communications, labelling, sources of information and assistance, case histories
Assessment: economic and general risk assessment, insurance, test methods, technical aspects of risk assessment of industrial hazards, reliability and consequence modelling, decision-making in risk management

A *Short Communication* is a concise but complete description of an investigation which will not be included in a later paper.

Submission of a manuscript implies that it is not under consideration for publication elsewhere and further that, with the exception of review papers, original work not previously published is being presented.

Preparation of papers

General
All papers should be concisely written. A Short Communication should preferably not exceed 5 printed pages (approx. 2500 words, or the equivalent in tables and illustrations). The language of the journal is English (American or British spelling, but with use of only one form in the same paper), but papers in French or German will also be considered. The author should remember that the journal is international and read widely by those whose first language may be other than that in which the paper is written. Clarity and precision are best achieved by the use of short words and simple sentences.

Papers should be submitted to one of the Editors:

Three hardcopies of the manuscript (and a floppy disk if possible) should be submitted in double-spaced typing on pages of uniform size with a wide margin on the left. This applies also to tables, legends for illustrations, references, and footnotes. The margin and double spacing greatly facilitate editorial processing. Each table should be typed on a separate page, and the legends to illustrations in sequence on a separate page, widely spaced. Typescripts should be preceded by a sheet of manuscript paper bearing the name and address of the person to whom proofs are to be sent, and indicating the number of pages in the typescript. Words or letters in the text which are to be printed in italics should be underlined.

Some flexibility of presentation will be allowed but authors are urged to arrange the subject matter clearly under such headings as: Introduction, Theory, Experimental, Results, Discussion, Conclusions, etc.

Title

Papers should be headed by a concise but informative title. This should be followed by the names of authors and by the name, address, telephone and fax numbers of the laboratory in which the work was performed. If the address of the author at the time when the paper will appear will be other than that where the work was carried out, this may be stated in a footnote. Acknowledgements for financial support should not be made by a footnote to the title or name of the author, but should be included in Acknowledgements at the end of the paper.

Abstract

A full-length paper should have an Abstract. (This is also required for Short Communications.) Authors of papers in French and German should supply in addition a translation in English of the Résumé or Zusammenfassung. The Abstract (preferably 100–200 words) should comprise a brief and factual account of the contents and conclusions of the paper, as well as an indication of any new information presented, and its relevance. Complete sentences should be used, without unfamiliar abbreviations or jargon.

Introduction

A full-length paper should have a short Introduction. This should state the reasons for the work, with brief reference to previous work on the subject.

References
    The references should be numbered consecutively throughout the text and collected together in a reference list (headed References) at the end of the paper.
    The list of references should be given on a separate sheet of the manuscript. Footnotes and legends should not include bibliographic material, and reference lists should not include material that could more appropriately appear as a footnote. Authors should ensure that every reference appearing in the text is in the list of references, and vice versa. Numerals for references are given in square brackets; numerals referring to equations are enclosed in parentheses.
    The following system of giving references is required:

Journals
1   U.C. Mishra, B.Y. Lalit and T.V. Ramachandran, Radioactivity release to the environment by thermal power stations, Sci. Total Environ., 14 (1980) 77–83.
(Journal titles will be abbreviated in accordance with the *Bibliographic Guide for Editors and Authors* (Chemical Abstracts Service, The Ohio State University, Columbus, OH 43210, USA). Authors unfamiliar with this system may give full titles without abbreviation.)

Monographs, Multi-author volumes, Proceedings
2   N. Sax, Dangerous Properties of Industrial Materials, Van Nostrand Reinhold, New York, 6th edn., 1984, p. 413.
3   H. Beller and J.M. Wilkinson, Acetylene, In: D.F. Othmer (Ed.), Encyclopaedia of Chemical Technology, Vol. 1, 2nd edn., Interscience, London, 1967, p. 171.
4   H.J. Fissan, H. Franzen and C. Helsper, Particle size distribution of combustion aerosols, In: M.M. Benarie (Ed.), Atmospheric Pollution 1978, Proc. 13th Int. Colloq., Paris, France, 1978, Elsevier, Amsterdam, 1978, pp. 263–266.

    References to a "private communication" are not to be given. A "personal communication" should be referred to only when permission has been obtained from the person who made the personal communication. A reference to "in press" implies that the paper has been accepted for publication.
    In the text, an author's name is given without initials, except where it is wished to avoid confusion with namesakes.
    When reference is made to a publication written by three or more authors, it is preferable to give only the first author's name in the text, followed by et al., or the name of one of the authors, followed by "and coworkers". In the list of references, the names and initials of all authors must be given.

Tables
    Careful thought should be given to the layout of tables (and figures) so that the significance of the results may be quickly grasped by the busy reader. Often a table of results can be understood more readily if columns and lines are interchanged. It should also be remembered that the length of a printed page is greater than its width. Tables should be numbered with arabic numerals and should have headings

that make their general meaning understandable without reference to the text. The units in which results are expressed should be given at the top of each column (in parentheses) and not repeated on each line of the table. Footnotes should be indicated by the use of lower-case letters (a, b, c, etc.), as superscripts without parentheses.

Illustrations

All illustrations should be numbered consecutively in the text, using arabic numerals, and one complete set should be in a form suitable for reproduction. In line drawings the lettering should be of such a size that they can be reduced by a factor of two or three. They should be drawn in Indian ink on drawing paper. Glossy prints are also acceptable; photocopies are not. The degree of reduction will be determined by the publisher, but in general it should be assumed that the same degree of reduction will apply to all line drawings in the same paper. Each illustration should bear the author's name, title of the paper, and the figure number. Original illustrations are not returned except by special request.

Legends should not be typed or written on the illustrations, but should be typewritten in sequence on a separate page, widely spaced. The legends should begin with a title of the same type as a table heading, followed by any other necessary descriptive material.

Photographs should be high-contrast, glossy, black-and-white prints, and should contain only material necessary to illustrate the matter under discussion. In the case of photomicrographs, magnifications must be given on the photograph. The top of the photograph should be indicated when this is not obvious. Colour illustrations can be reproduced at the author's expense.

Proofreading

Authors will receive proofs, which they are requested to correct and return as soon as possible.

Since priority is established by the date of receipt of a paper, it is essential that no new material be inserted in the text at the time of proofreading. A "note added in proof" will be accepted only if permission from the editors has been obtained; this will bear the date of receipt.

Reprints

A total of 50 reprints of each paper will be supplied free of charge to the author(s). Additional reprints can be ordered at prices shown on the reprint order form which will accompany the galley proofs.

Symbols, formulae and equations

Symbols, formulae and equations should be typed with great care, capitals and lower case letters being distinguished where necessary. Also, a clear distinction in

typewritten text should be made between the figure 1 (one) and the lower case l (ell) and between zero (0) and the letter O. Particular care should be taken in writing mathematical expressions containing superscripts and subscripts. Greek letters and unusual symbols employed for the first time should be defined by name in the left-hand margin.

The solidus ' / ' may be used in equations to economize vertical space, but its use should be consistent. For example

$$A/b = x^2/(u + v)^{1/2}$$

but it is pointless to write

$$A/b = \frac{x^2}{(u + v)^{1/2}}$$

Formulae should be regarded as part of the text as far as punctuation is concerned.

It is recommended that natural or Naperian logarithms should be denoted by ln while decade logarithms should be denoted by log. Powers of e are often more conveniently denoted by exp( ).

The multiplication sign should be used in floating point numbers to avoid confusion, *i.e.* 4.25×10^5, not $4.25 \cdot 10^5$. The decimal point should always be denoted by a full stop.

Units

SI units are preferred. However, if the work on which the paper is based has been carried out in other units, SI units should be given in parentheses, after the units used.

Compuscripts: Manuscripts on floppy disk

Nowadays, most authors of scientific articles use word processors to prepare their manuscripts. This allows the text of the article to be converted directly to the typesetting computer. The advantages of this are clear: no errors will be introduced into the text during the typesetting phase, and publication of the article can be faster than is normally the case. Elsevier is therefore providing authors with the opportunity to submit their papers on floppy disk. In order to distinguish between the traditional manuscript form and papers submitted on floppy disk, the latter will hereafter be referred to as "compuscripts".

How to submit a compuscript
When submitting a compuscript, please adhere to the following guidelines:
– The disk (3.5 or 5.25 in.) should be formatted to be MS-DOS, PC-DOS or Macintosh compatible.
– The text should be prepared in any of the commonly used word processor formats such as WordPerfect, Microsoft Word, Displaywrite, First Choice, Multi-mate, Professional Writer, Samna Word, Sprint, Volkswriter. Wang PC, Wordstar, T$_E$X or L$_A$TEX.

- The text should be saved on disk in the normal word processor format.
- The names of the text files, the word processing system used, as well as the title of the article and the authors' names, should be indicated on the disk.

How to prepare a compuscript

Non-reproducible characters should *not* be left as a blank space in the file or filled in by hand, but be replaced by a character or a series of characters not used elsewhere, and used consistently, e.g. ⟨gamma, capital⟩, ⟨lower case gamma⟩, ⟨gG⟩ or ⟨gg⟩ to indicate the use of Greek symbols in the text. The use of such non-standard characters should be indicated in a separate list, giving all the symbols used. The typesetter can then easily replace these strings of characters with the appropriate symbol.

Figure captions and tables (if included in the file) should be placed at the end of the text.

Any figures, photographs, schemes, structural formulae, etc. should be submitted in normal paper form. Digitized images cannot be reproduced with sufficient quality.

What should be sent with the disk?

Three hard copies (exact print-outs of the text) should be mailed with the disk, as well as (original plus two copies of) figures, schemes, photographs and tables that could not be included in the disk file. The hard copies will be used for refereeing the article, and as a back-up in case the disk turns out to be unusable. (In order not to delay the publication, your article will, in that case, be typeset in the conventional manner.) The hard copies should be identical to the disk text file. Loose copy which is not on the disk file may be overlooked and not added to the typeset text.

Copyright regulations

Upon acceptance of an article for publication in the Journal, author(s) will be asked to transfer the copyright of the article to the publisher. This transfer will ensure the widest possible dissemination of information.
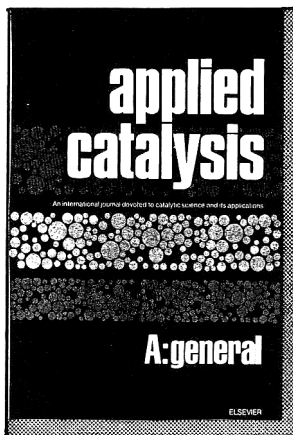
Audience

Surface, Organic and Polymer Chemists; Chemical Engineers.

AIMS AND SCOPE

Applied Catalysis provides rapid publication of communications on:

❖ catalytic phenomena occurring in industrial processes or in processes in the stage of industrial development. Both heterogeneous and homogeneous catalysis are included;

❖ scientific aspects of preparation, activation, ageing, poisoning, rejuvenation, regeneration and start up transient effects of commercially interesting catalysts;

❖ methods of catalyst characterizat on when they are both scientific and of interest for industrial catalysts;

❖ aspects of chemical engineering ⁻elevant to an improved understanding of catalytic phenomena;

❖ new catalytic reactions of potential practical interest. New catalytic routes.

A **News Brief** section, provided by correspondents, contains information gathered from patents, technical journals etc.

Ful! texts are incorporated in CJELSEVIER, a file in the Chemical Journals Online Database available ɔn STN International®.

ABSTRACTED/INDEXED IN: API Abstracts: Catalysts & Catalysis, ChemInform, Chemical Abstracts, Current Contents/Engineering, Technology & Applied Sciences, Current Contents: Physical, Chemical & Earth Sciences, Engineering Index, Metals Abstracts, Research Alert, SCISEARCH, Science Citation Index, Theoretical Chemical Engineering Abstracts.

I would like ☐ a free sample copy of Applied Catalysis A: General
☐ Instructions to Authors.
☐ to enter a subscription for 1993.
Please send me a Proforma Invoice.

Name _____

Address_____

_____

_____

The Dutch Guilder price (Dfl.) is definitive. US$ prices are for your convenience only and are subject to exchange fluctuations. Customers in the European Community should add the appropriate VAT rate applicable in their country ɔ the price(s).

711\414\144\178\3

SUBMISSION OF PAPERS

Submission of a manuscript implies that it is not under consideration for publication elsewhere and further that, with the exception of review papers, original work not previously published is being presented.

Papers should be submitted to Dr. G.F. Bennett, Department of Chemical Engineering, University of Toledo, 2801 W. Bancroft Street, Toledo, OH 43606, U.S.A. or Dr. R.E. Britter, Department of Engineering, University of Cambridge, Cambridge CB2 1PZ, Great Britain. Authors in the Far East should submit papers to Dr. T. Yoshida, Chemical Engineering Laboratory, Department of Mechanical Engineering, Faculty of Engineering, Hosei University, 7-2 Kajino-cho 3-chome, Koganei-shi, Tokyo 184, Japan.

MANUSCRIPT PREPARATION

Three copies of the manuscript should be submitted in double-spaced typing on pages of uniform size with a wide margin on the left. The top copy should bear the name and the full postal address of the person to whom the proofs are to be sent. An abstract of 100–200 words is required.

References should be numbered consecutively throughout the text and collected together in a reference list at the end of the paper. Journal titles should be abbreviated. The abbreviated title should be followed by the volume number, year (in parentheses), and page number.

ILLUSTRATIONS

Line drawings should be in a form suitable for reproduction, drawn in Indian ink on drawing paper. They should preferably all require the same degree of reduction, and should be submitted on paper of the same size as, or smaller than, the main text, to prevent damage in transit. Photographs should be submitted as clear black-and-white prints on glossy paper. Each illustration must be clearly numbered. Colour illustrations can be reproduced at the author's expense.

Legends to the illustrations must be submitted in a separate list.

All tables and illustrations should be numbered consecutively and separately throughout the paper.

LANGUAGE

The principal language of the journal is English, but papers in French and German will be published.

PROOFS

Authors will receive page proofs, which they are requested to correct and return as soon as possible. No new material may be inserted in the text at the time of proofreading.

REPRINTS

A total of 50 reprints of each paper will be supplied free of charge to the principal author. Additional copies can be ordered at prices shown on the reprint order form which accompanies the proofs.

> A pamphlet containing detailed instructions on the preparation of manuscripts for JOURNAL OF HAZARDOUS MATERIALS may be obtained from the publishers.

JOURNAL OF HAZARDOUS MATERIALS

CONTENTS